AN EVALUATION OF THE NON-LINEAR VISCOELASTIC PROPERTIES OF THE HEALING MEDIAL COLLATERAL LIGAMENT

by

Steven David Abramowitch

BS, University of Pittsburgh, 1998

Submitted to the Graduate Faculty of

School of Engineering in partial fulfillment

of the requirements for the degree of

Doctor of Philosophy

University of Pittsburgh

2004

UNIVERSITY OF PITTSBURGH

SCHOOL OF ENGINEERING

This dissertation was presented

by

Steven David Abramowitch

It was defended on

July 15th, 2004

and approved by

Patrick J. McMahon, M.D.

Michael S. Sacks, Ph.D.

Richard E. Debski, Ph.D.

Savio L-Y. Woo, Ph.D., D.Sc.
Dissertation Director

AN EVALUATION OF THE NON-LINEAR VISCOELASTIC PROPERTIES OF THE HEALING MEDIAL COLLATERAL LIGAMENT

Steven David Abramowitch, PhD

University of Pittsburgh, 2004

Injuries to knee ligaments are frequent, demanding an increased understanding of the healing process. Clinically, the injured medial collateral ligament (MCL) has been found to heal without surgical intervention. However, laboratory studies have shown that, even one year after injury, the biomechanical properties, biochemical composition, and histomorphological appearance of the healing MCL remains suboptimal. While research has focused on the changes in mechanical properties (i.e. stress-strain behavior) of the healed MCL, studies on its viscoelastic properties are limited. Yet, this knowledge is critical to determine the overall kinetic response of the knee joint.

The quasi-linear viscoelastic (QLV) theory proposed by Professor Y.C. Fung has been frequently used to model the viscoelastic properties of the MCL. This theory was developed based on an idealized step-elongation during a stress relaxation test. As this is experimentally impossible, the constants of the theory may not be representative when they are determine based on experiments that utilize finite strain rates. Thus, the overall objectives of this dissertation were to 1) develop and validate a novel experimental and analytical approach that accounts for finite strain rates and provides an accurate determination of the viscoelastic properties of the normal MCL, 2) apply this new approach to describe the viscoelastic behavior of the healing MCL, and 3) to determine whether the new approach can describe the response of the MCL to harmonic oscillations.

This work demonstrated that a newly developed approach could be utilized to determine the constants of the quasi-linear viscoelastic theory and successfully describe the viscoelastic behavior of both the normal and healing MCLs. Interestingly, the healing ligaments display a lower initial slope of the stress-strain curve and a greater propensity to dissipate energy, suggesting other structures within the knee would have to play a compensatory role in knee function. It was also found that the mechanisms governing the viscoelastic response of the MCL to harmonic oscillations may not be the same as that which governs stress relaxation behavior. Thus, a more general theory may be necessary to describe both phenomena.

TABLE OF CONTENTS

LIST OF TABLES

LIST OF FIGURES

PREFACE

When I started this journey, I truly had no idea what was in store for me. Who could have guessed that the next five years would teach me how to ask and answer interesting research questions at such a high level; but at the same time, also present me with personal challenges that forced me to answer deep philosophical questions. In the process, I was taught the satisfaction of finishing something that I once thought was impossible, and the emptiness of failing at something that I promised I would always pass; the power and prestige of being the best in your field, as well as the elegance and grace of being who you are; the beauty of science, and importance of human emotion. There were so many experiences that have changed my life for the better. Most importantly, however, were the people behind those experiences.

To my primary academic advisor and mentor, Professor Savio L-Y. Woo: Aside from my family, I have never learned more from anyone. You have taught me life lessons that I will never forget and academic principles that will take me to great heights. As a tribute to you, I dedicate my life to teaching others the lessons I have learned in the hope that I may one day impact someone's life to the degree that you have impacted mine. I am deeply honored to be your student!

To my friends at the Musculoskeletal Research Center: You can never know how much you mean to me. We laughed and cried together, shared the deepest moments of our lives, and supported one other through all of the ups and downs. It simply amazes me that, even as people come and go, the one thing that stays constant is the willingness to be there for one another. You are the warmest group of people. I look forward to the future with you.

To my parents, family, and friends: I have been absolutely blessed to be surrounded by so many people that want nothing but the best for me. Growing up, that is all I knew. I had no idea that life is not like that for everyone. You have always seen something in me that I never saw in myself. You have always put your feelings aside to do what is best for me. Thank you for helping me become the person I am today.

Finally, I would like to thank all my committee members, Drs. Debski, McMahon, and Sacks, for all of their help and guidance along the way. Additionally, I would like to acknowledge the Department of Bioengineering and the NIH grant AR 41820 for their funding support.

This work is dedicated to my Grandparents whose lives have ended, but will always remain deep within my heart- Erna Hass, Jeanette and Nathan Abramowitch, Leroy Wentzel.

1.0 MOTIVATION

Severe injuries to knee ligaments can be devastating, commonly resulting in surgery and extended absences from work or athletic competition. They often lead to damage of other structures and arthritis. With the increasing activity level and average life span of the general population, the rate of injury has been on the rise. The current incidence of knee ligament injuries is 2 per 1,000 people per year in the general population [74], with a much higher rate for individuals involved in sports activities [52, 63, 72]. Of these injuries, ninety percent involve the anterior cruciate ligament (ACL) and the medial collateral ligament (MCL) [74].

Clinical and basic science studies have revealed that some knee ligaments, such as the MCL, can heal following isolated injury [32, 45, 49, 50, 127] while others, such as the ACL and PCL, do not heal and in the majority of cases require surgical reconstruction [26, 42, 51, 88]. In addition, ACL and PCL injuries rarely occur in an isolated state. ACL injuries are often accompanied by meniscal damage and injury to the MCL, and PCL injuries often involve damage to the posterior lateral corner. In these cases, surgery is definite and outcomes are less successful. For the patients with isolated MCL injuries, however, their prognosis is favorable with a return to pre-injury activity levels following 12 weeks of limited weight bearing and physical therapy. Concomitantly, basic science studies have also found that a non-operative treatment modality in animal models resulted in the stiffness of the healing femur-MCL-tibia complex (FMTC) approaching that for normals at this time period. However, these studies have further shown that the mechanical properties of the ligament substance (i.e. quality of tissue) are

well below normal and remain so for one to two for years after injury. These differences have been associated with a wide array of biochemical and histmorphological changes.

Ligaments also exhibit time- and history- dependent viscoelastic properties. Although the viscoelastic behavior of ligaments is widely recognized as an important factor that mediates normal joint function, relatively few studies have investigated how injury and the subsequent healing response affects the viscoelastic behavior of these ligaments. To date, it has been shown that healing MCLs display a greater percentage of stress relaxation or creep. In addition, during cyclic loading and unloading, the tangent modulus of healing MCL was found to be lower but increases more rapidly with additional cycling than for non-injured ligaments [17, 112]. However, these parameters are insufficient to fully describe the viscoelastic behavior of these tissues [2, 18, 34, 59, 82, 110]. On the other hand, mathematical models have been developed to describe the complexity of these behaviors that could include the microphysical interactions of various constituents. Models can be an important tool in understanding tissue structure-function relationships and elucidating the effects of injury, healing, and treatment [24, 108, 109]. The quasi-linear viscoelastic (QLV) theory, developed by Professor Y.C. Fung, is arguably the most widely used model to describe the viscoelastic properties of soft-tissues. It has been utilized to describe the viscoelastic behavior of the normal MCL, anterior cruciate ligament (ACL), as well as many others [15, 19, 24, 34, 36, 48, 57, 67, 76, 108, 109, 121, 138].

Nevertheless, there are limitations with the application of the QLV theory, i.e. the ability to accurately estimate the constants describing the viscoelastic behavior (C, τ_1, τ_2, A, and B) [15, 23, 36, 57, 67, 76, 83]. As will be described more completely in the following sections, the QLV theory describes the time and strain dependent stress within a tissue by the convolution of a strain dependent elastic function and a time dependent reduced relaxation function. The theory

was developed on the basis that the reduced relaxation function describes the normalized stress response of a specimen in response to a step increase in strain. Since it is experimentally impossible to apply a step change in strain, many investigators have attempted to load specimens at high rates and assumed that no relaxation has occurred during loading. This approach proves to be technically challenging in terms of performing tests while measuring strain accurately as vibrations are a common occurrence when using fast strain rates [36]. In addition, the small amount of relaxation that occurs during loading when using finite strain rates causes significant errors in the estimates of the constants of the QLV theory (A, B, C, τ_1, and τ_2).

A number of authors have implemented methods to account for the latter issue in order to better approximate the "true" constants of the QLV theory. These methods include normalization procedures, iterative techniques, as well as extrapolation and deconvolution [56, 68, 76, 83]. However, these approaches all require the use of fast strain rates and are therefore significantly affected by experimental errors resulting from vibrations. Therefore, the results from different laboratories for the same type of tissue can vary dramatically as each test is dependent on the testing protocol and the approach utilized to determine the constants of the theory. In addition, the variability resulting from these approaches reduces statistical power, making differences between groups of tissues virtual undetectable.

Ideally, if there was an approach that could allow for the utilization of slow strain rates to avoid the errors resulting from vibration and also account for the relaxation manifested during loading, it would be possible to determine the true constants of the QLV theory that describe the viscoelastic behavior of a tissue. Then, the QLV theory can be utilized to describe the viscoelastic behavior of the healing and sham-operated MCL. Comparing these results would allow for the changes in viscoelastic behavior resulting from injury to be elucidated. In

addition, this approach would allow for investigators from different laboratories to compare their results. These investigators can provide clinicians and physical therapists with a further understanding of the contribution of the healing MCL to knee function and recommend an appropriate time frame to return to normal activity. Finally, these data may one day pave the way for future studies which may correlate viscoelastic behavior with structural or biological changes within the healing tissue such that fundamental questions regarding the roles of specific biochemical constituents can be answered.

2.0 BACKGROUND

2.1 STRUCTURE AND COMPOSITION OF THE NORMAL MCL

Anatomically, the MCL runs from the medial femoral epicondyle distally and anteriorly to the postero-medial margin of the metaphysis of the tibia (Figure 1). In the human, it consists of two bands, the superficial and deep. The superficial band runs on the anterior side of the MCL from the medial epicondyle to an anterior medial attachment to the tibia. The deep band runs along the posterior side of the MCL and attaches to the medial meniscus. In animals, these bands are not distinct and the MCL appears less broad. These differences likely correspond to the increased stability required at the knee for bipedal locomotion compared to quadrapedial locomotion. Yet, despite these differences, there are some fundamental similarities between the MCLs of human and animals.

The MCL is designed to help maintain varus-valgus and anterior-posterior stability during normal knee joint motion. Microscopically, the predominant cell type of the MCL is spindle shaped fibroblasts interspersed in between the parallel bundles of extracellular matrix which are composed mainly of collagen (Figure 2). Collagen is organized into a cascade of levels with pro-collagen assembled into microfibrils which in turn aggregate to form subfibrils. Multiple subfibrils combined to form fibrils which are the elemental constituent of collagen fibers [53, 54]. Collagen fibers are the functional macrostructural element of ligaments and

groups of these fibers form fascicular units which are readily observed upon inspection. As many as twenty or more of these fascicular units are bound together to form fasciculi that are up to several millimeters in diameter. Hundreds of fasciculi agglomerate to form the MCL [53, 54].

Figure 1 A photograph of a goat knee (medial view) displaying the MCL.

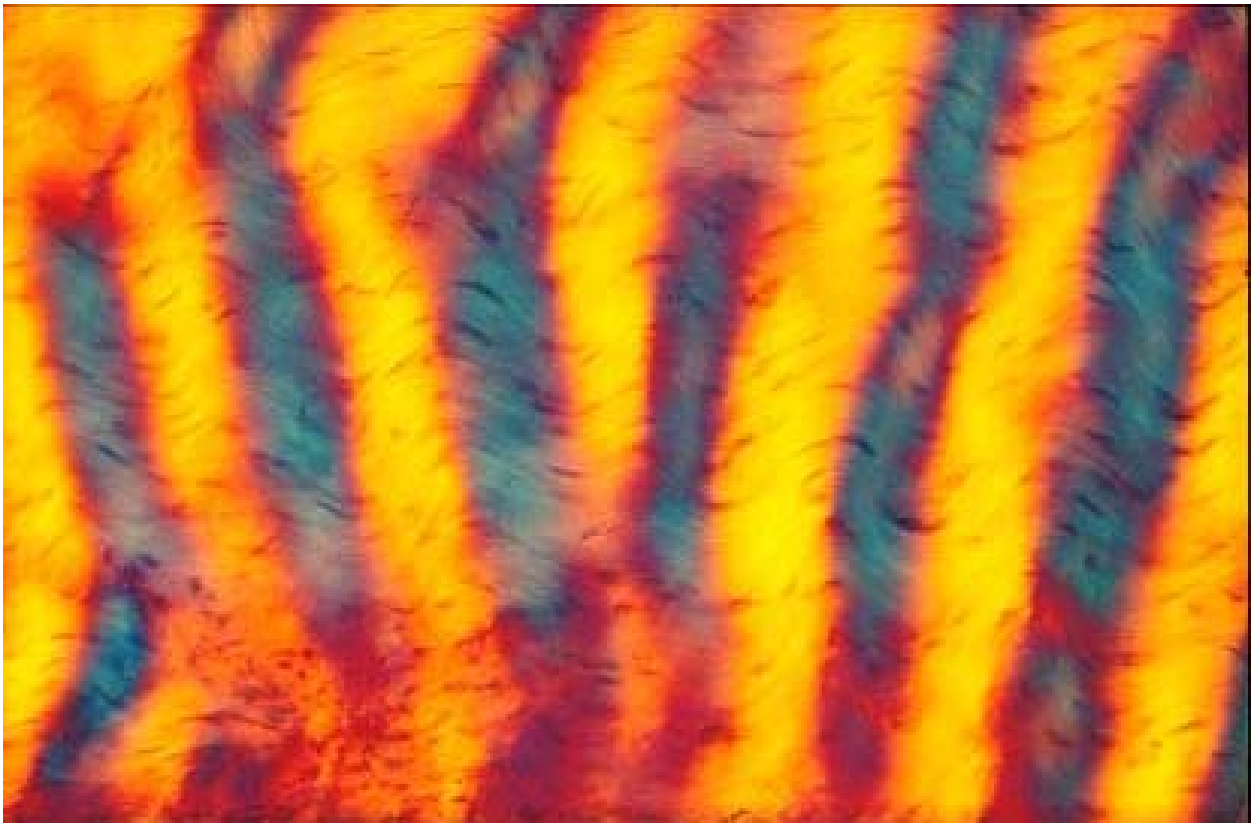

Figure 2 H&E stained histology slide of the MCL midsubstance at a magnification of 20x.

The MCL's femoral insertion is classified as direct, which means the fibers attach directly into the femur thru a transition of ligamentous tissue to bone in four zones: ligament, fibrocartilage, mineralized fibrocartilage and bone [124]. The tibial insertion of the MCL is designed to cross the epiphyseal plate so that it can be lengthened in synchrony as the bone grows between the plate and the joint. Prior to epiphysial closure, the tibial insertion is indirect whereby the superficial fibers are attached to periosteum while the deeper fibers are directly attached to the bone at acute angles via Sharpey's fibers [124]. A uniform microvascular system

originating in the femoral insertion from the medial superior genicular artery provides nutrition to the cell population, which maintain the ligament in terms of matrix synthesis and repair.

The biochemical constituents of the MCL consist of fibroblasts surrounded by aggregates of collagen, elastin, proteoglycans, glycolipids and water [119]. Between 65 and 70% of the MCLs total weight is composed of water. Type I collagen is the major constituent (70-80% dry weight) and is primarily responsible for a ligament's tensile strength. Type III collagen (8% dry weight), is strongly associated with disorganized scar tissue, and Type V collagen (12% dry weight) has been suggested to regulate the diameter of collagen fibrils [10, 69]. Type XII collagen (< 1% dry weight) has been observed more recently and is thought to provide 'lubrication' between collagen fibers [86]. The collagen types at the bone-MCL interface have also been studied, with types X, IX, and XIV being identified [10, 69, 85, 86]. The functional roles of these collagens are not clear, but they are thought to aid in reducing stress concentrations as ligamentous tissue transitions into bone. Proteoglycans and elastin constitute a small percentage of the MCLs dry weight, making up the ground substance which surrounds collagen fibers. The functional roles of these molecules are to attract water into the ligament and return the MCL to its original shape following deformation, respectively.

2.2 STRUCTURE AND COMPOSITION OF THE HEALING MCL

MCL injuries can result from a variety of mechanisms. However, the most common involve a high valgus stress resulting from a direct blow to the lateral side of the knee or upper leg with the foot firmly planted on the ground (Figure 3). The healing process of an isolated

MCL tear, although affected by various systemic and local factors, is somewhat similar to those for the vascular tissues [31]. Clinically, Grade I and II MCL injuries heal well within 11 to 20 days post-injury [22]. Healing of a Grade III MCL tear, however, may continue for years after initial injury.

Figure 3 Photograph depicting the common mechanism of an MCL injury.

A typical midsubstance tear of the MCL is characterized by the mop-end appearance of its torn ends. Roughly, ligament healing can be divided into four overlapping phases: i.e.

hemorrhage, inflammation, repair, and remodeling [127]. Between these torn ends, the hemorrhage phase begins with blood flowing into the gap created by the retracting ligament forming a hematoma. In response to the increased vascular and cellular reactions resulting from the injury, inflammatory and monocytic cells migrate into the injury site and convert the clot into granulation tissue and engage in phagocytosis of necrotic tissue. This marks the beginning of the inflammatory stage. After approximately 2 weeks, a continuous network of immature, parallel collagen fibers replaces the granulation tissue. The inflammatory phase concludes with the formation of extracellular matrix in the central region of the ligament from a random and disorganized grouping of fibroblasts (Figure 4).

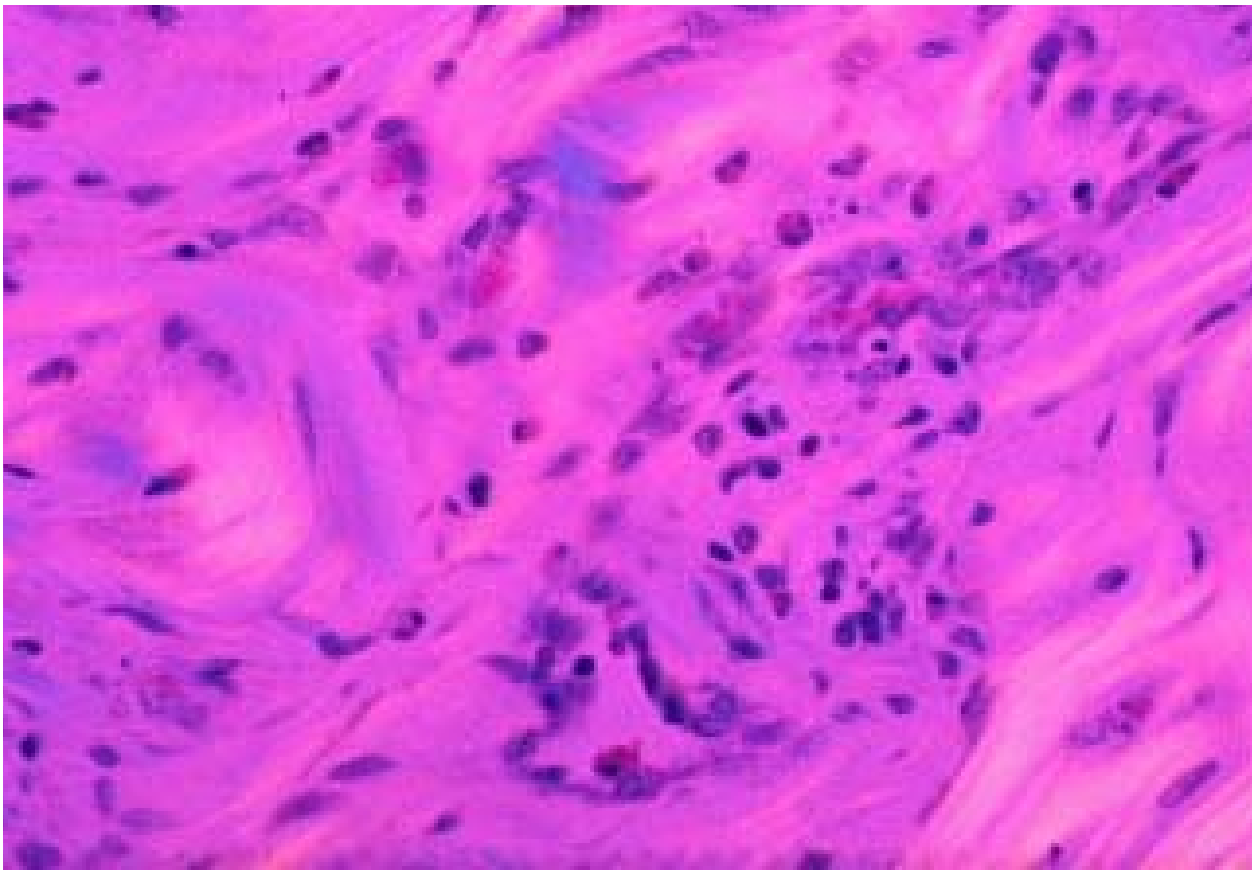

Figure 4 Histology of the midsubstance of the rabbit MCL at ten days following injury. Polarized light magnification at 100x.

The formation of extracellular matrix by fibroblasts also marks the beginning of the reparative phase. The ligament superficially resembles its pre-injury appearance. The torn ends of the ligament are no longer visible, and the granulation tissue has been replaced by immature, parallel collagen fibers. New blood vessels begin to form, while fibroblasts continue to actively produce extracellular matrix. This phase overlaps with the inflammatory phase, and concludes after several weeks.

Overlapping with the reparative phase, the remodeling phase begins several weeks after injury and continues for months. It is marked by collagen fibers continuing to align along the long axis of the ligament and the increased maturation of collagen matrix. The continued alignment of these fibers has been shown to correlate directly with an improvement in the structural properties of the ligament.

Based on the results of long-term animal studies, healing ligaments still have a different histological and morphological appearance compared to the uninjured ligament. When viewed using transmission electron microscopy, the number of collagen fibrils increased, but their diameters and masses are significantly smaller after 2 years of healing [28, 29]. Additionally, "crimping" patterns within the healing ligament remain abnormal for up to one year, and collagen fiber alignment remains poor [32, 118].

Further, the extracellular matrix of the healing MCL exhibits increases in glycosaminoglycans, changes in elastin, and differences in other glycoproteins in the short-term [14, 16, 31, 116, 140]. The changes in collagen distribution are also evident, with more type III and V than in normal ligaments [84]. Long-term studies (> 10 months) have shown that levels of glycosaminoglycans and collagen type V remain elevated, collagen fibrils remain small, and the crimp patterns remain irregular [29, 31, 84, 139, 141]. The number of mature collagen cross-links is only 45% of normal values after one year [30, 132]. Most importantly, a relationship has been demonstrated between inferior biomechanical properties of the MCL and the smaller number of collagen cross-links, as well as the decrease in mass and diameter of the collagen fibers [132].

2.3 TENSILE PROPERTIES

Due to the limited length of ligaments and logistical difficulties in clamping soft-tissue, tensile testing of ligaments is usually performed using a bone-ligament-bone complex [122, 123, 126]. In a single test, the structural properties of the bone-ligament-bone complex and the mechanical properties of the ligament substance can both be obtained [123].

2.3.1 Structural Properties of the FEMUR-MCL-TIBIA Complex

Structural properties of the bone-ligament-bone complex are extrinsic measures of the tensile performance of the overall structure. As a result, they depend on the size and shape of the ligament in question, in addition to the variations of the unique properties from tissue to the insertion into bone. These properties are obtained by loading a ligament to failure and are represented in the resulting load-elongation curve (Figure 5). From this curve, the stiffness (N/mm) is the slope of the load-elongation curve between two defined limits of elongation; the ultimate load (N) is the highest load placed on the complex before failure; the ultimate elongation (mm), is the maximum elongation of the complex at failure; and the energy absorbed at failure (N-mm) is the area under the entire curve which represents the maximum energy stored by the complex. These parameters represent the performance of a complex in response to uniaxial tension.

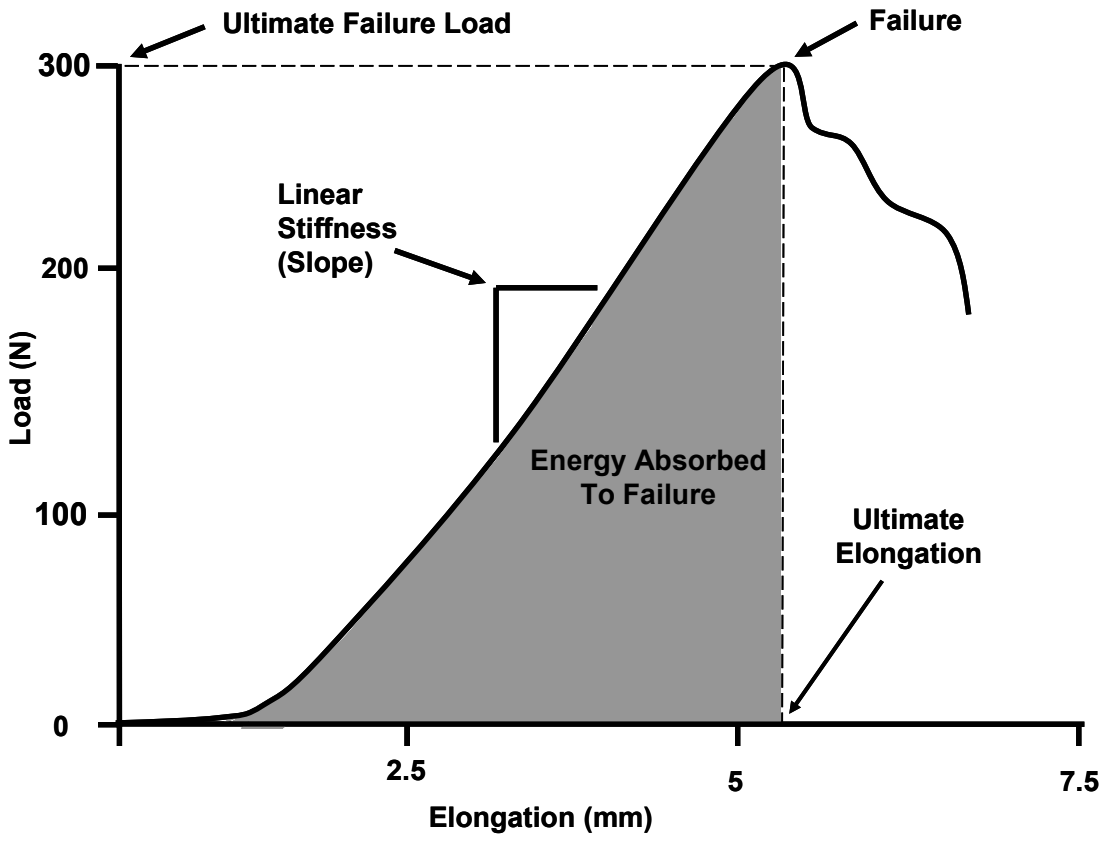

Figure 5 A typical non-linear load-elongation curve representing the structural properties of a rabbit femur-MCL-tibia complex.

2.3.2 Mechanical Properties of MCL Substance

Mechanical properties, on the other hand, are intrinsic measures of the quality of materials and are represented by a stress-strain curve (Figure 6). From this curve, the tangent modulus (N/mm^2 or MPa) is obtained from the linear slope of the stress-strain curve between two limits of strain; the tensile strength (N/mm^2) is the maximum stress achieved; the ultimate strain (in percent) is the strain at failure; and the strain energy density (MPa) is the area under the stress-strain curve, are parameters obtained to represent tissue quality. In order to determine the

mechanical properties of the ligament, video techniques have been used to track markers deployed in one-dimensional or two-dimensional patterns on the ligament's surface and the relative motions of the markers is used to determine the strain values [58, 64, 106, 123, 144]. In addition, measurement of the ligament cross-sectional area is required for stress calculations. Laser micrometry is a good method that has been employed for accurate measurement of the cross sectional area of ligaments without deforming the cross section of soft tissues [65, 120]. A specimen is placed perpendicular to a collimated laser beam and rotated 180 degrees. Using the specimen's shadow, profile widths of the specimen are recorded by a computer, and the shape and area of the specimen's cross-section are reconstructed digitally.

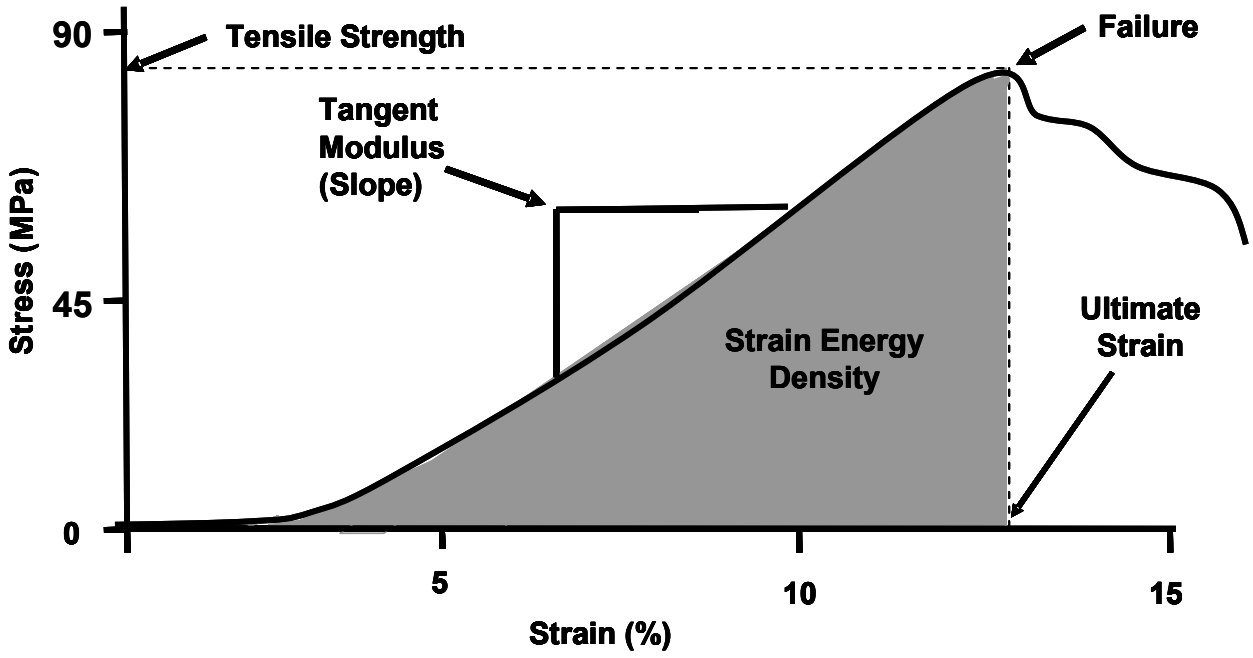

Figure 6 A typical non-linear stress-strain curve representing the mechanical properties of the rabbit ligament substance.

2.3.3 Viscoelastic Properties

The MCL, like all biological materials, possess time- and history- dependent viscoelastic properties [11, 17-19, 121, 129, 131]. Thus, the loading and unloading of a specimen in uniaxial tension yields different paths of the load-elongation curve for each testing cycle, forming a hysteresis loop. This represents the energy lost as a result of a non-conservative or dissipative process. These viscoelastic properties result from complex interactions of its constituents, i.e. collagen, water, surrounding protein, and ground substance [17, 18, 24].

Three classic experimental tests used to characterize the viscoelastic behavior are stress relaxation and creep tests, as well as the application of small harmonic excitation (i.e. dynamic mechanical analysis). A stress relaxation test involves stretching a specimen to a constant length and allowing the stress to vary with time. A creep test involves subjecting a specimen to a constant force while the length gradually increases with time. For a linear viscoelastic material, the stress in response to harmonic excitation of strain will be out of phase by some difference, δ, where $0° < \delta < 90°$ (perfectly viscous). Therefore, the stress can be resolved vectorially as

$$\sigma = \epsilon E' + i \epsilon E''$$

Dividing by strain gives the dynamic modulus of the tissues which is written as the complex ratio

$$E^* = \sigma/\epsilon = E' + i E''$$

Where E' is the in phase or storage modulus and E" is the out of phase or loss modulus. Both of these components are related to δ by

$$E' = \sigma_0/\epsilon_0 \ \mathrm{Cos}(\delta)$$

and

$$E'' = \sigma_0/\epsilon_0 \ \mathrm{Sin}(\delta)$$

where σ_0 and ϵ_0 are the maximum amplitude of stress and strain, respectively. Thus, by measuring δ, one can determine the degree of elastic versus viscous behavior for a specimen (Figure 7).

For soft tissues, the amplitude of oscillation must be small in order for stress and strain to oscillate harmonically, thus allowing for the application of linear viscoelastic theory. Previous studies of vascular tissue have shown linear viscoelastic theory can be applied if sinusoidal strains remain below 4% [93].

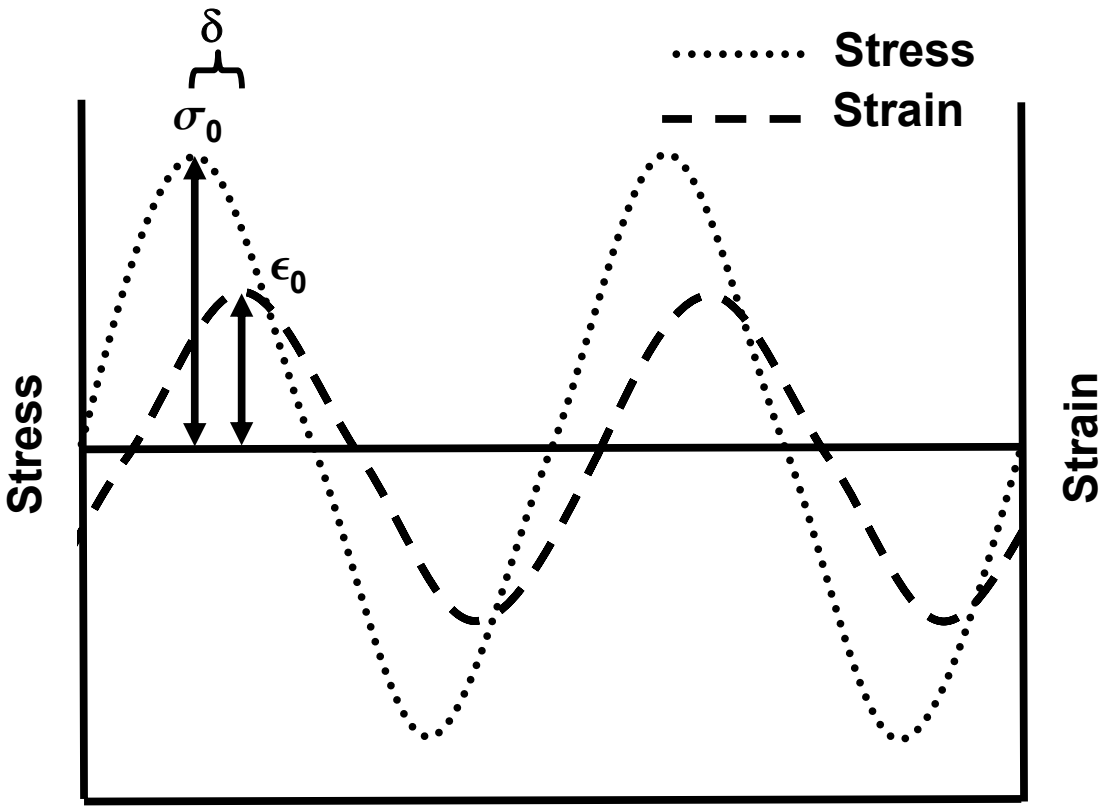

Figure 7 Sinusoidal oscillations showing the phase lag of stress to strain for a viscoelastic material.

2.3.4 Factors Affecting the Properties of the Normal MCL

A large range of experimental methods have been employed by investigators in the measurement of their mechanical properties. Difficulties encountered during testing include gripping of ligaments, strain measurement, definition of the initial length, determination of the cross-sectional area, specimen orientation, and so on. Furthermore, other factors including temperature, dehydration, freezing and sterilization techniques used during testing can also cause different outcomes in the experimental data. For more information on these factors, the readers are encouraged to study the chapter by Woo and co-workers entitled, "Biology, Healing and

Repair of Ligaments" in Biology and Biomechanics of the Traumatized Synovial Joint: The Knee as a Model, 1992 [133].

Biological factors including species, skeletal maturity, age, immobilization, and exercise have a significant influence on the mechanical properties of ligaments. Studies have shown that that the relationship between different levels of activity and the properties of the MCL follows highly non-linear relationship [62, 79, 80, 87, 89, 117, 124, 125]. Limbs subjected to periods of immobilization displayed marked decreases in the structural properties. Remobilization was found to reverse these negative changes, but at a much slower rate. Up to one year of remobilization was required for the properties of ligaments to return to normal levels following up to 2 months of immobilization [124]. Exercise, on the other hand, only showed marginal increases in the biomechanical properties of ligaments [61, 130].

Maturation has also been shown to cause significant changes to the MCL. A study looking at the changes resulting from skeletal development using the rabbit model have shown that the stiffness and ultimate load increased dramatically from 6 to 12 months of age [134]. This corresponded with a change in failure mode from the tibial insertion to the midsubstance reflecting closure of the tibial epiphysis during maturation [136]. However, these values reached a plateau up to four years of age. This exemplifies that each ligament is a unique structure and it is not possible to extrapolate age related changes from one ligament (ex. MCL to ACL) or species (ex. rabbit to human) to another.

2.3.5 Properties of the Healing MCL

The MCL of animals has served as a suitable model for studies of ligament healing because it can heal spontaneously after rupture [37, 115]. It is anatomically accessible and has suitable

length-width ratio and relatively uniform cross-sectional area for uniaxial tensile testing. The rabbit and canine MCLs have been studied extensively [14, 37, 38, 40, 41, 70, 75, 84, 105, 115, 128, 141].

The results of these experiments have revealed that conservative treatment produces similar results when compared to surgical repair with and without immobilization [12, 115, 124]. Similar results have been reported in clinical studies whereby patients respond well to conservative treatment without immobilization by plastercasts [25]. Immobilization after an MCL tear has been found to lead to significant changes in collagen synthesis and degradation, a greater percentage of disorgnized collagen fibrils, decreased structural properties of the FMTC, decreased mechanical properties of the ligament substance, and slower recovery of the resorbed insertion sites [8, 27, 37, 39, 124, 128]. These findings have led to a change in the paradigm of clinical management, i.e. shifting from surgical repair with immobilization to non-operative management with early controlled range-of-motion exercises [46, 100].

The changes in the histomorphological appearance and biochemical composition of the healing MCL are reflected in its biomechanical properties. One of the more severe injury models creates a "mop-end" tear which mimics injuries observed clinically [115]. A "mop-end" tear of the MCL substance is created by placing a stainless steel rod beneath the MCL and pulling medially, rupturing the MCL in tension and causing a midsubstance tear and damage at the insertion sites. Immediately after injury (Time 0), the valgus rotation more than doubles as compared to sham operated controls, and is still approximately 20% greater than controls at 12 weeks of healing [115]. The structural properties also differ from normal with the stiffness of the healing FMTC only approaching normal levels by 52 weeks after injury. This return to normal is largely due to an increase in the cross-sectional area of the healing ligament to as much

as 2 ½ times its normal size [91]. Thus, mechanical properties of the healing MCL midsubstance remain consistently inferior to those of the normal ligament and do not change with time (Figure 8) [91, 115].

Most likely, more than one ligament is damaged when the knee is traumatically injured, such as a combined ACL and MCL injury. These injuries are usually do not heal as successfully as the isolated MCL injuries [141]. Animal studies have revealed that with ACL reconstruction, the structural properties of the FMTC, and mechanical properties of the healing MCL were improved compared to those without ACL reconstruction. However, they remained worse than for isolated MCL injuries, suggesting that the gross joint instability may disrupt the healing process of the MCL [6]. Additionally, no long-term advantages were found between groups with the MCL repaired or without [141]. Thus, for a combined ACL and MCL injury, many clinicians reconstruct the ACL and treat the MCL non-operatively.

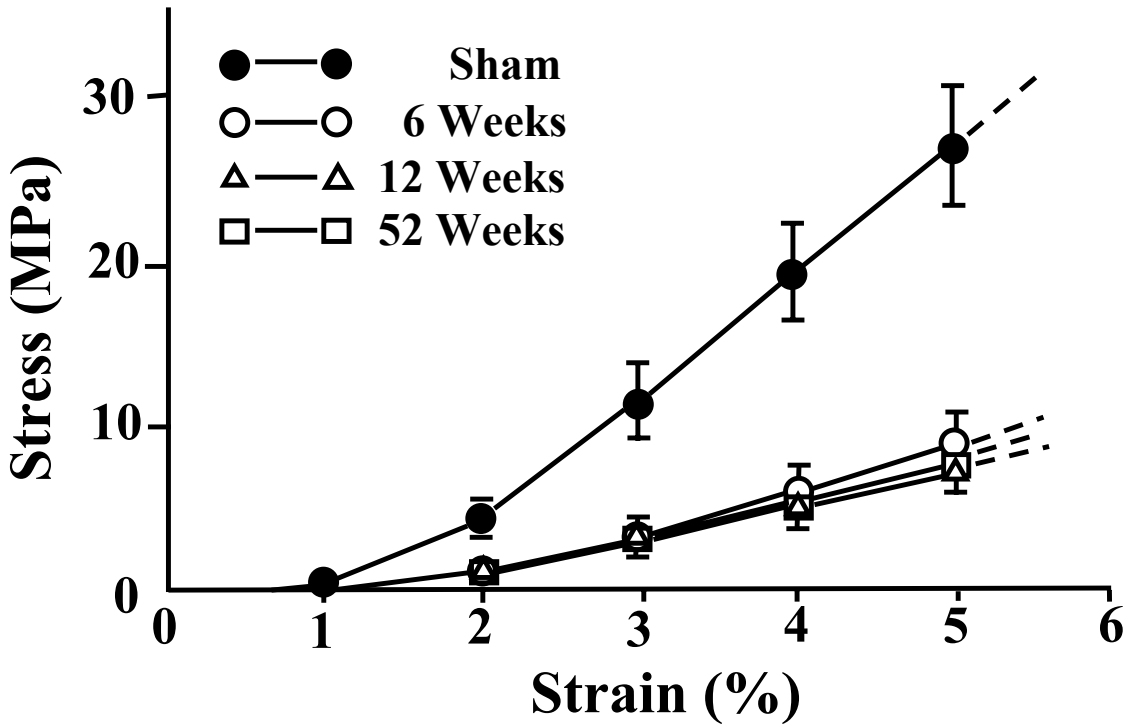

Figure 8 Stress-strain curves representing the mechanical properties of the MCL substance for sham control, as well as 6, 12, and 52 weeks after injury (printed with permission from [90]).

While most research has been performed using the rabbit model, its sedentary nature may not mimic healing as seen in the clinical situation. As a result, a goat model has been developed recently and used for MCL healing studies because of its large size, robust activity level, and the previously published success of ACL reconstructions using this animal [81, 82]. A comparison between the tensile properties of the healing goat MCL and the healing rabbit MCL indicates that the stiffness and ultimate load of the healing goat FMTC are closer to control values at earlier time periods, probably due to their increase activity level [1]. However, the tangent modulus and morphology of the healing ligament for the goat and rabbit models demonstrate that the tissue is of similar quality.

This model was then extended to study combined ACL and MCL injuries because of the difficulties of performing ACL reconstructions on smaller animals [6]. Functional evaluations of the knee demonstrated that the initially high *in situ* forces in the ACL graft were transferred to the healing MCL during the early stages of healing (i.e. from time zero to six weeks). These excessively high loads likely contributed to the observed decrease in the structural properties of the FMTC and tangent modulus of the MCL substance when compared to the isolated MCL injury [6, 104].

In terms of the viscoelastic behavior of healing ligaments, the current knowledge is less conclusive as less than a handful of studies have investigated this topic [17, 33, 128]. All of these studies are based on experiments which measured the percentage of stress relaxation or creep over a defined time period. Regardless of the injury model utilized, these studies have shown that the percentage of stress relaxation and creep is increased for healing ligaments in the first 3 months after injury. However, some studies suggested that these values returned to normal levels after this time period [17, 33, 128], while others suggested they remained increased [79].

2.4 QUASI-LINEAR VISCOELASTIC THEORY

The nonlinear time- and history- dependent viscoelastic behavior of soft biological tissues has been widely described by the QLV theory formulated by Fung (1972) [15, 19, 24, 34-36, 44, 48, 57, 76, 99, 103, 108, 109, 113, 121, 138]. This theory has been adopted for modeling the viscoelastic behavior of ligaments and tendons by many laboratories [19, 24, 36, 48, 57, 67, 99, 108, 109, 113, 121]. In our laboratory, the QLV theory has been successfully used for modeling

the viscoelastic properties of the canine MCL [121], the porcine ACL [57], and the human patellar tendon [48].

2.4.1 Fundementals

In the late 60's, Professor Y.C. Fung made two key observations about soft tissue mechanical behavior that could not be described using linear viscoelastic theory. The first observation was that the percentage of stress relaxation was linearly related to the applied stress. In other words, an increase of the applied stress resulted in an increase in the total amount of stress relaxation. Yet, the same overall percentage of relaxation would be observed when the stress relaxation was normalized by the peak stress. The second major observation was that the stress-strain behavior of soft tissues in nonlinear. Linear viscoelastic theory can describe the first observation only if there is a linear relationship between stress and strain. Since this behavior was nonlinear, Professor Fung realized that a new viscoelastic theory would be necessary. Based on the framework of linear viscoelastic theory, Professor Fung developed the QLV theory to describe these observations. It assumes that the stress relaxation behavior of soft-tissue can be expressed as

$$\sigma(t) = G(t)*\sigma^e(\varepsilon) \qquad (1)$$

where $\sigma^e(\varepsilon)$ is a nonlinear function describing the stress in response to an instantaneous input of strain (i.e. the elastic response). $G(t)$ is the reduced relaxation function that represents the time-dependent stress response of the tissue normalized by the peak stress following a step input of strain [i.e., $t = 0^+$, such that $G(t) = \sigma(t)/\ \sigma(0^+)$, and $G(0^+) = 1$].

To describe a non-instantaneous strain history (i.e. strain is dependant on time), the Boltzmann superposition principle can be assumed and the stress at time *t*, σ(*t*), is given by the convolution integral of the strain history and *G*(*t*):

$$\sigma(t) = \int_{-\infty}^{t} G(t-\tau)\frac{\partial \sigma^{e}(\varepsilon)}{\partial \varepsilon}\frac{\partial \varepsilon}{\partial \tau}\partial \tau \qquad (2)$$

In the experimental setting, we can assume that the history begins at $t = 0$. These equations describe the general theory to model the viscoelastic behavior of soft tissues. However, to apply this theory to experimental data obtained for a specific tissue, it is necessary to define functions for G(t) and $\sigma^{e}(\varepsilon)$ that describe the relaxation of a tissue following a step-elongation and the stress resulting from an instantaneous strain, respectively.

2.4.1.1 Reduced Relaxation Function

While any choice can be made for the function G(t), the specific form that has been the most popular choice for many studies was also developed from a few additional key observations by Professor Fung. While testing rabbit mesentery, he noticed that the hysteresis was not dependent on the strain rate of the experiment (i.e. the amount of damping or energy loss was constant versus frequency). In addition, the dynamic modulus increased linearly versus the logarithm of frequency. With his strong background and experience in aeroelasticity, he soon recalled that these were design criteria considered for airplane wings to respond to turbulence and a mathematical representation had previously been described [78].

The reduced relaxation function chosen by Professor Fung can be derived on the basis of a standard linear solid model (Figure 9).

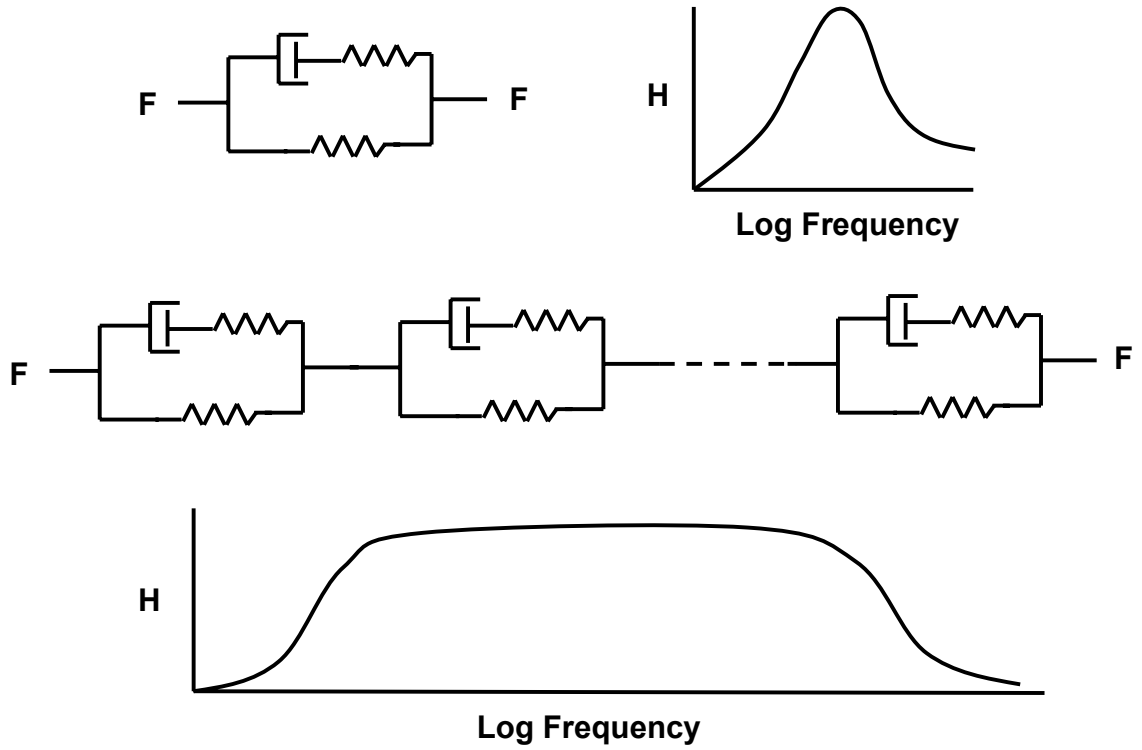

Figure 9 Models of a standard linear solid can be combined in series to create a model with a continuous spectrum of relaxation (adapted from [34]).

The differential equation for this model takes the form

$$\sigma + \tau_\epsilon \sigma' = E_R (\epsilon + \tau_\sigma \epsilon') \quad (3)$$

where τ_ϵ is the relaxation time constant for constant strain, τ_σ is the relaxation time constant for constant stress, and E_R the constant that determines the level of stress or strain after a long relaxation, $t \rightarrow \infty$. For a suddenly applied stress $\sigma(0)$ and strain $\epsilon(0)$, this equation is subjected to the initial condition

$$\tau_\epsilon \sigma(0) = E_R \tau_\sigma \epsilon(0) \quad (4)$$

which describes instantaneous behavior of two springs in parallel since the dashpot behaves as a rigid solid for a step input of strain. However, to force this equation to describe normalize relaxation versus time, the condition G(0) = 1 is necessary. Thus, for a unit step increase of strain

$$\tau_\epsilon = E_R \tau_\sigma \quad (5)$$

or

$$E_R = \tau_\epsilon/\tau_\sigma. \quad (6)$$

With these conditions, the stress in response to a unit step increase of strain can be obtained by solving equation 3:

$$G(t) = E_R [1 + (\tau_\sigma/\tau_\epsilon - 1) e^{-t/\tau\epsilon}] \mathbf{1}(t) \quad (7)$$

With the substitution

$$S = \tau_\sigma/\tau_\epsilon - 1 \quad \text{and} \quad E_R = 1/(1+S) \tag{8}$$

equation 7 becomes

$$G(t) = 1/(1+S)\,[1 + S\, e^{-t/\tau\epsilon}] \tag{9}$$

To implement the idea of a relaxation spectrum, which is equivalent to connecting an infinite number of standard linear solid models in series and providing a distribution of spring and dashpot constants throughout, τ_ϵ is replaced by a continuous variable, τ. Thus, equation 9 becomes

$$G(t) = \frac{1 + \int_0^\infty S(\tau) e^{-\frac{t}{\tau}} d\tau}{1 + \int_0^\infty S(\tau) d\tau} \tag{10}$$

The standard linear solid was chosen because, like most soft tissues, this model does not completely stress relax to zero. Instead, it reaches a finite platue for long relaxation times. However, the constant hysteresis versus frequency (i.e. spectrum of relaxation) that is characteristic of soft tissues is not observed with this model. In order to describe the phenomenon of a constant spectrum of relaxation, a special definition of $S(\tau)$ must be considered

$$S(\tau) = C/\tau \qquad \text{for} \qquad \tau_1 \le \tau \le \tau_2 \tag{11}$$
$$= 0 \qquad \text{elsewhere}$$

where C is a dimensionless constant. With this definition, the reduced relaxation function describing a constant spectrum of relaxation takes the form

$$G(t) = \frac{1 + C[E_1(t/\tau_2) - E_1(t/\tau_1)]}{1 + C\ln(\tau_2/\tau_1)} \tag{12}$$

where $E_1(y) = \int_y^\infty \frac{e^{-z}}{z} dz$ is the exponential integral, and C, τ_1, and τ_2 are material constants. For a stress relaxation experiment, the constant C determines the magnitude of viscous effects present and is related to the percentage of relaxation. The time constants τ_1 and τ_2 govern initial and late relaxation, respectively, relating to the slope of the stress relaxation curve at early and late time periods [102].

2.4.1.2 Sinusoidal Strain History and G(t)

As mentioned, the choice for the expression of G(t) was made partially because the hysteresis for many soft tissues is independent of strain rate. While equation 12, which describes stress relaxation in response to a step input of strain, was obtained by solving equation (3) for a step input of strain, the stress response to a sinusoidal input of strain can be determined in a similar fashion. For a sinusoidal oscillation,

$$\epsilon(t) = \epsilon_0 e^{i\omega t} \tag{13}$$

the stress response can be described as

$$\sigma(t) = \sigma_0 e^{i\omega t} \tag{14}$$

where $\omega = 2\pi f$. Thus, an expression for the complex or dynamic modulus, i.e. σ_0/ϵ_0 can be obtained by substituting these equations into equation 3:

$$M = \frac{1+i\omega\tau_\sigma}{1+i\omega\tau_\varepsilon} E_R \tag{15}$$

With the same substitution for S as described in the previous section

$$M = \frac{1}{1+S}\left(1 + S\frac{\omega\tau_\varepsilon}{\omega\tau_\varepsilon + \frac{1}{\omega\tau_\varepsilon}} + iS\frac{1}{\omega\tau_\varepsilon + \frac{1}{\omega\tau_\varepsilon}}\right) \tag{16}$$

Then, allowing τ_ϵ to be replaced by a continuous variable τ gives

$$M(\omega) = \frac{1}{1+\int_0^\infty S(\tau)d\tau}\left(1 + \int_0^\infty S(\tau)\frac{\omega\tau}{\omega\tau + \frac{1}{\omega\tau}}d\tau + \int_0^\infty iS(\tau)\frac{1}{\omega\tau + \frac{1}{\omega\tau}}d\tau\right) \tag{17}$$

With the definition of a constant spectrum of relaxation, the dynamic modulus can be described as

$$M(\omega) = \{1+C/2[\mathrm{Ln}(1 + \omega^2\tau_2^2) - \mathrm{Ln}(1 + \omega^2\tau_1^2)] + i\ C[\mathrm{Tan}^{-1}(\omega\tau_2) - \mathrm{Tan}^{-1}(\omega\tau_1)]\}\{1 + C\ \mathrm{Ln}(\tau_2/\tau_1)\}^{-1} \quad (18)$$

By dividing the magnitude of the complex portion of this expression by the real portion, an equation describing the damping or internal friction is as follows

$$\mathrm{Tan}(\delta)=(C[\mathrm{Tan}^{-1}(\omega\tau_2) - \mathrm{Tan}^{-1}(\omega\tau_1)])/(1+1/C/2[\mathrm{Ln}(1 + \omega^2\tau_2^2) - \mathrm{Ln}(1 + \omega^2\tau_1^2)]) \quad (19)$$

As the choice for the relaxation function, G(t) for ligaments is based on the framework of linear viscoelasticity and incorporates the concept of a constant spectrum of relaxation [34, 35], it is described by 3 constants (C, τ_1, and τ_2). The degree of energy loss per cycle (described by the dimensionless constant C) during cyclic loading of a specimen is constant for a wide range of frequencies. The frequencies described by $1/\tau_2$ and $1/\tau_1$ bound the lower and upper limits of this range, respectively.

Previous work has shown that creep cannot be predicted from stress relaxation using the QLV theory [111]. In fact, Professor Fung in his book *Biomechanics* (2^{nd} edition; 1993 [34]) described this phenomenon by suggesting "…creep is fundamentally more nonlinear, and perhaps does not obey the quasi-linear hypothesis." While many studies have indeed shown that this theory does well when it is used to describe and subsequently predict stress relaxation

phenomenon, it is less clear whether the constants obtained from a stress relaxation experiment can be utilized with the QLV theory to describe the response of ligaments to harmonic oscillations (i.e. hysteresis).

2.4.1.3 Elastic Response

For the elastic response, there have been many expressions which describe the nonlinear concave upward shape that is characteristic of many soft tissues. One of these expressions has become popularly utilized to describe the stress-strain behavior of ligaments and tendons [121]. The expression consists of an exponential function with a linear constant A and a nonlinear constant B.

$$\sigma^e(\varepsilon) = A(e^{B\varepsilon} - 1) \tag{20}$$

The physical significance of these constants has been examined. The physical significance of B and the product AB are the rate of change of the slope of the stress-strain curve and the initial slope of the curve, respectively. This is shown in the following derivation:

$$\sigma(\varepsilon) = A*[e^{B\varepsilon} - 1]$$

$$\frac{\partial\sigma(\varepsilon)}{\partial\varepsilon} = AB*e^{B\varepsilon}$$

$$= AB*e^{B\varepsilon} - AB + AB$$

$$= B*[Ae^{B\varepsilon} - A] + AB$$

$$\frac{\partial\sigma(\varepsilon)}{\partial\varepsilon} = B\sigma + AB$$

Note that the slope of the stress-strain curve is linearly related to stress by constant B. When the stress is zero or near zero, the slope of the stress-strain curve is governed by the term AB.

2.4.2 Errors Involved with the Application of the QLV Theory

The most common approach to determine the constants of the QLV theory (A, B, C, τ_1, and τ_2) utilized until the mid 1980s was the instantaneous assumption approach as utilized by Woo et al. (1981) [121]. This approach is based on curve-fitting the equations describing the elastic response and reduced relaxation function separately to the stress-strain curve obtain during loading and the normalized and time-shifted relaxation data from a static stress relaxation experiment. It assumes that the loading phase of the stress relaxation test occurred instantaneously [23]. It is, therefore, necessary to simulate a step increase in strain as closely as possible to minimize errors resulting from that assumption. Thus, previous investigators have applied extensions at relatively high rates and assumed that the stress relaxation portion of the

experiment begins at t = 0. This allows separate curve-fitting of equations 19 and 12 to the loading and relaxation portions of the experimental data, respectively, to estimate the 5 constants. It was later found that even short (< 1 sec) loading times significantly erred all of the estimated constants, with constant τ_1 most significantly affected [23].

As a result, researchers developed approaches designed to account for the relaxation manifested during short loading times. These methods included normalization procedures, iterative techniques, as well as extrapolation and deconvolution methods [15, 23, 36, 57, 67, 76, 83]. While these approaches improved the estimates of constants, they are still dependant on fast ramp times (~0.01 to 0.1 sec). Not only does this prove to be technically challenging as it is difficult to measure strain accurately, but investigators later found that obtained constants are significantly affected by experimental errors associated with high extension rates (ex. overshoot, vibration, poorly approximated strain histories) (Figure 10) [36]. The constants obtained demonstrate high variability because they are dependent on the testing equipment, testing protocol, and an individual investigator's subjectivity on defining the time at which the stress relaxation portion of the test begins. Table 1 lists the range of values reported in the literature for ligaments and tendons for the 5 constants (A, B, C, τ_1, and τ_2) of the QLV theory [19, 24, 36, 48, 57, 67, 99, 108, 109, 113, 121]. Similar ranges of values have been reported for all types of tissue in which this theory has been applied. It should be noted that the reported values span at least 2 orders of magnitude, likely reflecting the errors from the sources described above.

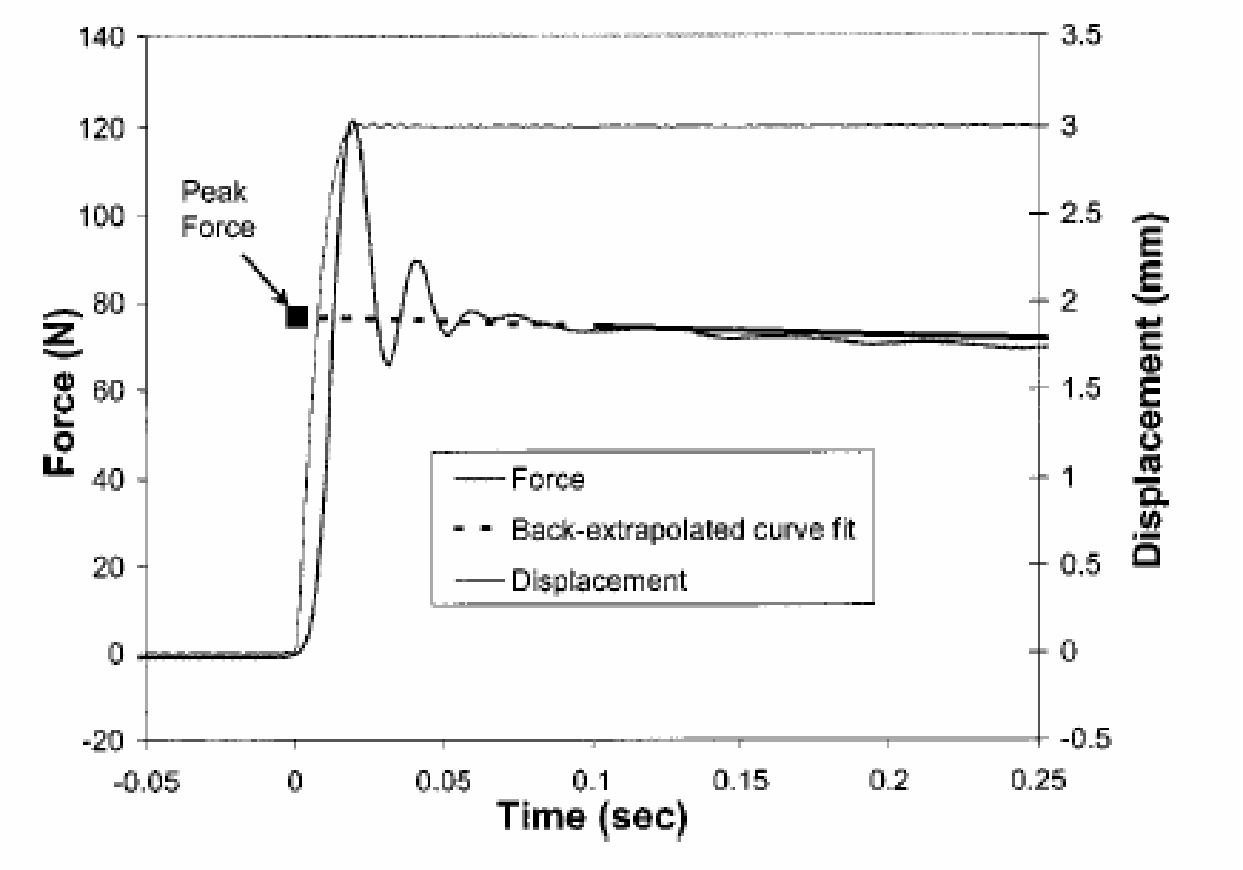

Figure 10 Vibrations induced while performing a ramp and hold strain history at high rates (printed with permission from [36]).

Table 1 A range of values reported in the literature for the constants of the QLV theory describing the viscoelastic behavior of ligaments and tendons.

A (MPa)	B	C	τ_1 (sec)	τ_2 (sec)
0.2 to 281	0.6 to 161	.099 to 2.01	.041 to 1.6	323 to $5.03(10^6)$

Thus, there is currently no approach that allows for the use of slow strain rates to minimize experimental errors and can also account for the relaxation manifested during the loading portion of the static stress relaxation test. While the current approaches can account for the relaxation manifested during the loading portion of a stress relaxation experiment, the wide range of values reported in the literature suggest that these constants are highly sensitive to the experimental protocol and analytical approach utilized. With this degree of variability, the obtained constants cannot be compared between laboratories or between tissues.

3.0 OBJECTIVES

3.1 BROAD GOALS

The broad goal of this dissertation is to more thoroughly describe the viscoelastic behavior of the healing MCL after 12 weeks of injury (i.e. the time period in which most patients would be allowed to return to normal activities) using the QLV theory and to make comparisons to those for the normal MCL. Because there is no one approach in the determination of the constants of the QLV theory that minimizes the errors resulting from finite strain rates nor the experimental errors from a fast strain rate test, the objective of this work was to develop a novel mathematical approach to determine the constants of the QLV theory and then validate these results experimentally. In addition, this new approach can yield unique and accurate estimates of constants to allow for statistical comparisons of the constants describing healing and sham operated MCLs.

The new analytical methodology and its application to the healing MCL is designed to address the three proposed Specific Aims below.

3.2 SPECIFIC AIMS

Specific Aim 1: The first Aim of this dissertation is to develop a new analytical approach that can determine the constants describing the functions $\sigma^e(\varepsilon)$ and G(t) based on an experiment that utilizes a slow strain rates (i.e. loading time >1 sec). This approach will allow for experimental errors to be minimized while accounting for relaxation that is manifested during loading.

Specific Aim 2: The second Aim of this dissertation is to utilize this new strain history approach to describe the viscoelastic properties of the healing goat MCL at 12 weeks after mop-end tear injury and compare the obtained constants with those for sham-operated controls.

Specific Aim 3: The third Aim of this dissertation is to assess whether the constants obtained using the approach described in Specific Aim 1 can be utilized to make conclusions regarding the response of ligaments to harmonic oscillations. To complete this Aim, a predicted spectrum of relaxation using the new strain history approach will be compared to that obtained experimentally via dynamic mechanical analysis (DMA).

3.3 HYPOTHESES

The hypotheses that correspond to Specific Aims 2 and 3 are as follows:

Hypothesis 2a: Based on previous studies that have shown that collagen within the healing MCL to be disorganized, the number of mature collagen cross-links to be decreased, and the tangent modulus of healing MCLs to be inferior to sham-operated controls, the constants A*B, which describe the initial slope of $\sigma^e(\varepsilon)$, will be significantly lower for healing MCLs compared to sham-operated controls.

Hypothesis 2b: Previous studies have also shown that healing MCLs exhibit a larger hysteresis and greater percentage of relaxation compared to sham-operated controls, then constant C, which is related to the degree of energy loss, will be significantly greater for healing MCLs compared to sham-operated controls.

Hypothesis 3: In order to make conclusions regarding the response of a ligament to harmonic oscillations based on the results of a stress relaxation test, both viscoelastic phenomenon must be governed by the same mechanisms and described by a constant spectrum of relaxation. Thus, if the constants obtained from analytical approach described in Specific Aim 1 describe this constant spectrum of relaxation, then the experimentally obtained spectrum of relaxation (i.e. Tan δ vs. frequency) obtained from sinusoidal loading of a specimen at small strains will be predicted using the approach described in Specific Aim 1 with an R^2 value greater than 0.9.

4.0 EXPERIMENTAL MODEL

Inanimate models are unsuitable for investigations of the healing process of the MCL, and invertebrate animals lack mammalian-type knee joints and MCLs. Different vertebrate species (including rabbits, dogs, and goats) have been used in our laboratory to study various aspects of the normal and healing MCL [79, 104, 123, 138, 141]. The NZW rabbit is of sufficient size to allow surgery to be performed easily. Furthermore, specimens from these animals have been shown to provide tissue samples large enough for successful biomechanical testing. However, due to the relative activity levels following injury, the rabbit has recently been suggested to be less analogous to humans and therefore considered an inferior model to the goat for studying ligament healing. The goat has been a preferred animal model because of its relatively large knee joint and robust post-operative activity level compared to that of the rabbit model [1, 81, 82, 92]. A study from our laboratory has shown that the structural properties of the FMTC are closer to controls at earlier time points for the goat which may be related to their activity level. Thus, we selected goats as our model for MCL healing studies. When healing was not considered (i.e. to evaluate whether the results obtained from static stress relaxation experiments could be utilized to predict those obtained from dynamic mechanical testing), the rabbit model was utilized because of its cost.

4.1 SURGICAL PROCEDURE

All surgical procedures were performed using well-established protocols developed in our research center [1, 104, 115, 140]. Since goats were utilized for the healing portion of this dissertation, the following surgical procedures are described specifically for goats. Animals were given an intramuscular (IM) preanesthetic dose of xylazine HCl 0.1 mg/kg and ketamine HCl (10 mg/kg), and a preoperative antimicrobial dose of 20-25 mg/kg Cephazolin. General anesthesia was maintained with 1.5-2.0% isoflurane supplemented by oxygen and nitrous oxide. The fur was shaved from the hind limbs, and the exposed area was sterilized with betadine solution.

An isolated MCL injury was created by making an anteromedial incision, centered over the joint line and carried down to the deep fascia. The fascia was incised, exposing the MCL, which was undermined. The knee was positioned to 90° of flexion. In the right knee (experimental), a stainless steel rod (4-mm-diameter) was passed beneath and perpendicular to the ligament, just inferior to the attachment of the medial meniscus, and pulled medially to rupture the ligament [1, 104, 115, 140]. The ruptured ends were re-approximated but not repaired (Figure 11). This technique was designed to simulate an MCL tear that is seen clinically. This injury consists of a mid-substance tear with simultaneous damage to the insertion sites. The left knees of all animals served as sham-operated controls [1, 104, 115, 140]. All incisions were closed using Dexon 2-0 sutures and standard suture technique. Skin incisions for the shams were the same as those for the experimental groups. The fascia over the MCL was incised, and the MCL was undermined but not ruptured for all shams.

Figure 11 Photograph of a "mop-end" tear created in the mid-substance of the MCL.

Postoperatively, all animals were allowed free cage activity (cage area: 3 m^2 for goats). No immobilization was used. The status of weight bearing, general health condition, as well as food and water intake of all animals was monitored during recovery. An experienced veterinary technician cared for the animals. Cephazolin (20-25 mg/kg) was administered twice a day for five days post-operatively for infection prophylaxis. Xylazine was injected intramuscularly (0.05-0.3 mg/kg) twice a day for three days postoperatively as an analgesic. Pain was assessed by monitoring changes in level of cage/pen activity and eating habits.

A lethal injection of sodium pentobarbital intravenously (50-100 mg/kg) while under sedation was used to humanely euthanize the animals at the time of sacrifice. This surgical procedure has been approved by the University of Pittsburgh Institutional Animal Care and Use Committee (IACUC). In addition, the methods are consistent with the recommendations of the Panel on Euthanasia of the American Veterinary Medical Association. (University of Pittsburgh Assurance Number A3187-01, Protocol Number 0699055A; University of Pittsburgh Assurance Number A3187-01, Protocol Number 0002023A-2, goats and rabbits, respectively).

4.2 SPECIMEN PREPARATION

Following sacrifice, hindlimbs were disarticulated at the hip joint, wrapped in saline-soaked gauze, placed in double plastic bags, and immediately stored at –20°C until testing [135]. On the day prior to testing, the saline soaked specimens were removed from the freezer and thawed overnight at room temperature. An orthopaedic surgeon examined specimens for joint abnormalities during dissection. All extraosseous and periarticular tissues around the knee joint

were removed leaving the MCL intact and connected via its insertion sites to the femur and tibia (i.e. a femur-MCL-tibia complex or FMTC). The femur and tibia were then cut to a length of 7-8 cm from the joint line to allow for placement within a laser micrometer system and testing clamps. The tibial platue and femoral condyles were cut parallel to each other with the knee flexed at 60°. Care was taken not to disturb the insertion sites. Cutting the platue and condyles allowed for an unobstructed line of sight for multiple cross-sectional area measurements along the length of the MCL and a more rigid fixation within our testing clamps.

5.0 EXPERIMENTAL METHODS

5.1 CROSS SECTIONAL AREA MEASUMENTS

A laser micrometer was developed in our research center to measure the cross sectional area and shape of soft tissues without contacting the tissue substance [65, 120] (Figure 12). The accuracy of the cross-sectional area measurement was been determined to be less than 0.1 mm^2. For the MCL, measurements were taken at three locations: (1) at the center of the joint line, (2) just distal (approx. 2.5 mm) to the femoral insertion, and (3) just proximal (approx. 2.5 mm) the tibial insertion [1, 104]. The three measurements were averaged, and this average was used for calculating Lagrangian stress (force/initial cross-sectional area).

Figure 12 FMTC mounted on a laser micrometer system.

5.2 STRAIN MEASUREMENTS

Two rectangular reflective markers (2 mm wide) were attached to the ligament substance for strain measurements. The markers were positioned approximately 1 cm apart along the long axis of the MCL and centered about the joint line (Figure 13). The motion of these reflective markers was recorded using a video analysis system (Motion Analysis™ VP320). This system was able to digitize the inner edge of each marker (i.e. the edge closest to the midsubstance of the ligament) based on contrast. The distance between these edges were used for the calculation of strain. Prior tests revealed that the errors in the accuracy of strain measurement with this system are less than 0.2% [1, 91, 104, 106].

Recent literature suggests that the viscoelastic behavior of the MCL may be nonlinear [96]. To address this potential limitation, it was important to utilize consistent levels of strain for experiments involving ligaments in order to make statistical comparisons between groups. A study by Provenzano et al. demonstrated that the rate of relaxation was constant for strains above 2.5% (i.e. the QLV theory would apply to strains above this magnitude). Further, this group has also shown that ligament damage occurs at strains greater than 5% for the rat model [97]. Therefore, the stain levels utilized in this dissertation were are all between 2.5% and 5% strain.

However, the strain output can not be used to control our testing system. Therefore, it was necessary to determine the elongations to apply to the sham-operated and healing MCL to yield equivalent strains. The data from a previous study which evaluated the mechanical properties of the healing goat MCL at 6 weeks after injury was utilized to determine elongations that would correspond to strains within 2.5 and 5%. Based on these data it was determined that elongations of 3 mm would fall safely within this range for both groups.

5.3 UNIAXIAL TENSILE TESTS

The FMTCs were rigidly fixed into custom-designed clamps at 60° of knee flexion. The clamps were immersed in a 32° C saline bath [1, 104]. One clamp was attached through a tensile load cell to the crosshead of the materials testing machine (model 4502; Instron, Canton, MA) and the other was attached to the base. The MCL was centered beneath the load cell and its long axis was aligned with the loading axis (Figure 13). After allowing 1 hour for the specimen to equilibrate to the environment, each specimen was preloaded to 2 N and the gauge length was zeroed. This was followed by preconditioning between 0 and 2 mm of extension for 20 cycles.

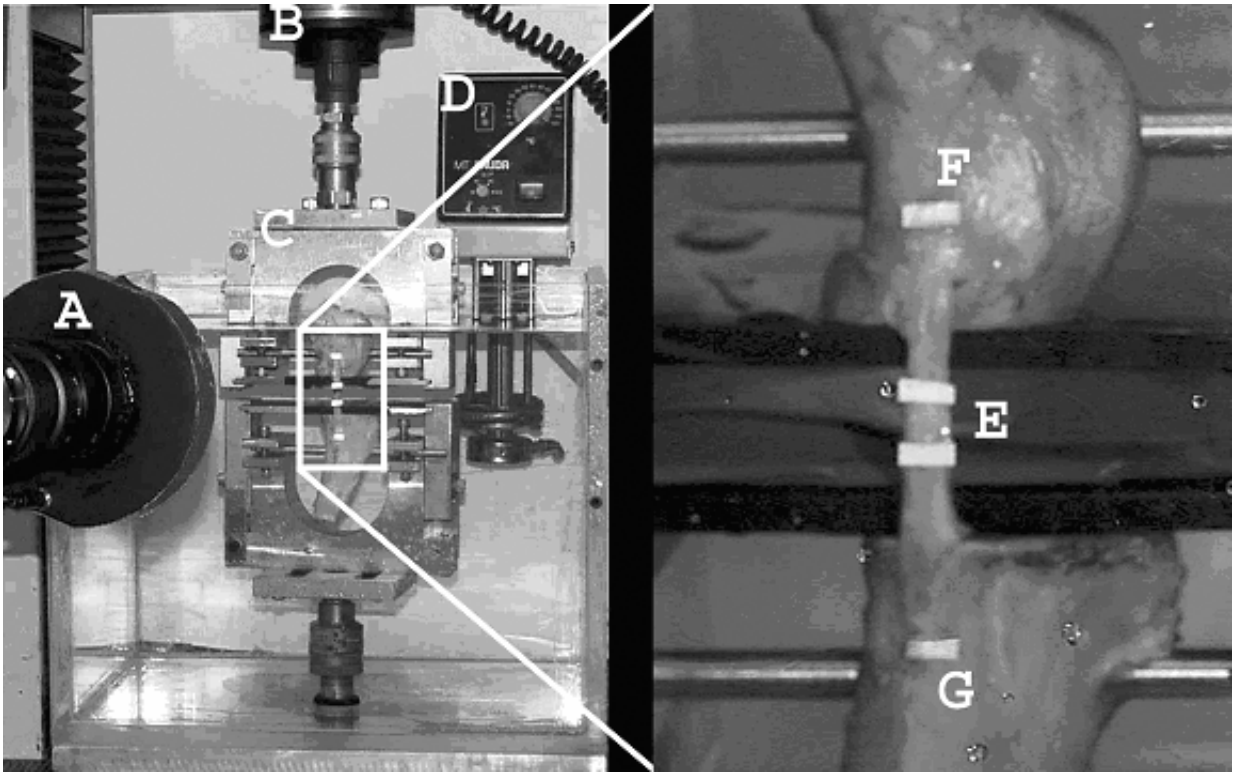

Figure 13 Photograph of an FMTC mounted on a materials testing machine. A) Video Camera B) Load cell C) Clamp-specimen construct D) water bath heater E) reflective markers on the midsubstance of the MCL F) Femur G) Tibia (printed with permission from [1]).

Each FMTC underwent a stress relaxation test whereby specimens were elongated from 0 to 3 mm at 10 mm/min and held for a period of 60 minutes (Figure 14). The time until peak load was t_0 = 18.4 seconds. The loading rate was chosen to avoid potential experimental errors associated with fast strain rates (i.e. overshoot, vibrations, and inaccurate measurements of tissue strain) [36]. Thus, the strain-time curve was linear to t_0 and constant for $t>t_0$. The total percentage of stress relaxation was defined as the difference between the peak stress at t_0 and the stress measured at the end of the test, normalized by the peak stress, and multiplied by 100. The nonlinear stress-strain and stress-time curves were obtained from the loading and relaxation phases of this test. A second test was performed to measure the cyclic stress relaxation behavior

of the MCL. In this test, each FMTC was subjected to 10 cycles of elongation between 2 and 3 mm at 10 mm/min and the corresponding peak stresses were recorded and utilized for validation (Figure 15). Prior to each test, specimens were held at a zero-load position and allowed to equilibrate within the saline bath for one hour.

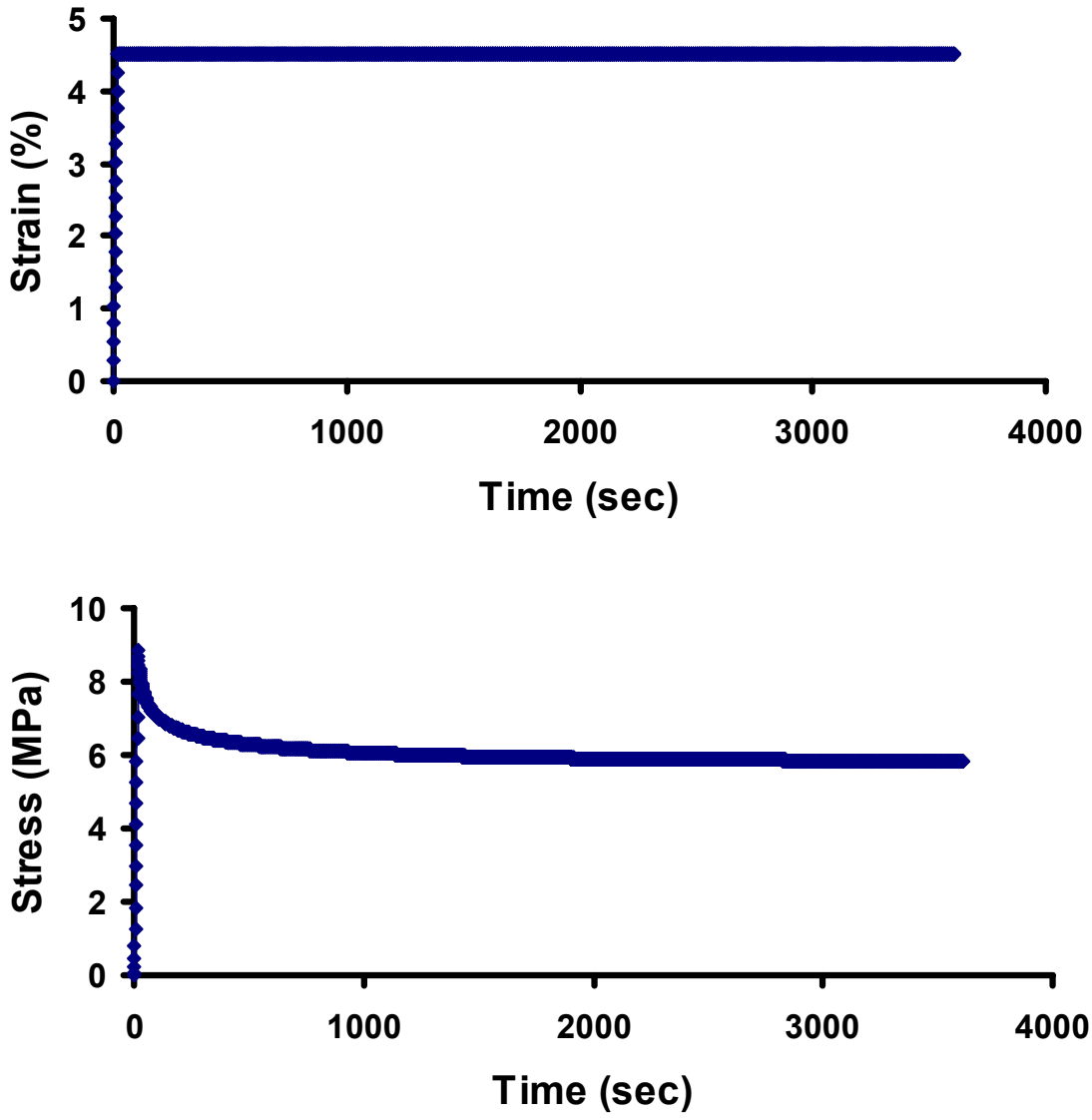

Figure 14 Strain and stress data versus time depicting a typical static stress relaxation test.

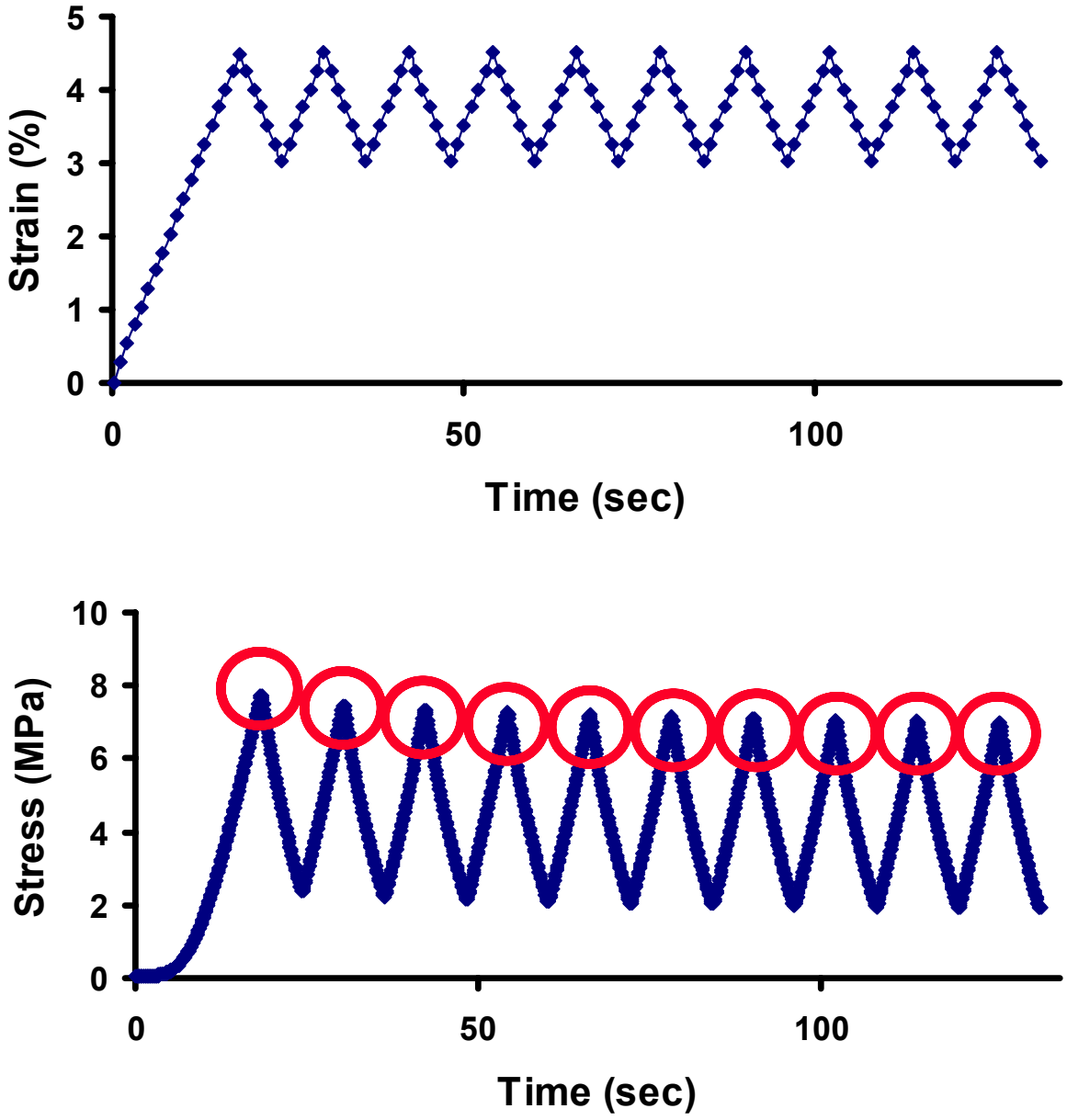

Figure 15 Strain and stress data versus time depicting a typical cyclic stress relaxation test. The circled peaks emphasize that these data were used for validation.

5.4 DYNAMIC MECHANICAL TESTING

For the dynamic mechanical test, six rabbit MCLs were isolated from the insertion sites of the knees. The geometry was standardized by cutting the ligaments into a dog bone shape with a length to width ratio of 6.8 ± 0.8 (width 1.6 ± 0.2 mm). The specimens were fixed in custom made soft tissue clamps and mounted on a laser micrometer system. Measurements were taken in 3 locations along the length of the tissue sample and averaged for stress calculations. Then the tissue sample-clamp construct was mounted to an Enduratec™ (Elf 3200) testing machine (Figure 16). Reflective markers were placed on the tissue sample to track strain using a Motion Analysis™ system. A heated saline drip was utilized to hydrate the tissue sample and maintain temperature at a constant 37ºC. The tissue sample was aligned along the loading axis using an x-y table and then was left unloaded for 30 minutes to acclimate. Next, a 0.5 MPa pre-stress was placed on the ligament and the ligament was elongated to a displacement of 0.5 mm while strain was recorded. Assuming a linear relationship between displacement and midsubstance strain, this initial elongation combined with the strain data collected during this elongation allowed for a determination of the displacement levels that corresponded to the strain levels of interest for this experiment. Immediately, the ligament was unloaded and given 30 minutes to reach equilibrium. A 0.5 MPa pre-stress was again placed on the ligament and this position served as the starting point for all subsequent tests. A 35 min stress relaxation test was performed by elongating the specimens to a predefined level of strain (5%). The stress relaxation reached a plateau after 35 minutes as the percent reduction in stress was less than 0.05% during the last 10 minutes of the test. Afterwards, the strain level was maintained and each specimen underwent sinusoidal perturbations (amplitude 0.25% strain) at frequencies of

0.01, 0.1, 1, 10, 25, and 50 Hz centered at 4.75% strain. Between tests at each frequency, the ligament was returned to the 5% strain level.

For each frequency, 10 cycles of stress versus time and strain versus time data were collected after the first 10 cycles of loading. These data were then curve-fit with the following equations:

$$\sigma(t) = y_\sigma + A_\sigma \, \mathrm{Sin}[\omega \, t + 2 \, \mathrm{Pi} \, \delta_\sigma] \tag{21}$$

$$\epsilon(t) = y_\epsilon + A_\epsilon \, \mathrm{Sin}[\omega \, t + 2 \, \mathrm{Pi} \, \delta_\epsilon] \tag{22}$$

where y is the mean value of stress or strain, A is the amplitude of the sinusoidal oscillations, ω is the testing angular frequency ($\omega = 2 \pi f$ where f is frequency), and δ is the phase shift of the data relative to 0. Subtracting $\delta_\sigma - \delta_\epsilon$ gives the phase difference, δ, between the stress versus time and the strain versus time data. The experimentally obtained spectrum of relaxation was obtained by plotting Tan δ versus frequency. The dynamic modulus was determined by A_σ / A_ϵ.

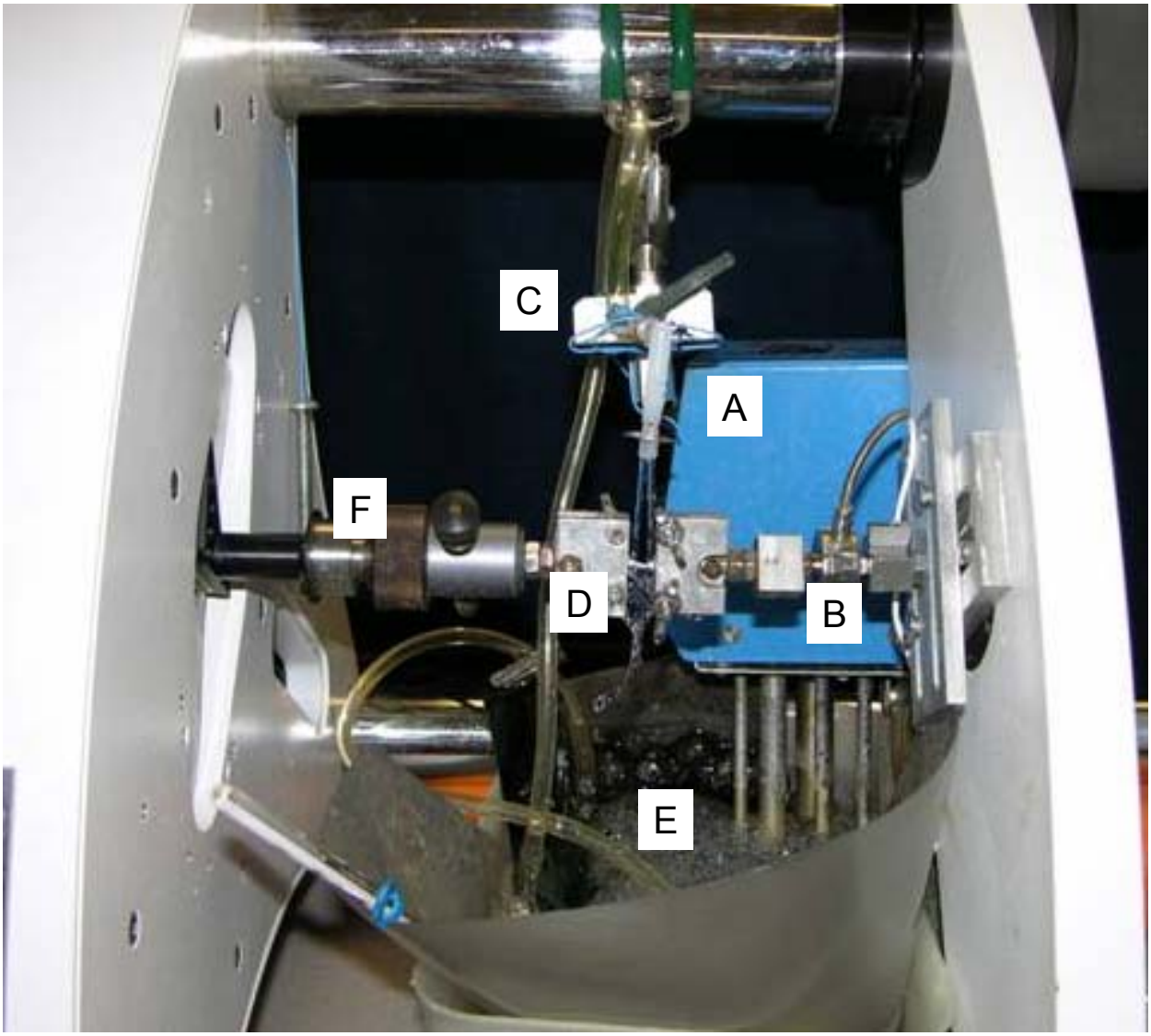

Figure 16 Photograph of a specimen mounted within an Enduratec™ Testing Machine. A) Water Heater B) Load Cell C) Saline Drip D) Specimen in soft tissue clamps E) Heated Saline Bath F) Actuator of the Enduratec™ Testing Machine.

.

6.0 THEORETICAL DEVELOPMENT AND EVALUATION

The main advantage to the assumption of a step-elongation is that it allows for separation of the elastic response and reduced relaxation function. Thus, one can obtain the constants of the QLV theory by separately curve-fitting each of these functions to the loading portion and the relaxation portion of a stress relaxation experiment. As discussed previously, this approach fails to account for the relaxation that is manifested during loading which leads to significantly erred estimates of constants. To truly describe the stress during loading and the subsequent relaxation, the elastic response and reduced relaxation function must be convoluted in the form of a convolution integral.

The new approach described in this dissertation is centered on curve-fitting the convoluted integral expression of the QLV theory to experimental data from a stress relaxation experiment. Thus, it is necessary to ensure that curve-fitting algorithms are global convergent (i.e. the solution is not dependent on the initial guess), and ensure that the approach is numerical stable (i.e. insensitive to systematic deviations between data and the theory as well as random noise). Finally, it is necessary to demonstrate that the approach is indeed accounting for the component of relaxation manifested during loading and the obtained constants can be validated by predicting the result of a separate experiment. The development of the new approach and its evaluation are presented in the following sections.

6.1 THE NEW STRAIN HISTORY APPROACH

A new analytical approach to determine the constants of the QLV theory was developed for the applicaton of modeling experimental data obtained using slow strain rates. The time dependent stress, σ, resulting from a constant strain rate γ between the times $0 < t < t_0$ can be written by substituting equations 20 and 12 into equation 2 (from section 2.4):

$$\sigma(t : 0 < \mathrm{t} < \mathrm{t}_0, \theta) = \frac{AB\gamma}{1 + C\ln(\tau_2 / \tau_1)} \int_0^t \{1 + \mathrm{C}(\mathrm{E}_1[(\mathrm{t} - \tau)/\tau_2] - \mathrm{E}_1[(t - \tau)/\tau_1])\} e^{\mathrm{B}\gamma\tau} \partial\tau \qquad (23)$$

where $\theta=\{A,B,C,\tau_1,\tau_2\}$.

Similarly, the subsequent stress relaxation from t_0 to $t = \infty$, can be described as

$$\sigma(t : \mathrm{t} \geq \mathrm{t}_0, \theta) = \frac{AB\gamma}{1 + C\ln(\tau_2 / \tau_1)} \int_0^{t_0} \{1 + \mathrm{C}(\mathrm{E}_1[(\mathrm{t} - \tau)/\tau_2] - \mathrm{E}_1[(t - \tau)/\tau_1])\} e^{\mathrm{B}\gamma\tau} \partial\tau \qquad (24)$$

The loading portion of the experimental data was defined as (t_i,$\mathbf{R_i}$), from $0 < t_i < t_0$ and the relaxation data as (t_i,$\mathbf{S_i}$), from t_0 to $t = \infty$. Thus, the sums of squares difference between the experimentally obtained data and the theory can be expressed as:

$$f(\theta) = \sum_i \left[\mathbf{R_i} - \sigma(t_i : 0 < t_i < t_0, \theta)\right]^2 \qquad (25)$$

and

$$g(\theta) = \sum_i \left[\mathbf{S_i} - \sigma(t_i : t_o \le t_i < t, \theta)\right]^2 \tag{26}$$

Since equations 25 and 26 are both functions of θ, the strain history approach minimizes these equations simultaneously. A nonlinear optimization algorithm, called the algorithm modified Levenberg-Marquardt algorithm that was used to minimize f(θ) + g(θ). The code for this algorithm was written using Mathematica (Wolfram Research, Inc. Champaign, IL), and was largely based on the algorithm outlined in the book *Numerical Recipes in C* [95].

This approach gives a direct fit of equations 23 and 24 to the experimental data with no modification of the theory or normalization of the data. Assuming that the theory provides a perfect Gaussian curve-fit of the data and a global minimum of f(θ) + g(θ) can be uniquely determined, the constants obtained that describe the instantaneous elastic response (A and B) and the spectrum of relaxation (C, τ_1, and τ_2) would be those obtained if a true step-elongation were to have been applied. This is because the actual strain history can be well approximated at slow extension rates.

It was found that constants A and τ_1 became significantly correlated as loading time increases. Since constant A is not required to describe the reduced relaxation following ramping at a constant strain rate [57], it was held fixed for each individual regression analysis. Its value was determined by curve-fitting equation 20 to the ramping portion of the experimental data. This is further justified by previous work which has shown that the stress-strain curves of ligaments are insensitive to strain rates ranging over 4 decades [137].

To provide an example of the correlation between constants A and τ_1, we selected a specimen at random from our preliminary analyses and increased constant A by 2.5%, 5%, and

10% of the value used in the original analysis. We based the percentage increase on the results reported in Woo et al., 1990, where the magnitude of mean stress at 3.5% strain varied by no more than 10% for specimens ramped at an extension rate similar to ours versus those ramped 3 orders of magnitude faster [137]. Table 2 demonstrates the resulting changes in each of the other constants in terms of percentage of their original value. Positive values indicated an increase of that constant, and negative values indicate a decrease for that constant. It should be noted that increasing constant A has the effect of decreasing constant τ_1 on the same order. More importantly, a 17% decrease of constant τ_1 was equivalent to decreasing τ_1 from 0.63 sec to only 0.52 sec.

Table 2 Percent differences of each constant when the value for constant A is increased.

% Increase of Constant A	B	C	τ_1	τ_2
2.5	-0.9%	-0.1%	-4.2%	0.2%
5	-1.8%	-0.2%	-8.4%	0.4%
10	-3.5%	-0.4%	-17.3%	0.7%

6.2 EVALUATION OF THE STRAIN HISTORY APPROACH

6.2.1 Effect of Initial Guess

Using a rabbit specimen, the FMTC was mounted onto customized clamps in an Instron™ testing machine and tested in a saline bath at 32° C as describe in previous sections. A rabbit was utilized for this analysis because the experimental time required to reach a platue in stress relaxation is roughly half as long compared to that of the goat. Thus, the number of data points and computation time required to perform the analysis was reduced significantly. A stress relaxation test was performed by elongating the FMTC to 1.5 mm (≈5% strain) and holding the strain constant for 25 minutes. Midsubstance strain was measured using a Motion Analysis™ system with reflective tape markers. The strain rate during the loading portion of the test was 0.45 %/sec (mean ± SD) and the time until the peak load was 9.3 sec. The constants of the QLV theory were determined using the strain history approach whereby the nonlinear regression algorithm was initiated with 100 different guesses. The average of the residuals for each guess was required to be within 30% of the average experimental stresses over the entire experiment. Further, the ranges of valid guesses for the constants were limited to a range of values (Table 3). These conditions forced each guess to provide a reasonable estimation of the experimental data.

Table 3 Range of values utilized to determine an initial guess. Note: Constant A is determined prior to this analysis as described in section 6.1. Its value was 2.52 MPa for this analysis.

B	C	τ_1 (sec)	τ_2 (sec)
10 - 100	0.01 - 0.25	0.0001 - 1	10 - 10000

For each initial guess, a coefficient of variation was computed for the obtained solution by dividing the standard deviations for each constant by the mean value and multiplying by 100. The algorithm was considered globally convergent if a coefficient of variation less than 2% was achieved. If the coefficient of variation was larger than 2%, that would suggest that the algorithm is sensitive to the initial guess. Thus, there would be less confidence that the solutions obtained from an individual regression analysis were meaningful since a different initial guess may result in a completely different solution.

Experimentally, the specimen stress relaxed by 17.2% following ramping to a peak stress of 21.5 MPa. The relaxation was considered to have reached a plateau after 25 minutes as there was no measurable stress relaxation during the last 10 minutes of the test. Regardless of the initial guess, the model fit the data well with R^2 values consistently measuring 0.996. This corresponded with the algorithm consistently converging to the same minimum χ^2 value of 8.33342 for each initial guess. The algorithm also converged to the same solution within a small variance. Below, Table 4 shows 7 of the initial guesses utilized and Table 5 shows the solution to those guesses. Finally, Table 6 shows the means, standard deviations, and coefficient of variation for all 100 solutions.

Table 4 Seven initial guesses utilized in the analysis.

Guess	B	C	τ_1 (sec)	τ_2 (sec)	Initial χ^2
1	60.0	0.062	0.003	143	6345.37
2	65.2	0.155	0.256	1321	3874.82
3	65.6	0.228	0.901	286	3463.54
4	54.0	0.067	0.396	1745	11628.50
5	67.4	0.156	0.252	4059	16879.60
6	55.2	0.085	0.715	1469	10236.80
7	62.4	0.101	0.989	7805	18026.60

Table 5 Seven solutions for the initial guesses in Table 4.

Solution	B	C	τ_1 (sec)	τ_2 (sec)	Final χ^2
1	54.9	0.047	0.319	240	8.33
2	54.9	0.047	0.319	240	8.33
3	54.9	0.047	0.319	240	8.33
4	54.9	0.047	0.319	240	8.33
5	54.9	0.047	0.319	240	8.33
6	54.9	0.047	0.319	240	8.33
7	54.9	0.047	0.319	240	8.33

Table 6 Means, standard deviations, coefficient of variations for all 100 initial guesses.

Solution	B	C	τ_1 (sec)	τ_2 (sec)	Final χ^2
mean	54.9	0.047	0.319	240	8.33
SD	0.0	0.000	0.000	0	0.00
CV	1.95E-06	4.84E-06	9.51E-05	9.15E-06	2.3E-16

Overflow errors were observed for 2 of the initial guesses. In other words a calculation was attempted for which exceeded the range of machine precision (Max: $1.920224672692356585420469060 6*10^{646456887}$:

Min: $5.207723940958923854615605332 8*10^{-646456888}$). The initial χ^2 values for these guesses where both greater than 30000 and therefore considered unreasonable. Overall, these data demonstrate that the strain history approach converges to the same solution for a broad range of initial guesses. Thus, the algorithm consistently converged to a unique solution which was assumed to be the global minimum.

6.2.2 Assessment of Numerical Stability

Further analysis of this approach showed that the theory did not provide a perfect Gaussian curve-fit to the experimental data. Thus, it was necessary to assess the variability of constants that may result from systematic deviations between the model and the experimental data, experimental noise, and numerical instabilities. A bootstrapping procedure was utilized to determine the sensitivity of the constants to systematic deviation between the theory and experimental data. To obtain the experimental data for this analysis, femur-MCL-tibia

complexes (N=6) were prepared from goat knees that had underwent a sham operation for a separate experiment [6]. Using a laser micrometer system, the cross-sectional area of the MCL was measured. Each FMTC was then mounted onto customized clamps in an Instron^{TM} testing machine and tested in a saline bath at 32° C. A stress relaxation test was performed by elongating the FMTC to 3 mm (≈5% strain) and holding the strain constant for 60 minutes. Midsubstance strain was measured using a Motion Analysis^{TM} system with reflective tape markers. The average strain rate during the loading portion of the test was 0.15± 0.06 %/sec (mean ± SD) and the time until the peak load was 18.4 sec. Following 1 hour of recovery, a second test was performed to measure the cyclic stress relaxation behavior of the MCL. In this test, each FMTC was subjected to 10 cycles of elongation between 2 and 3 mm at 10 mm/min and the resulting stress response was recorded. Data was collected rate of 5 Hertz.

This dissertation utilized a bootstrapping analysis that was previously described by Yin et al. [143]. First, the data from each specimen was curve-fit individually using the strain history approach. Residual plots for each specimen were then curve-fit with a polynomial function to obtain a pool of curves representing systematic error. Taking the difference between the systematic error curves and the residuals allowed for a random noise distribution for each specimen to be obtained. Finally, a randomly selected systematic error curve and random error distribution were added to predicted stresses that were obtained by curve-fitting the theory to averaged experimental data. This created a set of data whose systematic error and random noise distributions were representative of those that could be observed experimentally. Constants A, B, C, τ_1, and τ_2 for this new data set were obtained using the strain history approach. One hundred new data sets were generated using this methodology. A coefficient of variation was calculated for each constant to assess the sensitivity of the new approach.

The coefficient of variation was based on 95% confidence intervals as the data did not follow a normal distribution. Thus, the formula was (upper bound- the median)/the median*100, for each constant. The algorithm was considered numerically stable if this coefficient of variation less than 2% was achieved for each constant. If the coefficient of variation was large (ex. > 2%) for a particular constant, then that constant is sensitive to systematic deviations between the model and the experimental data, experimental noise, and numerical instabilities. Thus, there would be less confidence that the solutions obtained from an individual regression analysis were meaningful since a data set with a slightly different distribution of random noise or systematic error may result in a completely different solution.

Six goat specimens were utilized for this analysis. The specimens stress relaxed by 32 ± 11% following ramping to a peak stress of 15.3 ± 5.40 MPa. The relaxation was considered to have reached a plateau after 60 minutes as the stress relaxed by only 0.25 ± 0.26% during the last 10 minutes of the test. The model fit the data for each specimen well with R^2 values measuring 0.993 ± 0.006 (Figure 17). Typical systematic and random error plots utilized in the Bootstrapping analysis are show in Figures 18 and 19. The bootstrapping analysis showed that none of the constants displayed large variability as measured by the coefficient of variation (Table 7). 95% confidence intervals were utilized to express these data as they did not follow a normal distribution.

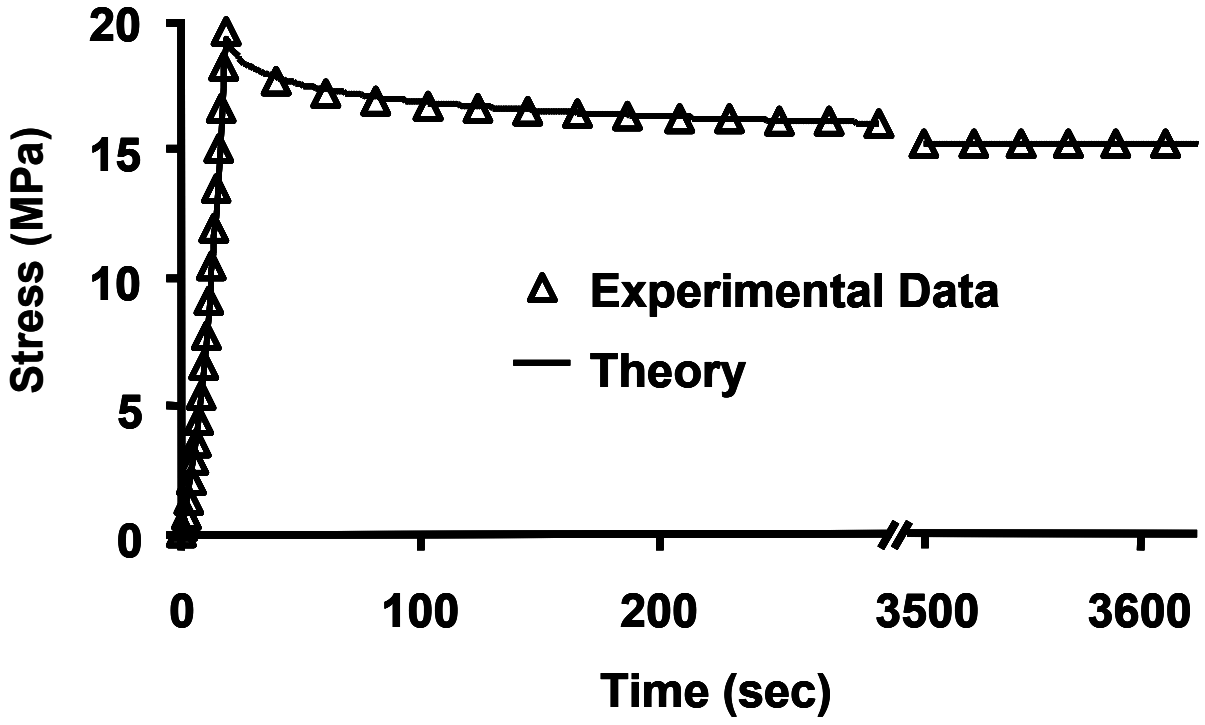

Figure 17 A typical fit to experimental data using the strain history approach (printed with permission from [4]).

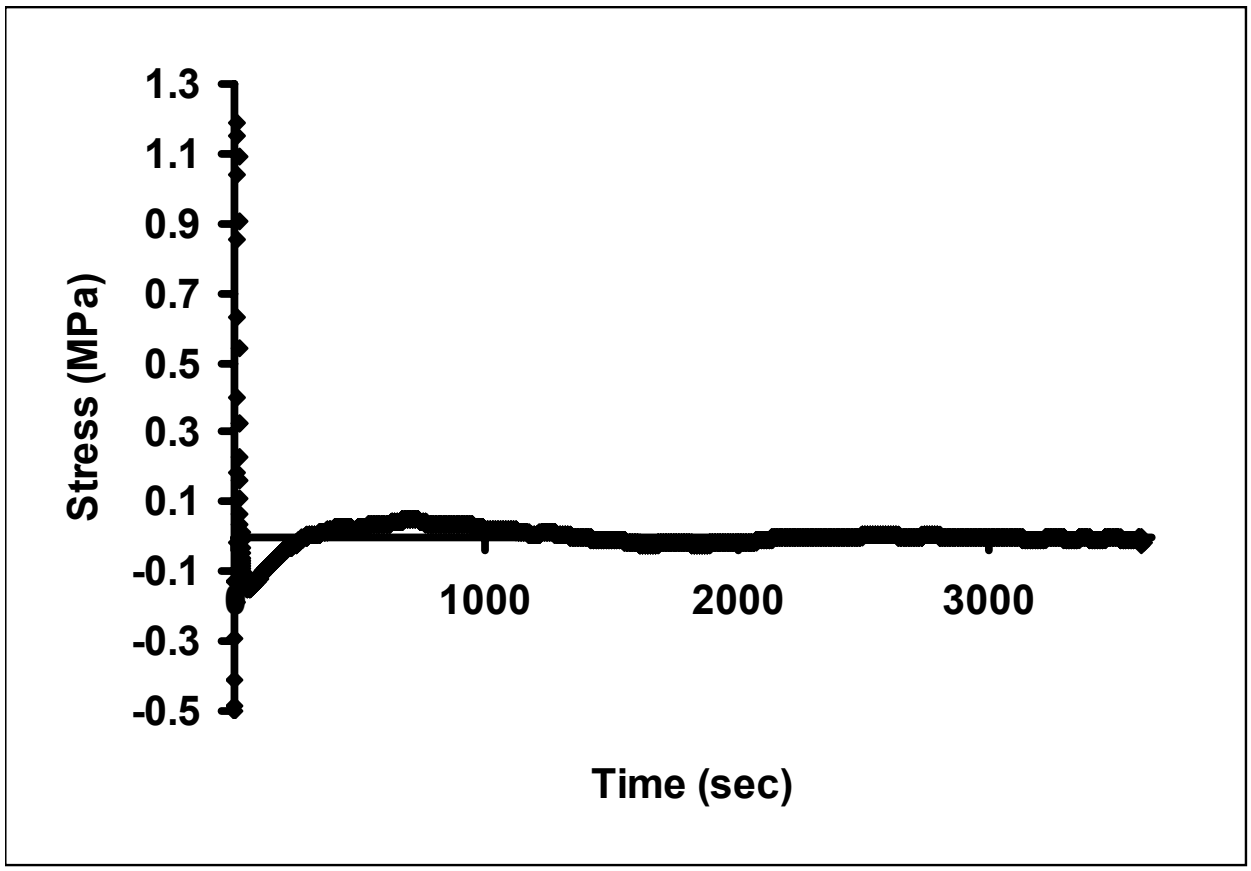

Figure 18 A typical residual plot demonstrating systematic deviations between the model prediction and experimental data (printed with permission from [4]).

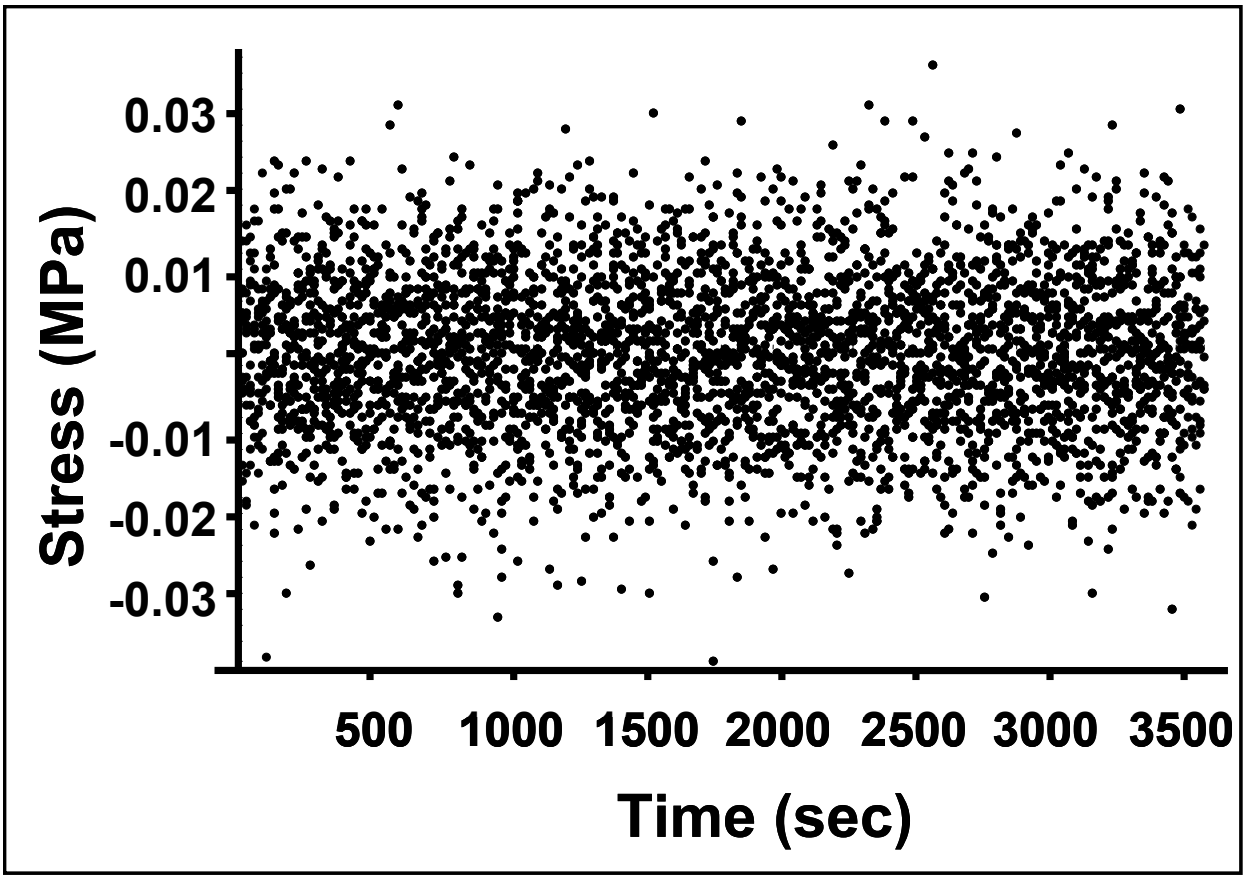

Figure 19 A typical random error plot with distribution 0 ± 0.00874 (mean ± SD) (printed with permission from [4]).

Table 7 95% confidence intervals (upper and lower bounds) of the solutions for the 100 bootstrapped replicates (printed with permission from [4]).

A	B	C	τ_1 (sec)	τ_2 (sec)
5.8	47.2	0.072	0.62	1469
6.00	48.2	0.072	0.63	1488

In terms of the constants describing the instantaneous elastic response, all values for constant A were within 1.7% of its median value. For constant B, the strain history approach determined its value within approximately 1% of the median value. In terms of the constants describing the reduced relaxation function, confidence intervals for constant C were within 1% of the median values. Similarly, the confidence intervals for constants τ_1 and τ_2 were also determined values to be within 1% of their median values, respectively. Thus, this approach was deemed insensitive to systematic deviation between the theory and experimental data and experimental noise.

6.2.3 Comparison to Previous Approach

The experimental data obtained from the same 6 specimens utilized in the bootstrapping analysis were utilized to obtain the constants of the QLV theory with another approach. The instantaneous assumption approach as utilized by Woo et al. (1981) assumes that the ramping phase of the stress relaxation tests occurred instantaneously [121]. Therefore, G(t) and $\sigma^e(\varepsilon)$ are assumed to be separable functions. Constants A and B can be obtained by fitting equation 20 to the experimentally obtained stress-strain curve, and constants C, τ_1, and τ_2 can be obtained by fitting equation 12 to the time shifted relaxation data normalized by the peak stress at t_0 where t_0 is set to t=0. Thus, this approach does not account for relaxation that occurred during ramping which may result in increasingly erred estimates of constants as loading times increase [23]. For all 6 specimens, the experimental data was curve-fit using both approaches and the obtained constants were compared. A nonparameteric two-tailed Wilcoxon sign-rank test and z-score statistic were used for statistical comparison and to calculate p-values [101]. Significance was set at $p<0.05$.

In terms of the solutions obtained from curve-fits of each individual specimen's data (Table 8), constant B was determined to be significantly greater when obtained using the strain history approach (53.1 ± 27.0; mean ± SD) compared to the instantaneous assumption approach (49.8 ± 25.4), indicating a more nonlinear instantaneous elastic response ($p<0.05$; Figure 20).

Table 8 Constants describing the reduced relaxation function obtained by curve-fitting individual specimens using the strain history and instantaneous assumption approaches. * significant difference between the two approaches ($p<0.05$) **(printed with permission from [4])**.

	A (MPa)		B	
Specimen #	Strain History	Inst. Assum.	Strain History	Inst. Assum.
997	6.75	6.75	73.5	61.8
965	3.04	3.04	78.5	76.3
422	2.75	2.75	76.8	75.5
41	7.19	7.19	41.6	38.5
26	32.86	32.86	13.9	13.5
19	5.65	5.65	34.0	33.1
Mean ± SD	9.7 ± 11.5	9.7 ± 11.5	53.1 ± 27.0*	49.8 ± 25.4

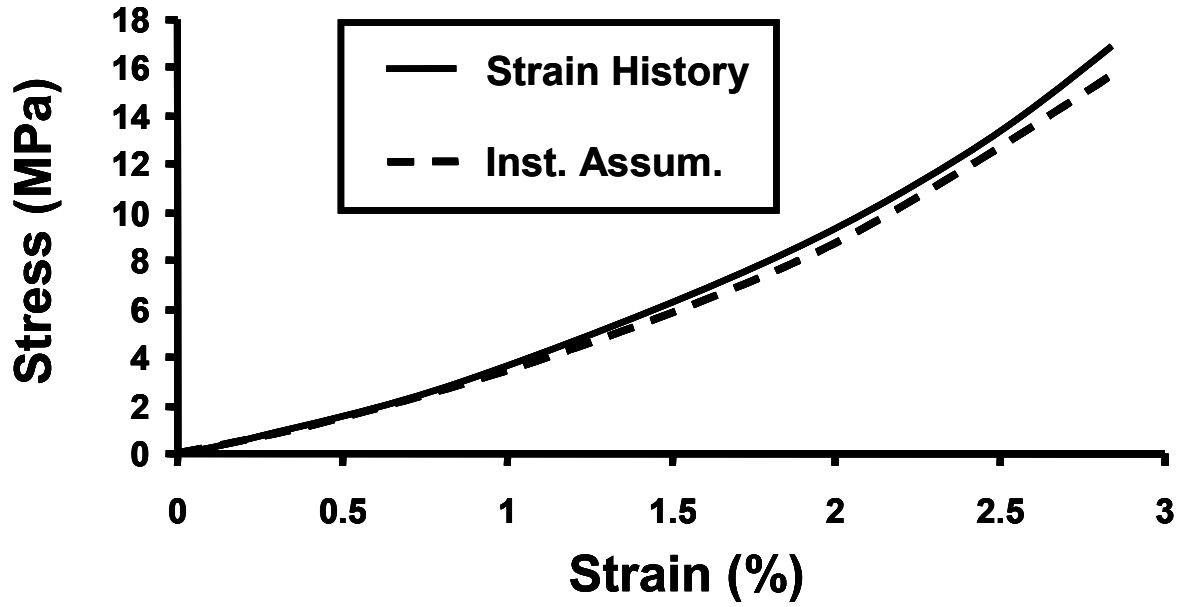

Figure 20 The elastic response as determined using the instantaneous assumption approach and the strain history approach.

For the constants describing the reduced relaxation function (Table 9), the strain history approach consistently estimated significantly higher values for constant C (0.089 ± 0.057 versus 0.076 ± 0.053) for each individual specimen ($p<0.05$). Estimates for constant τ_1 obtained using the strain history approach (0.54 ± 0.15 sec) were an order of magnitude lower than those obtained using the instantaneous assumption approach (2.13 ± 0.98 sec; $p<0.05$). Further, estimates for constant τ_2 were also significantly lower when determined with the strain history approach (1602 ± 581 sec versus 2222 ± 821 sec; $p<0.05$). Thus, it can be seen that the strain history approach consistently predicts a reduced relaxation function with a greater percentage of relaxation, steeper initial slope, and earlier time to reach equilibrium (Figure 21).

Table 9 Constants describing the reduced relaxation function obtained by curve-fitting individual specimens using the strain history and instantaneous assumption approaches. * significant difference between the two approaches ($p<0.05$) (printed with permission from [4]).

	C		τ_1 (sec)		τ_2 (sec)	
Specimen #	Strain History	Inst. Assum.	Strain History	Inst. Assum.	Strain History	Inst. Assum.
997	0.204	0.183	0.30	3.29	1972	2451
965	0.055	0.047	0.64	2.07	1997	2685
422	0.071	0.058	0.63	1.85	896	1163
41	0.084	0.073	0.54	2.97	2248	3030
26	0.066	0.050	0.44	0.51	1587	2786
19	0.056	0.045	0.70	2.09	910	1218
Mean ± SD	0.089 ± 0.057*	0.076 ± 0.053	0.54 ± 0.15*	2.13 ± 0.98	1602 ± 581*	2222 ± 821

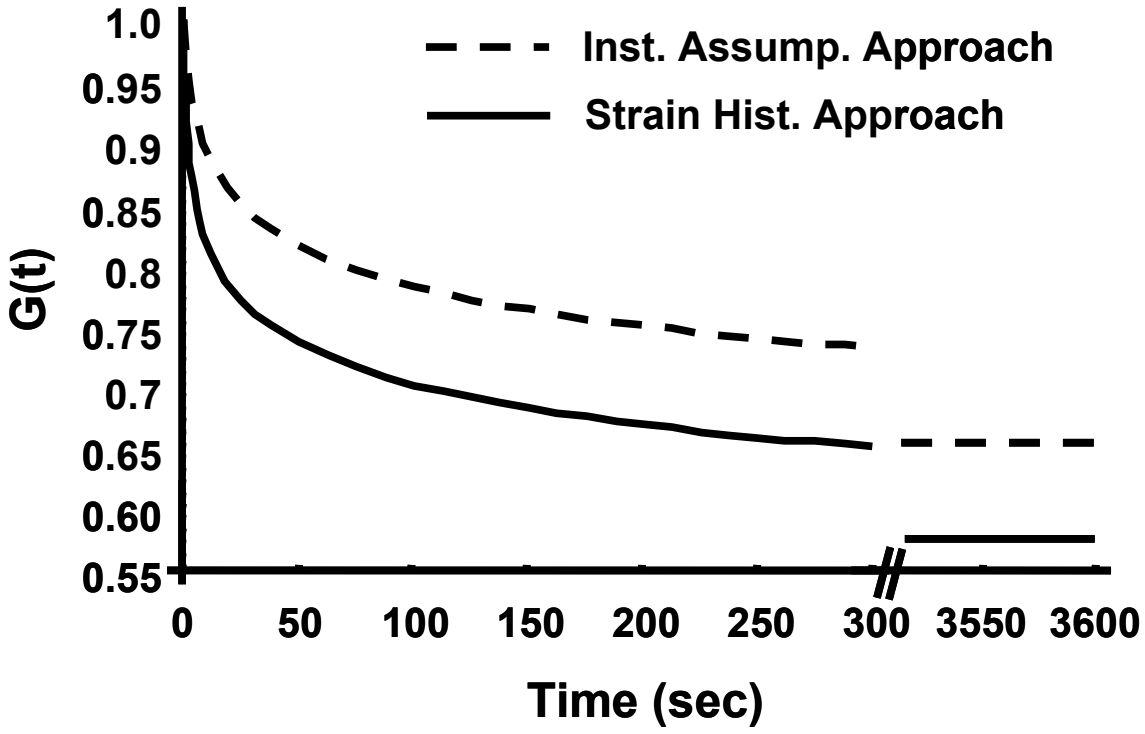

Figure 21 The reduced relaxation function as determined using the instantaneous assumption approach and the strain history approach (printed with permission from [4]).

6.2.4 Validation: Cyclic Stress Relaxation

To determine the predictability of QLV theory using the constants obtained from the strain history approach, the obtained constants A, B, C, τ_1, and τ_2 based on the experimental data from the original 60 minute static stress relaxation test were separately substituted into equation 2 to obtain the specific equations describing the stress response of the goat FMTC for each specimen. Using a previously described approximated strain-time history [121],

$$\varepsilon = \alpha t \qquad 0 < t < t_0 \tag{27}$$

$$\varepsilon = \varepsilon^{+} - \varepsilon^{-} \cos[\omega(t - t_0)] \qquad t_o < t < \infty \tag{28}$$

where α is the specimen's strain rate, determined experimentally, ω is the angular frequency of the cyclic stress relaxation experiment, and:

$$\varepsilon^{+} = \frac{\varepsilon_1 + \varepsilon_0}{2} \tag{29}$$

$$\varepsilon^{-} = \frac{\varepsilon_1 - \varepsilon_0}{2} \tag{30}$$

equation 2 can be solved by direct integration for the history-dependent peak stresses. Specifically, the peak stresses (t=t1,t2 … etc.) for the first 8 cycles were calculated with the following times as upper limits to the integral. The times for the peak stresses are

$$t = t_n = t_0 + (2n)\frac{\pi}{\omega} \tag{31}$$

The peak stress obtained from equation 2 were then compared to those obtained experimentally. The percent difference between the experimentally obtained and theoretical obtained peak stresses were calculated by the formula (theory-experimental)/experimental*100. Constants were considered validated if predictions were within 15%.

The constants A, B, C, τ_1, and τ_2 obtained using the strain history approach could accurately describe the experimental data of the cyclic stress relaxation test for each specimen.

Error between the prediction and experimental data ranged from 0.2% to 2.9% for the best prediction (Figure 22) and 9.3% to 16.2% for the worst prediction (Figure 23). In general, the prediction of the initial peak stress was the most erred for all specimens. Nonetheless, the average error for this peak measured only 6.3 ± 6.0% across all specimens.

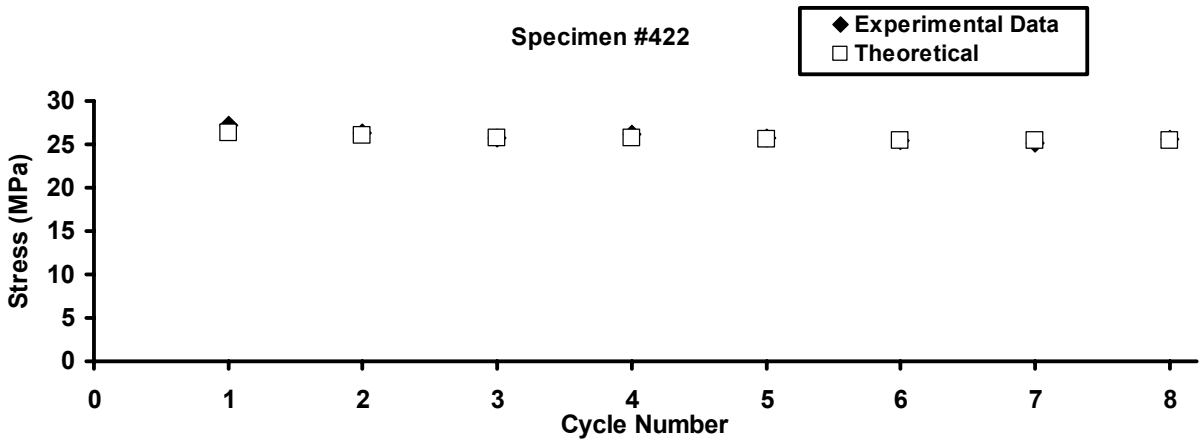

Figure 22 Prediction of the peak stresses of a cyclic loading history based on the constants obtained from the stress relaxation experiment using the strain history approach for individual specimens (Best Prediction) (printed with permission from [4]).

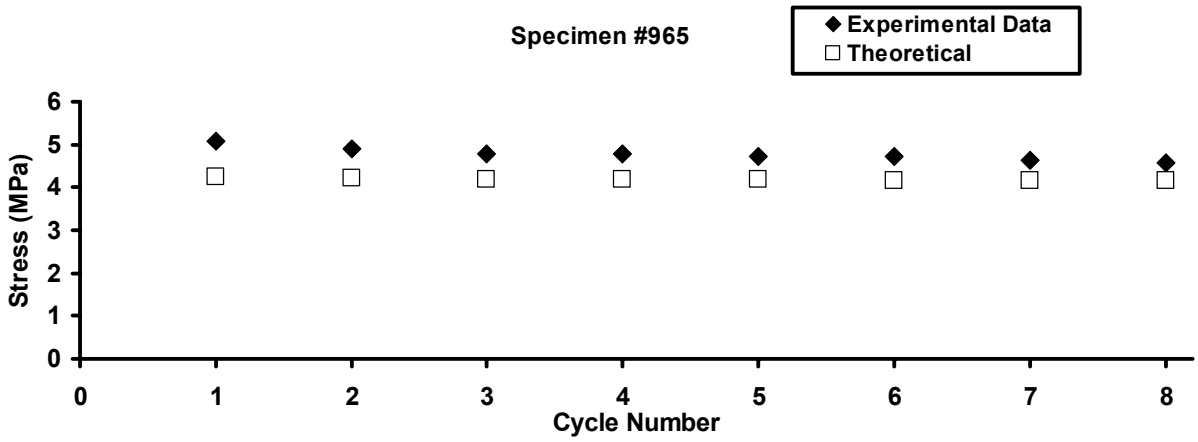

Figure 23 Prediction of the peak stresses of a cyclic loading history based on the constants obtained from the stress relaxation experiment using the strain history approach for individual specimens (Worst Prediction) (printed with permission from [4]).

7.0 APPLICATION OF THE STRAIN HISTORY APPROACH TO THE HEALING MCL

7.1 EXPERIMENTAL DESIGN

For Specific Aim 3, skeletally mature goats (N=6) were utilized. The right leg served as the healing group and the left leg served as the sham-operated controls. The experimental data obtained from a stress relaxation test for both groups was curve-fit using the strain history approach. To make statistical comparisons between the two groups, it was necessary to determine if the experimental data and obtained constants from individual specimens were normally distributed. As this portion of the dissertation utilized a paired approach, the normality of differences in the experimental data and obtained constants between individual paired samples were analyzed using a one sample Kolmogorov-Smirnov test [101]. Since a normal distribution was observed for all constants, a paired *t*-test was used for statistical comparisons [43]. The significance level was set at $p<0.05$.

7.2 EXPERIMENTAL RESULTS

When dissected, the MCLs in the control group appeared shiny, white and opaque, with well-defined edges. The healing MCLs, on the other hand, showed signs of an enlarged tissue mass at the original rupture site. Laser micrometer measurements confirmed gross observations, demonstrating that the cross-sectional area of the healing MCL (19.2 ± 5.3 mm^2) was almost 100% larger than for sham-operated controls (11.6 ± 1.9 mm^2; $p<0.05$).

During the loading phase of the stress relaxation test, tissue strain was found to increase linearly with time. Thus, the elongation rate of 10 mm/min was equivalent to a midsubstance strain rate, γ, of 0.26 ± 0.01 %/sec for healing specimens and 0.24 ± 0.01 %/sec for sham-operated controls. At the end of the loading phase, tissue strain was 4.7 ± 1.8% versus 4.4 ± 1.7%, respectively ($p>0.05$). The corresponding stress increased in a nonlinear fashion for both groups with the healing specimens measuring 4.4 ± 2.8 MPa, which was significantly lower than that of sham-operated controls (11.6 ± 5.8 MPa; $p<0.05$). The largest amount of stress relaxation occurred in the first 20 minutes (Figure 24). At 60 minutes, the total amount of stress relaxation was 49.0 ± 12.1% for healing MCLs versus 26.5 ± 8.1% for sham-operated controls ($p<0.05$). Curve-fits of the data of each individual specimen using the QLV theory were of good quality with R^2 values greater than 0.994 for both groups (Figure 25).

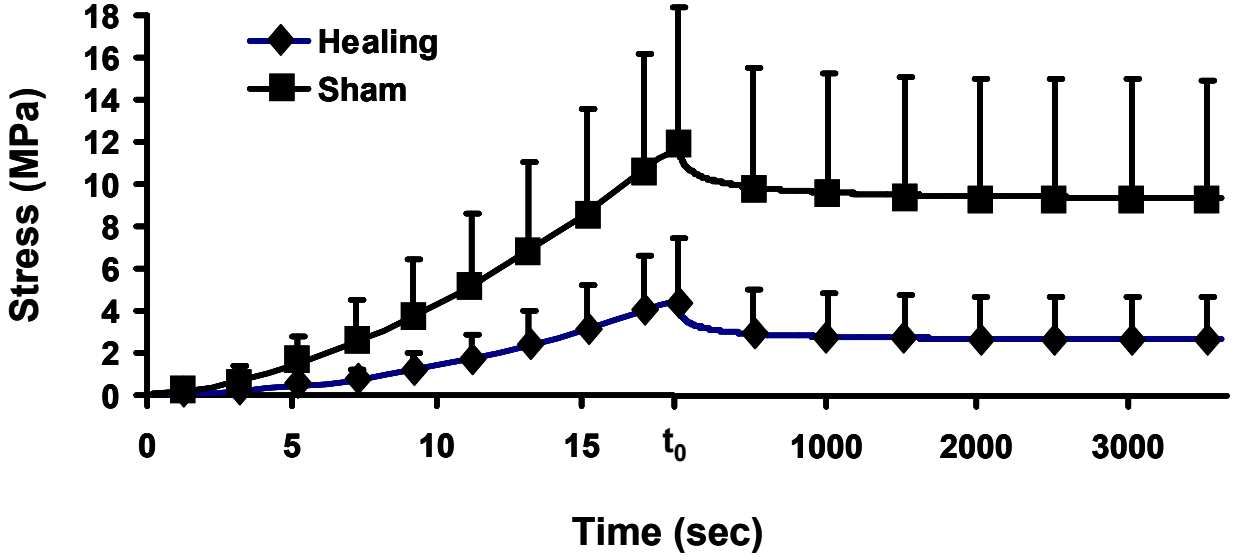

Figure 24 Experimental stress vs. time curves (mean ± SD) during the stress relaxation test for healing and sham-operated specimens. Note the time scale change at t0 = 18.4 sec separating the loading phase and relaxation phase of the experimental data (printed with permission from [5]).

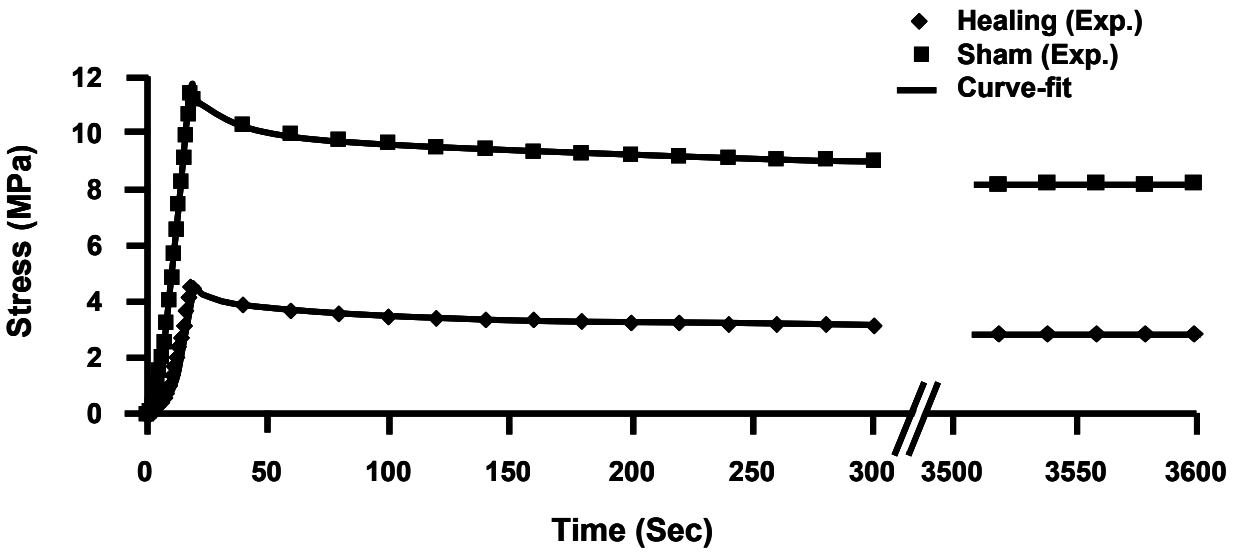

Figure 25 Typical curve-fitting of the experimental data with the QLV theory for a pair of specimens demonstrating an accurate description of these data by the theory. In this figure, the diamonds and squares represent the experimental data and the solid line is the curve-fit to these data (printed with permission from [5]).

7.3 ELASTIC RESPONSE

The constants describing the instantaneous elastic response for healing and sham-operated MCLs are shown in Table 10. The combination of constants A*B, i.e. the initial slope of the stress-strain curves, was greater for sham-operated controls compared to those for healing MCLs ($p<0.05$). Note that there were no statistical differences for constant A (0.7 ± 0.6 MPa versus 4.0 ± 4.2 MPa) or B (54.1 ± 18.9 versus 48.4 ± 23.1) between healing and sham-operated MCLs, respectively ($p>0.05$).

Table 10 Constants describing the instantaneous elastic response of the healing (n=6) and sham-operated MCLs (n=6). * indicates statistically significant differences between healing MCLs and sham operated controls (p<0.05) (printed with permission from [5]).

	A (MPa)		B		A*B (MPa)	
Specimen #	**Healing**	**Sham**	**Healing**	**Sham**	**Healing**	**Sham**
915	0.5	4.4	56.3	31.7	28.2	139.5
921	0.2	4.7	29.0	44.2	5.8	207.7
924	0.6	0.3	55.5	79.7	33.3	23.9
947	0.2	2.1	74.5	55.6	14.9	116.8
948	0.7	0.7	73.7	63.8	51.6	44.7
949	1.8	11.8	35.5	15.3	63.9	180.5
mean	0.7	4.0	54.1	48.4	32.94*	118.8
SD	0.6	4.2	18.9	23.1	21.9	73.0

7.4 REDUCED RELAXATION FUNCTION

The three constants describing the reduced relaxation function (C, τ_1, and τ_2) for the healing MCLs and sham-operated controls are detailed in Table 11. The dimensionless constant C was nearly 3 times greater for healing MCLs compared to sham-operated controls ($p<0.05$). Constant τ_2, on the other hand, was significantly smaller for healing MCLs measuring approximately 63% of that for sham-operated controls ($p<0.05$). No differences were found for time constant τ_1.

Table 11 Constants describing the reduced relaxation function of the healing (n=6) and sham-operated MCLs (n=6). * indicates statistically significant differences between healing MCLs and sham operated controls (p<0.05) (printed with permission from [5]).

	C		τ_1 (sec)		τ_2 (sec)	
Specimen #	**Healing**	**Sham**	**Healing**	**Sham**	**Healing**	**Sham**
915	0.112	0.073	0.58	0.73	1265	2002
921	0.380	0.098	1.65	0.67	1210	1385
924	0.207	0.039	0.52	1.96	1284	2440
947	0.260	0.096	0.82	0.69	1804	1627
948	0.113	0.068	0.61	0.58	1114	2152
949	0.134	0.037	0.60	0.72	939	1465
mean	0.201*	0.069	0.80	0.89	1269*	1845
SD	0.106	0.026	0.43	0.52	291	419

7.5 VALIDATION

In terms of validation of the constants using the data from the cyclic stress relaxation test, Figures 26 and 27 show that the average peak stresses of the theoretically predicted values closely match the average experimentally measured values for both the healing MCL and the sham-operated controls, respectively. For both groups, the theory predicted the initial peak stress most accurately, but the predictions tended to plateau more quickly when compared to the experimental data. However, the close agreement confirms the validity of the 5 constants for all specimens at the strain level utilized in this study.

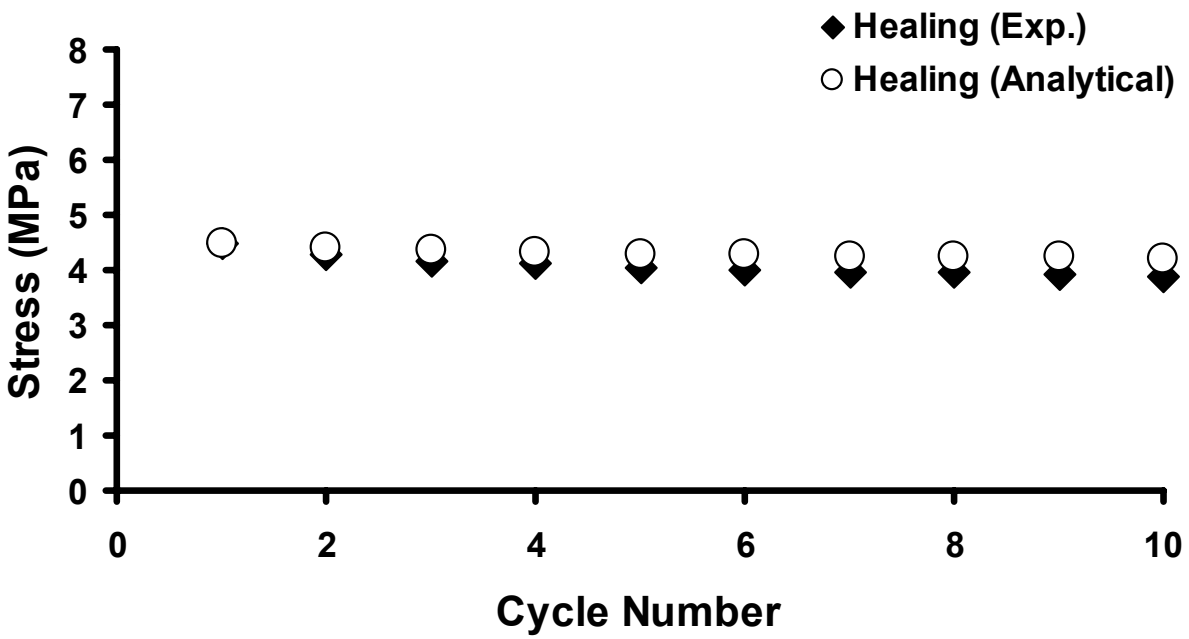

Figure 26 The average peak stresses of the theoretically predicted values versus the average experimentally measured values for the healing MCLs (printed with permission from [5]).

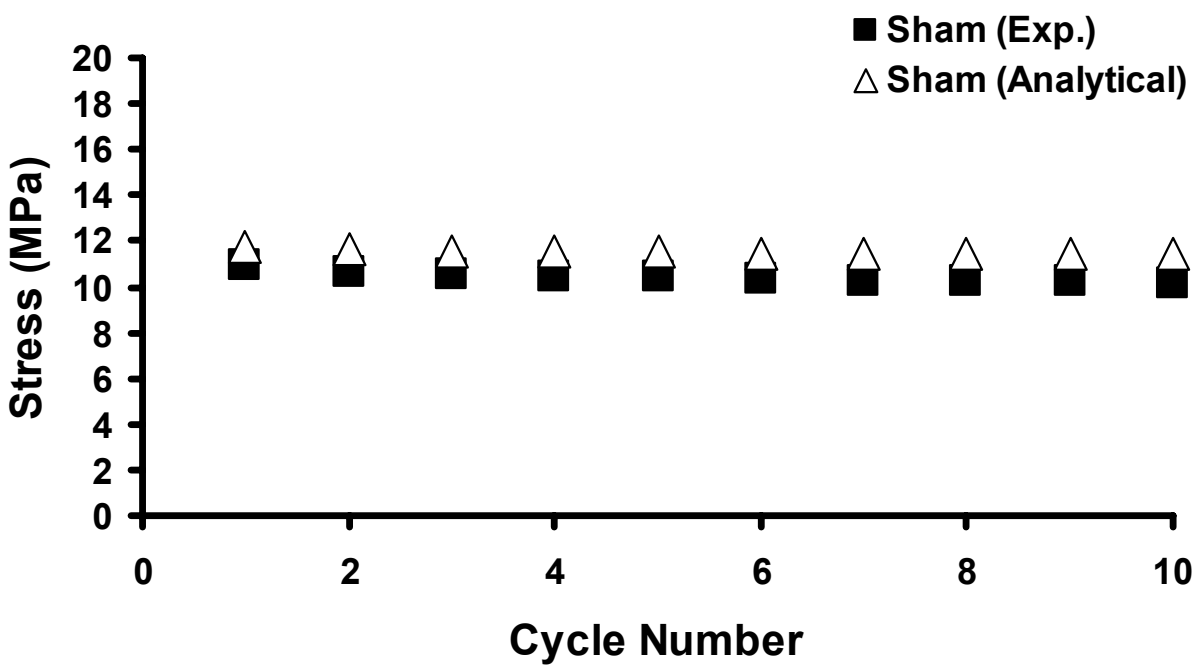

Figure 27 The average peak stresses of the theoretically predicted values versus the average experimentally measured values for the sham-operated controls (printed with permission from [5]).

8.0 DYNAMIC MECHANICAL TESTING

8.1 EXPERIMENTAL DESIGN

For Specific Aim 3, we wanted to assess whether the constants obtained utilizing the strain history approach can be used to determine the response of the MCL to sinusoidal loading, dynamic mechanical testing was performed. Utilizing sinusoidal strains of a small magnitude about an equilibrium value of strain allow for the application of linear viscoelastic theory. Details on the mathematical development are provided in Section 2.4.1.2. Thus, the spectrum of relaxation, i.e. Tan δ versus frequency, of a tissue can be experimentally determined [7, 20, 21, 44, 66, 94, 107, 142]. As the formulation of G(t) is based on linear viscoelastic theory, the experimental measures of Tan δ can be predicted from the results of a stress relaxation experiment [34]. As described in previous sections, a formula which describes the constant spectrum of relaxation has been written in terms of the constants C, τ_1, and τ_2:

$$\text{Tan}(\delta)=(C[\text{Tan}^{-1}(\omega\tau_2) - \text{Tan}^{-1}(\omega\tau_1)])/(1+1/C/2[\text{Ln}(1 + \omega^2\tau_2^2) - \text{Ln}(1 + \omega^2\tau_1^2)]) \quad (32)$$

Theoretically, the same constants obtained from a stress relaxation test of a tissue can also be utilized to describe its spectrum of relaxation, i.e. Tan(δ) versus frequency. Thus, the ability to infer the response of the MCL to harmonic oscillations based on the constants obtained from a static stress relaxation test can be assessed.

Using the experimental data from a stress relaxation test a previously described, the strain history approach was utilized to curve-fit the experimental data to obtain the constants of the QLV theory. These constants were then utilized in equation 32 to predict the spectrum of relaxation (i.e. Tan(δ) versus frequency). This prediction was compared to the actual experimentally determined spectrum of relaxation for the same specimens (Figure 28). An r^2 statistic was utilized computed based on the differences between the prediction and experimental data. Values greater than 0.8 suggests that the constants obtained using the strain history approach are predictive of the response of ligaments to harmonic oscillations.

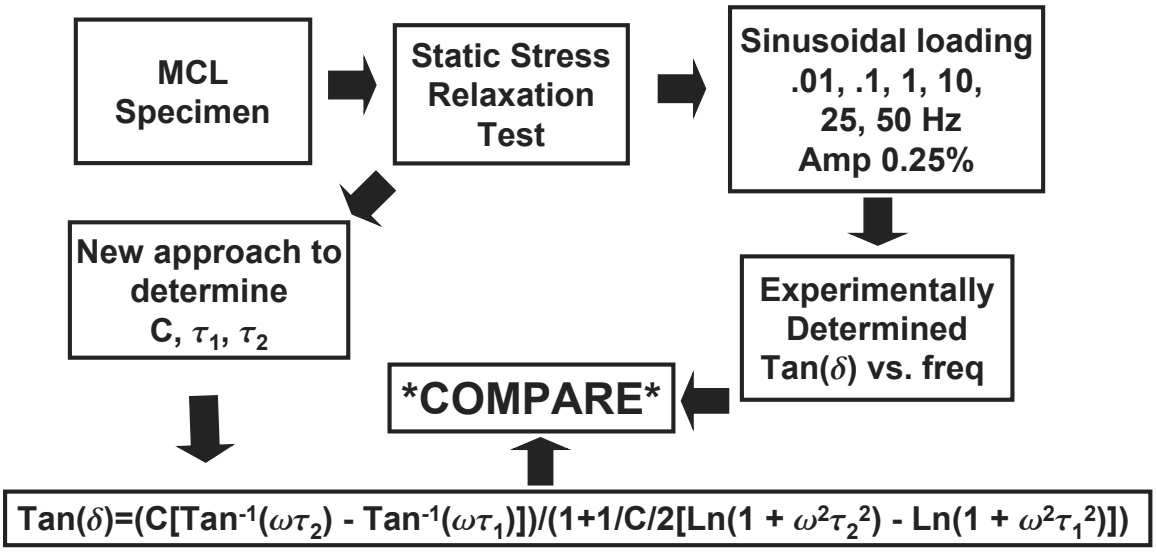

Figure 28 A flow chart displaying the comparison of experimental and theoretical results.

8.2 COMPARISON OF EXPERIMENTAL AND THEORETICAL RESULTS

The cross-sectional area of the 6 dog-bone shaped rabbit MCLs averaged 1.0 ± 0.3 mm^2. Specimens stress relaxed by 25 ± 3% following ramping to a peak stress of 13.4 ± 5.7 MPa. The relaxation was considered to have reached a plateau after 30 minutes as the stress relaxed by only 0.05 ± 0.35% during the last 10 minutes of the test. The model fit the static stress relaxation data well for each specimen well with R^2 values measuring 0.983 ± 0.005. The constants describing the reduced relaxation function are displayed in Table 12.

Table 12 Constants describing the elastic response and reduced relaxation function obtained by curve-fitting individual specimens using the strain history.

Specimen #	A (Mpa)	B	C	τ_1 (sec)	τ_2 (sec)
3176	4.3	18.9	0.050	0.28	1675
3696	4.5	23.4	0.069	0.33	647
3594	7.7	17.4	0.046	0.27	1139
3595	13.0	20.1	0.047	0.31	1151
3597	6.6	27.3	0.054	0.36	257
3349	8.3	21.2	0.054	0.32	758
Mean ± SD	7.4 ± 3.2	21.4 ± 3.6	0.053 ± 0.008	0.31 ± 0.04	938 ± 492

The Tan(δ) response and dynamic modulus to sinusoidal oscillations are shown in Figures 29 and 30, respectively. It can be seen that the rabbit MCL is relatively elastic for the frequencies tested as Tan(δ) is relatively close to zero. The experimentally obtained spectrum of relaxation is relatively constant in the range of 0.1 to 10 Hz. However, the specimens display more viscous behavior toward 0.01 Hz and 50 Hz as energy dissipation is 57% and 14% higher

than at 1 Hz, respectively. The dynamic modulus increased linearly with the logarithm of frequency between 0.01 to 50 Hz.

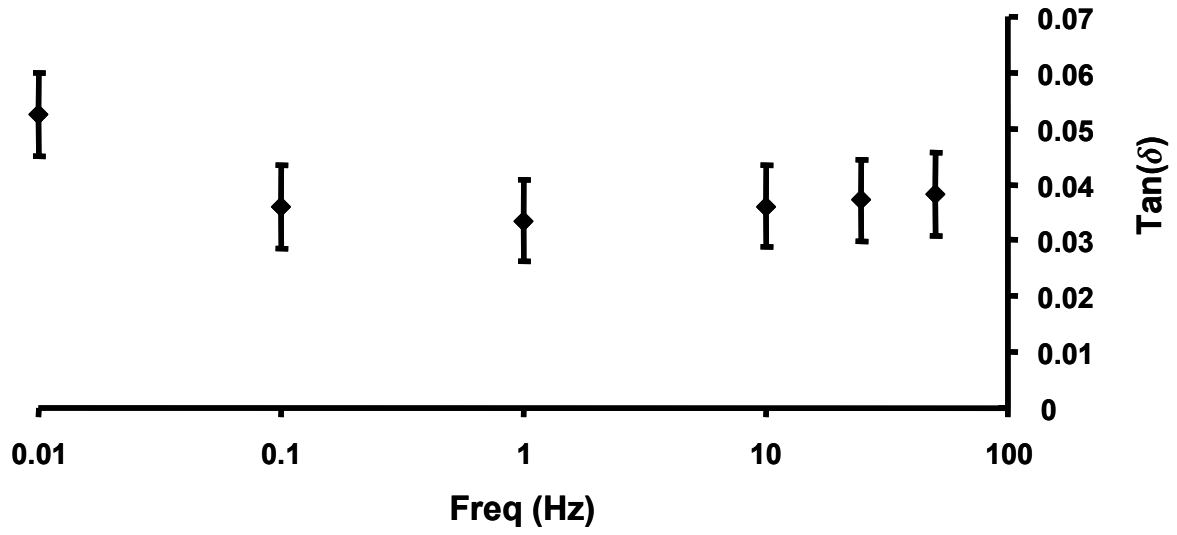

Figure 29 The experimentally obtained spectrum of relaxation for 6 rabbit MCLs.

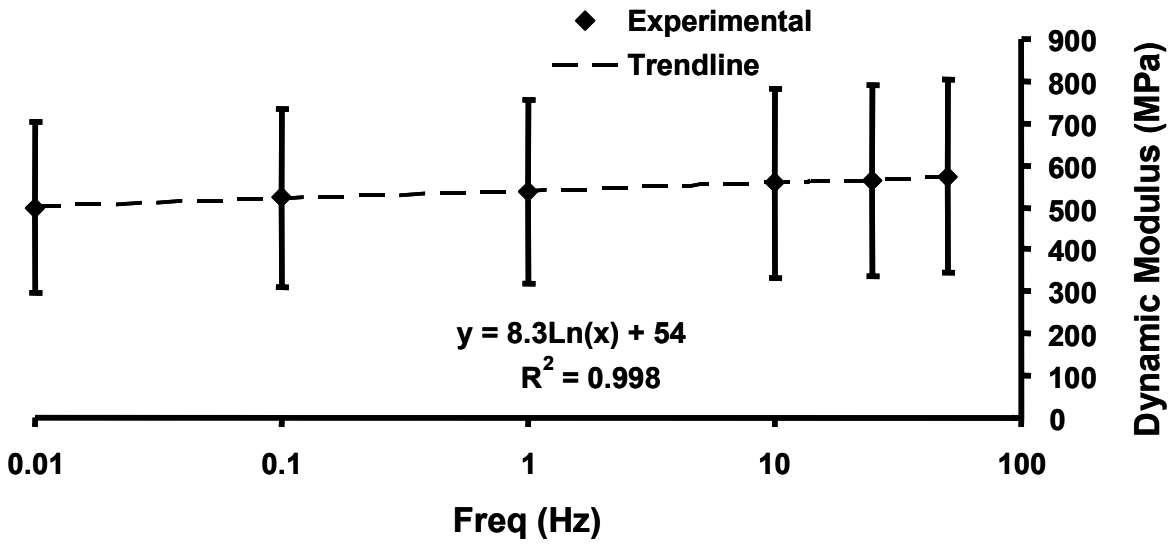

Figure 30 The experimental obtained dynamic modulus for 6 rabbit MCLs. Note that the data is linear on a logarithmic scale.

The theoretical prediction of the spectrum of relaxation based on the result of the static stress relaxation test are shown in Figure 31. At 0.01 Hz, the prediction matches the experimental data well. From 0.1 to 1 Hz, the predicted energy loss is overestimated. Then, from 10 to 50 Hz, the prediction significantly underestimates the experimental results. The theoretical curve based on a constant spectrum of relaxation can not display more viscous behavior towards both higher on lower frequencies with a more elastic response in the range of physiologic frequencies. Thus, the assumption of a constant spectrum of relaxation is not valid and conclusions regarding the response of the rabbit MCL to harmonic oscillations using the new approach are limited, especially for high frequencies (>1 Hz).

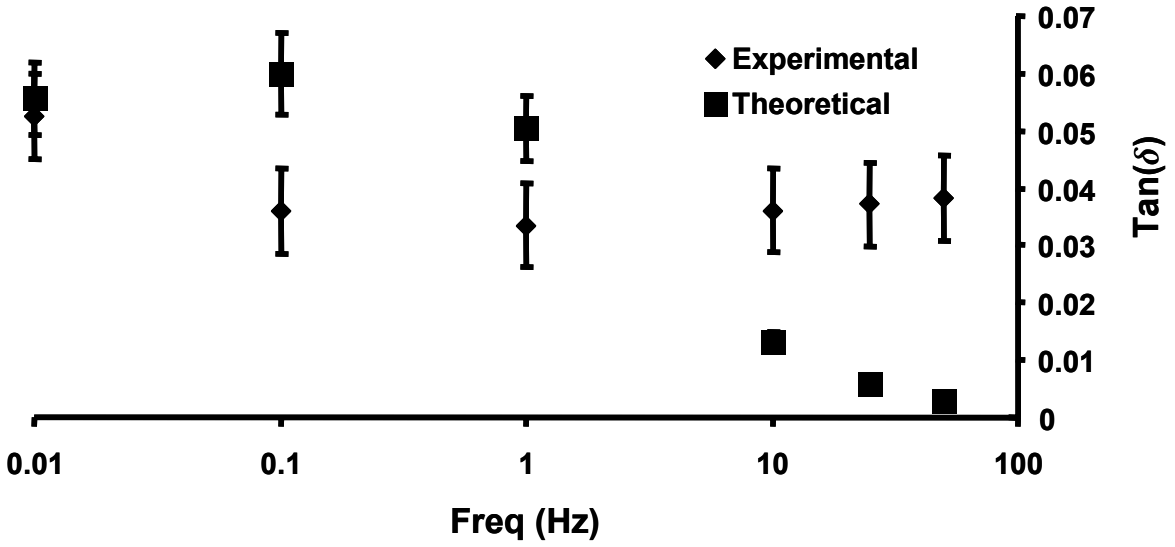

Figure 31 Experimental versus theoretical spectrum of relaxations for 6 rabbit MCLs

9.0 DISCUSSION AND CONCLUSIONS

In this dissertation, an improved analytical approach to obtain the constants of Fung's QLV theory (A, B, C, τ_1, and τ_2) was developed such that the time- and history- dependent viscoelastic properties of the MCL could be described during the early phase of healing. The current approach takes into account the utilization of finite strain rates during tensile loading; thereby, removing the assumption of a step change in strain. With the utilization of slower strain rates, the accuracy of stress and strain measurements can be improved and the experimental errors that result from fast strain rates can be avoided. The strain history approach also enables one to fit the entire experiment (i.e. the stress versus time data from the loading phase and the stress relaxation portion) and accurately determines the constants of QLV theory (A, B, C, τ_1, and τ_2). This results from the approach converging to a globally convergent and numerical stable solution with a reduction in variation and increased statistical power. Further, these constants were validated by comparing the theoretical viscoelastic behavior of all ligaments during a cyclic stress relaxation test to experimental data.

Even though the strain history approach provides an accurate description of stress relaxation behavior of the MCL using the QLV theory, data obtained via dynamic mechanical testing suggests that the results obtained from a stress relaxation test on the basis of a constant spectrum

of relaxation still needs to be proved to be predictive of the true response to harmonic oscillations for these ligaments.

9.1 VISCOELASTIC BEHAVIOR OF THE HEALING MCL

Our results showed that the percentage of stress relaxation for healing MCLs at 12 weeks after injury was significantly increased compared to sham operated controls. Previous studies found greater relaxation for the healing rabbit MCL up to 6 weeks post-injury compared to intact, but values were no longer statically different from controls by 14 weeks [17]. This may be due to injury model used in the previous study (i.e. 4 mm gap injury or a 4 mm saggital Z-plasty in the rabbit). On the other hand, the "mop-end" tear injury model used in this study creates significant damage to the insertion sites which may provide another path for the alteration in stress relaxation behavior. In fact, the differences observed in this study between healing MCLs and sham-operated controls are similar to those reported by Lam et al. (1993) when comparing the stress relaxation of skeletally mature rabbits versus those whose tibial insertion was immature [59]. Thus, the healing of the osseous insertion sites may provide another path for the alteration in stress relaxation behavior.

In terms of the constants describing the QLV theory, the key findings are that the initial slope of the instantaneous elastic response (i.e. constants A*B) was lower for healing MCLs compared to sham-operated controls, suggesting differences in the quality of tissue between the two groups. This is supported by a previous study on the same specimens that reported inferior mechanical properties for the healing MCLs as determined from a load to failure test [1].

Further, the viscoelastic properties of the healing MCL at 12 weeks had a larger viscous response than sham operated controls as shown by a larger value of C. Therefore, the healing MCL would dissipate more energy and have a longer recovery time upon removal of load.

Although there were no differences found for τ_1 which describes short-term relaxation, the values obtained for this constant are similar to those found in Specific Aim 1. Constant τ_2 measured more than 4 orders of magnitude larger than τ_1, suggesting that both groups display insensitivity to strain rates that span orders of magnitude. The significant difference between τ_2 for the sham and healing MCL indicates the long-term relaxation reaches a plateau earlier for the healing tissue. Although, there were no differences found for τ_1 which describes short-term relaxation, the values obtained for this constant are similar to those reported previously for the goat MCL and other ligaments and tendons [3, 24, 48, 71, 121].

9.2 A NEW APPROACH TO DETERMINE CONSTANTS OF QLV THEORY

The key finding was that the regression algorithm converged to a unique solution that was stable and validated by predicting the stress response of a separate experiment. By comparing the set of constants for individual specimens to those obtained for the instantaneous assumption approach, the effect of the assumption of a step change was elucidated. Finally, the behavior of the MCL was predicted for the cyclic stress relaxation test using the properties obtained from static stress relaxation test. Our prediction matched the experimental results, validating our values for the QLV constants.

9.2.1 Determination of Constants

The constants (A, B, C, τ_1, and τ_2) for sham-operated controls compare well to those reported previously for the goat MCL which utilized the same methodology as the current study [3]. Compared to a study on the canine MCL, in which the strain rate utilized in the loading phase was 2 orders of magnitude higher than that for the current study, the constants for sham-operated controls were also similar [121]. Most importantly, constant τ_1, which has been shown to be the most sensitive to the experimental strain rate [23], was on the same order of magnitude as reported in these previous studies of the MCL as well as for other ligaments and tendons [3, 24, 48, 71, 121].

Previous studies using QLV theory together with the assumption of a step change in strain do not account for the relaxation that occurred during ramping and base normalization of experimental data on an underestimated peak stress [23, 102, 103]. As a result, constants C and τ_1 are significantly underestimated and overestimated, respectively [23]. The current approach improves the estimates of these constants. The constant C was significantly higher and constant τ_1 was an order of magnitude lower than those determined using the instantaneous assumption approach. Further, the strain history approach estimates a more nonlinear instantaneous elastic response as indicated by the higher value for constant B. All of these improved approximations result from accounting for the strain history during ramping.

In spite of the fact that the ramp time used in this study is 1-2 orders of magnitude longer than those used previously, the constants obtained using the strain history approach are similar to those reported previously for ligaments and tendons [24, 48, 71, 121]. Most importantly, the determination of constant τ_1, which has been shown to be the most sensitive to the experimental ramp time, was on the same order of magnitude as these previous studies [23]. Further, the

ability for the model to predict the results of a second experiment for validation of the constants was similar to that reported by Woo et al., 1981 whose constants were also determined based on data with a ramp time that was 2 orders of magnitude shorter than that used in this study [121].

9.2.2 Comparison to Other Approaches

Previously our laboratory had used a two-step regression approach to obtain better estimates of the constants (A, B, C, τ_1, and τ_2) based on experiments with finite ramp times [57]. For this approach, however, two physically significant constants, B and τ_1, are highly correlated. As a result, regression algorithms either fail to converge or converge to solutions that are sensitive to systematic deviations between the theory and the experimental data for certain applications. This is demonstrated in Table 13 where the constants (A, B, C, τ_1, and τ_2) were determined for each individual specimen using this approach. Convergence failed for 3 of 6 specimens and the constants A, B, and τ_1 spanned more than 10 orders of magnitude.

Table 13 Constants describing the instantaneous elastic response and reduced relaxation function obtained by curve-fitting individual specimens using the approach described previously by our laboratory. ψ denotes convergence failure of the algorithm, for which the constants obtained for the iteration prior to failure are reported.

Specimen #	A (MPa)	B	C	τ_1 (sec)	τ_2 (sec)
997$^{\psi}$	<1E-10	2.1E+07	0.173	4.87	2287
965$^{\psi}$	15.62	36.3	0.068	5.25E-06	1275
422	10.95	46.2	0.071	9.05E-05	1568
41$^{\psi}$	<1E-10	2.5E+07	0.072	4.16	3186
26	1.68	90.0	0.071	1.34E-04	1657
19	2.67E-10	548.5	0.046	1.52	1197

A similar issue (i.e. the correlation of constants A and τ_1) was observed using the strain history approach. It was found that a relatively similar curve-fit could be achieved when both constants A and τ_1 are increased and decreased by the same percentage of their original value, respectively. Thus, this study chose to fix constant A based on work from two previous studies. One study showed that constant A is unnecessary to describe the reduced stress relaxation following a finite ramp time, and the other demonstrated that the stress-strain curve of ligaments is relatively insensitive to strain-rates ranging over 4 decades [57, 137].

This allowed for a significant improvement in the variability of the obtained constants when compared to an approach described previously by our laboratory [57]. It should be noted that this study did not compare to other approaches that account for the loading portion of the experiment as these approaches are fundamentally based on short ramp times [15, 76, 83]. These approaches were not developed to apply to the experimental protocol utilized in this study, but will perform adequately when applied appropriately.

It should also be noted that for tissues whose stress-strain curve is sensitive to strain-rate, an alternative means to determine constant A may be necessary. For this case, a high strain-rate experiment may still be required to determine constant A, but the remaining constants could be determined utilizing a second slower strain rate experiment along with the approach described in this dissertation. Although this methodology would still require accurate high-speed measurements of stress and strain to determine constant A, the errors caused by the inability of a testing machine to accurately perform a linear ramp and hold test at high strain rates can still be avoided.

9.2.3 Dynamic Mechanical Testing

While the strain history approach combined with the QLV theory performed well for modeling and predicting stress relaxation behavior, the result comparing the predicted and experimentally measured spectrum of relaxation did not match well. Most notably, the spectrum of relaxation was not constant for the rabbit MCL as assumed by the selection of the function for G(t). Yet, compared to the differences in frequency, the experimentally obtained spectrum of relaxation shows that ligaments are relatively insensitive to strain rates spanning nearly 4 orders of magnitude. This supports previous work by Woo et al. showing that ligaments are relatively insensitive to strain rate [137].

However, contrary to the assumption of a constant spectrum of relaxation, the rabbit MCL becomes more viscous for low and high frequencies, and more elastic for frequencies that correspond to those of daily activities. These experimental results support the work of a recent study investigating the response of the human MCL to harmonic oscillations [11]. The human MCL displays more elastic behavior for frequencies between 0.1 and 1 Hz, but energy

dissipation doubles for frequencies of 0.01 Hz and 15 Hz. Thus, the human MCL displays a smaller range of insensitivity to strain rate. These changes in energy dissipation versus frequency for both the rabbit and the human may provide insight into the molecular composition of the MCL. It can be hypothesized that the behaviors observed at the low and high ends of the frequency spectrum correspond to water interacting with proteoglycans and water interacting with collagen, respectively. With further investigation, this approach may be utilized to further answer questions regarding the mechanisms governing the viscoelastic behavior of ligaments.

With respect to the QLV theory, however, the variable phase angle versus frequency suggests that the assumption of a constant spectrum may not be valid. Professor Fung suggests there are certain ranges of frequencies of oscillations in which the assumption of a constant spectrum of relaxation does not represent a tissue accurately [34]. Any tissue may have local peaks and valleys in these data. Thus, it may be necessary to consider a broader range of frequencies than was tested in this dissertation.

However, because the strain history approach is based on the assumption of a constant spectrum of relaxation, it appears that the constants obtained can not be utilized to predict the response of the ligament to harmonic oscillations. This may suggest that different mechanisms govern these behaviors and a more general theory is necessary. On the other hand, these data might also suggest that peaks and valleys in the spectrum of relaxation have relatively little influence on the shape of the reduced relaxation function.

A future modification that could help resolve this issue would be to change the mathematical expression for G(t). Instead of a constant spectrum of relaxation, a variable spectrum can be considered whose amplitude can change with frequency [44]. Preliminary data based on a spectrum of relaxation that consists of 5 constants (C_1, C_2, C_3, τ_1, and τ_2) shows that it

has the potential to fit the experimental results for Tan(δ) versus frequency (Figure 32). However, the theoretical prediction of the reduced relaxation function based on this spectrum of relaxation displays a shape that that is not consistent with that obtained experimentally for the rabbit MCL (Figure 33). In fact, the shape of the experimentally obtained reduced relaxation function is more consistent with that described by a constant spectrum of relaxation. While more data is necessary regarding this point, these results suggest that the mechanisms which govern hysteresis are not identical to those that govern stress relaxation. Thus, the QLV theory and the new approach may be limited to only describing viscoelastic behaviors related to stress relaxation.

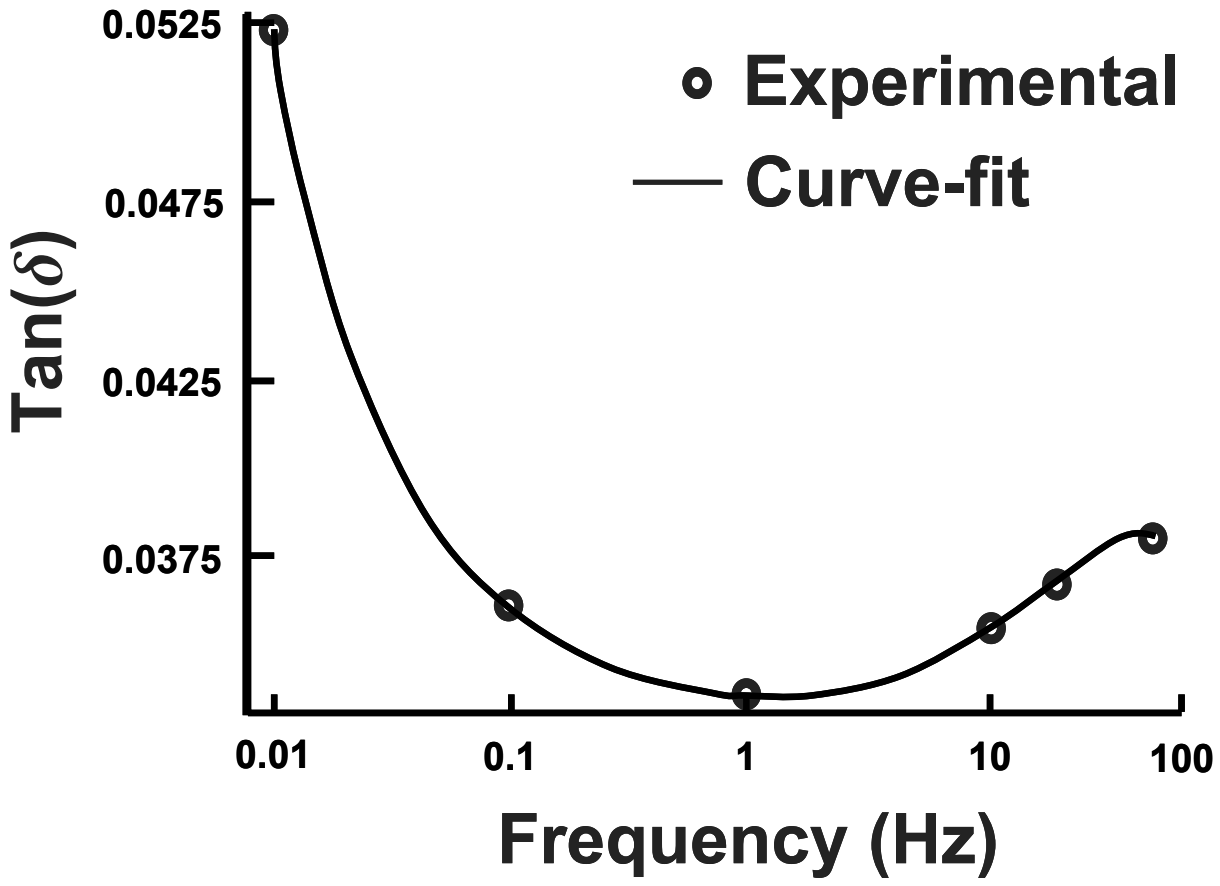

Figure 32 Curve-fit to experimental data for Tan(δ) versus frequency using a variable spectrum of relaxation description.

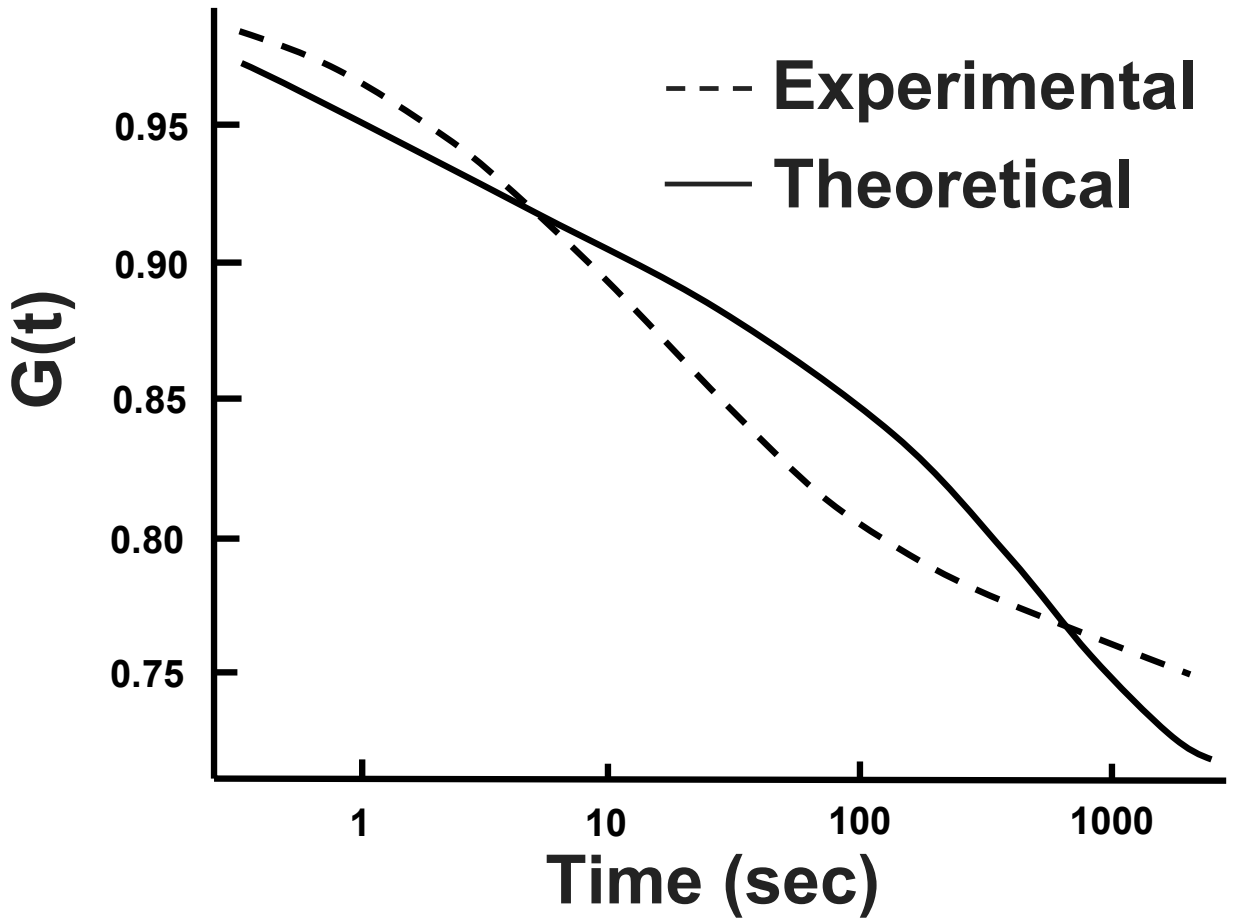

Figure 33 The experimental data for G(t) compared to the theoretical prediction based on the variable spectrum of relaxation determined from Figure 32.

An additional modification that may improve results is to use an alternative weighting schemes when curve-fitting the theory to the experimental data obtained from a stress relaxation test. For example, the energy dissipation at frequencies between 1 and 100 Hz from dynamic testing corresponds to energy dissipation from only 0.01 to 1 sec of a stress relaxation experiment. On the other hand, the energy dissipation at frequencies between 0.01 and 1 Hz corresponds to energy dissipation from 1 to 100 sec of a stress relaxation experiment. Thus, if a constant rate of data collection is utilized and all data are equally weighted, the data representing

lower frequencies and longer relaxation times will be weighted heavier when fitting data from a stress relaxation experiment by virtue of the fact that more data points are collected at longer times. A logarithmic weighting scheme would potentially equally weight both early and late relaxation times.

Finally, it should be noted that these results were obtained for the rabbit MCL. While the human shows similar behaviors, it can be seen from Tables 9 and 12 (in Sections 6.2.3 and 8.2) respectively) that the constants (specifically, C, τ_1, and τ_2) describing the viscoelastic behavior of the rabbit MCL tend to be lower than those for the goat. This suggests that the viscoelastic behavior between these models is different. Thus, thorough dynamic mechanical testing and analyses of the healing and sham operated goat MCL are necessary to definitively state how well the constants obtained in this dissertation are able to predict the response of the goat MCL to sinusoidal perturbations.

9.3 CONCLUSIONS

9.3.1 Clinical Significance

The most powerful clinical significance would be to correlate the constants obtained in this dissertation directly with the biochemical constituents or histomorphological appearance of the healing tissue. This would provide a direct relationship between the biology of the ligament and its function. As a result, new treatment strategies may be developed that specifically target the proteins that have the most significant effect on ligament function. This dissertation provides a first step in establishing those correlations. Based on the current knowledge available in the

literature, the differences between healing and sham operated controls at 12 weeks points to some significant clinical considerations.

In terms of the elastic response of the healing MCL, the most notable result was that the initial slope (constants A*B) was significantly decreased compared to sham-operated controls. Previous studies have associated collagen cross-link density with tangent modulus [30, 114]. In addition, ligament crimp has been suggested to significantly affect the mechanical properties of ligaments at low strains. Since it has previously been found that both of these components are altered in the healing MCL, this decrease in initial slope may be indicative of the changes in collagen cross-linking and crimp pattern. In addition, another potential mechanism that explains these results may be related to the random alignment of collagen in the healing MCL. Upon the application of a tensile load, randomly oriented collagen fibers will rotate to align along the loading axis of the ligament before being recruited to resist elongation. The toe region of disorganized tissues has previously been found to be significantly larger than that of tissues whose collagen is more aligned. While previous studies have shown that collagen alignment appears to improve from 6 to 12 weeks in the goat model, these data may suggest that alignment is still not ideal.

In terms of the constants describing the reduced relaxation function, the most significant result for the healing MCL was the increased viscous effects (i.e. a higher value of C). Previous biochemical studies showed that healing MCLs have increased GAG molecules and water content [17, 18, 31, 60]. In addition, it has been shown that tissues with a greater water content display a greater degree of stress relaxation. Thus, it could be hypothesized that these biochemical changes are correlated to the increase of constant C. This may provide a protective mechanism by which the healing MCL limits its exposure to high valgus stresses by dissipating

energy to a much greater degree. As a result, other structures within the knee may have to play more of a role to assist in stabilizing the knee. Therefore, it can be hypothesized that other valgus stabilizers (e.g the ACL) play an important role in the healing process of the MCL and the healing process of the MCL is significantly compromised when the ACL is injured.

For constant τ_2, the lower value for healing ligaments suggests that they reach a platue in their stress relaxation behavior earlier compared to normal ligaments. This suggests that fluid flow within the healing ligament reaches an equilibrium faster. This could also be potentially related to the disorganized collagen matrix as well as the increased number of voids and decreased collagen density that have been observed for healing ligaments. All of these factors provide fluid with more places and easier avenues to flow in order to reduce stress within the healing ligament.

Clearly, more studies are necessary to make stronger correlations between the constants that describe the QLV behavior of tissues and their biochemical constituents. However, the results of this dissertation show that the viscoelastic behavior of the healing MCL is significantly altered at 12 weeks after injury. The changes observed likely represent a means by which the healing response naturally protects the ligament from high stresses. That is, the inferior tissue quality prevents stresses from becoming too high. Yet, if stresses do become high, the healing tissue will stress relax to a greater degree and reach that lower equilibrium value faster than normal ligaments. While most patients with an isolated injury to the MCL are permitted to resume normal levels of activity at 12 weeks, clinicians and physical therapists should recognize that the knee is not functioning as it did prior to injury and that other structures within the knee may be playing more of a functional role to compensate for the compromised function of the MCL.

9.3.2 Significance of the Strain History Approach

By using the strain history approach to determine the constants of the QLV theory that allows for the use of slow strain rates, errors caused at fast strain rates including overshoot, vibrations, and inaccurate measurements of tissue strain are avoided. Researchers can focus on collecting accurate measurements of stress and strain at slower strain rates while still having the ability to determine meaningful constants describing the viscoelastic behavior of their specimens. the stability of the solutions obtained using the strain history approach reduces the variation of the constants and increases statistical power. Therefore, the strain history approach may allow for differences in the constants of the QLV theory to be determined that may have otherwise been unobserved due to the effects of a finite ramp time or performing experiments at fast strain rates.

As shown in this dissertation this approach can allow for more accurate comparisons of the constants describing injured, diseased, or treated tissues versus those of normal tissues so that researchers can quantitatively measure differences in viscoelastic behavior. This approach makes QLV theory a valuable tool that can be utilized to help elucidate structure-composition-function relationships such that fundamental questions regarding the roles of specific biochemical constituents can be answered. However, the application the QLV is much broader than ligaments. It has been used to describe vascular, lung, pharyngeal, myocardium, cartilage, skin, ureter, rectum, and many other tissues [9, 13, 15, 44, 47, 55, 73, 77, 145]. Ultimately, the analytical approach and knowledge gained in this dissertation can be applied to the majority of soft tissues and can be utilized to address questions in other fields.

Most importantly, the approach detailed in this dissertation will allow for researchers to compare their results to those obtained from different laboratories and can develop some idea of

a “realistic” range of values that should be expected from any given experiment. With this knowledge, investigators have a basis of comparison that will allow them to assess whether their experimental methods are sound and data are reasonable.

9.4 FUTURE DIRECTIONS

This dissertation outlines an experimental and analytical approach that can be utilized for future studies aimed to understand how the composition and morphology relate to the stress relaxation phenomenon in ligaments. However, this dissertation focused on one time period after injury. Future studies should aim to perform similar analyses at various time periods following injury to elucidate the changes in viscoelastic behavior throughout the healing process. In addition, with the advance of quantitative measures of biochemical constituents, future studies should look toward measuring viscoelastic properties and protein concentrations on the same specimens in order to establish potential correlations. Therefore, it is envisaged that this approach can be extended to better understand the relationship between tissue structure and function during tissue remodeling throughout the time course of healing. The approach described in this dissertation will lead to a greater understanding of stress relaxation behavior of ligaments and the effects of injury on this behavior.

This dissertation also demonstrated that the assumption of the constant spectrum of relaxation may not be valid for ligaments. As a result, conclusions regarding the response of ligaments to harmonic oscillations based on the constants obtained from this approach are limited. Future work should aim to describe stress relaxation, hysteresis, and creep phenomena within the framework of one theory. Continuum based models have shown the potential to do

this as well as account for nonlinear behaviors and large deformations. Recently, 1-D single integral formulations have been explored and shown to perform very well [96, 98]. However, to fully describe the nonlinear behavior of ligaments, more general continuum based models that account for multi-dimensional finite strains must be considered.

The single integral finite strain (SIFS) viscoelastic model describes finite deformation of a nonlinearly viscoelastic material within the context of a three-dimensional model. This model includes the concept of microstructural change to describe the nonlinear stress-strain relationship resulting from recruitment. In addition, fading memory is incorporated in the viscoelastic response to ensure that more recent states of strain have greater weight in determining the stress than earlier states. In fact, QLV theory can be obtained by an appropriate selection of strain invariants. Ultimately, mathematical models, such as the SIFS theory or a modified QLV theory, that can fully describe hysteresis, stress relaxation, and creep behaviors are necessary to gain a true understanding of the viscoelastic behavior of ligaments and the constituents that influence these behaviors.

APPENDIX A

OUR LABORATORY'S PREVIOUS APPROACH

To compare to a previously published approach that can account for the relaxation manifested during loading, we utilized an approach detailed by Kwan et al. 1993 [57]. Unlike other approaches that are limited to fast strain rates (see note following page), this approach was developed to apply to any strain history. Thus, we evaluated it for our data collected from a slow strain rate test in which experimental errors (i.e. overshoot) were minimized. For this approach, the instantaneous step strain is replaced by a linear ramp strain with a constant, finite strain rate γ to a strain level at time t_0. As stated previously, the corresponding stress rise during $0 < t < t_0$ can then be written as

$$\sigma(t) = \frac{AB\gamma}{1 + C\ln(\tau_2 / \tau_1)} \int_0^t \{1 + \mathrm{C}(\mathrm{E}_1[(\mathrm{t} - \tau)/\tau_2]\ \mathrm{E}_1[(t - \tau)/\tau_1])\} e^{\mathrm{B}\gamma\tau} \partial\tau \tag{33}$$

Similarly, the subsequent stress relaxation $\sigma(t)$, from t_0 to $t = \infty$, can be described as

$$\sigma(t) = \frac{AB\gamma}{1 + C\ln(\tau_2 / \tau_1)} \int_0^{t_0} \{1 + \mathrm{C}(\mathrm{E}_1[(\mathrm{t} - \tau)/\tau_2]\ \mathrm{E}_1[(t - \tau)/\tau_1])\} e^{\mathrm{B}\gamma\tau} \partial\tau \tag{34}$$

These two equations are then normalized by dividing equations 33 and 34 by the peak stress $\sigma(t_0)$ to eliminate constant *A*. This equation describes the stress relaxation normalized by the stress at time t_0 for a linear ramp and hold strain history:

$$\frac{\sigma(t)}{\sigma(t_0)} = \frac{\int_0^{\min(t,t_0)} \{1 + \mathrm{C}(\mathrm{E}_1[(\mathrm{t} - \tau)/\tau_2]\ \mathrm{E}_1[(t - \tau)/\tau_1])\} e^{\mathrm{B}\gamma\tau} \partial\tau}{\int_0^{t_0} \{1 + \mathrm{C}(\mathrm{E}_1[(\mathrm{t}_0 - \tau)/\tau_2]\ \mathrm{E}_1[(t_0 - \tau)/\tau_1])\} e^{\mathrm{B}\gamma\tau} \partial\tau} \tag{35}$$

We expanded this formulation because the integrals of equation 35 are difficult for most nonlinear regression software packages to evaluate. Further, the upper limit of the integral in the denominator represents a removable singularity. Thus, we integrated both the numerator and denominator in Equation 35 by parts and evaluated the denominator as the upper limit of the integral approaches t_0, to obtain an expand form,

$$\frac{\sigma(t)}{\sigma(t_0)} = \frac{-1 + e^{\alpha B t_0} - C\Gamma[\frac{t}{\tau_2}, \frac{t}{\tau_1}] + C\, e^{\alpha B t}(\Gamma[\alpha B t + \frac{t}{\tau_2}, \alpha B t + \frac{t}{\tau_1}] + \Gamma[\frac{(1+\alpha B\tau_1)(t-t_0)}{\tau_1}, \frac{(1+\alpha B\tau_2)(t-t_0)}{\tau_2}]) + C e^{\alpha B t_0}\Gamma[\frac{t-t_0}{\tau_2}, \frac{t-t_0}{\tau_1}]}{-1 - C\Gamma[\frac{t_0}{\tau_2}, \frac{t_0}{\tau_1}] + e^{\alpha B t_0}(1 + C(\Gamma[\alpha B t_0 + \frac{t_0}{\tau_2}, \alpha B t_0 + \frac{t_0}{\tau_1}] + \ln[\frac{1+\alpha B\tau_2}{1+\alpha B\tau_1}])} \tag{36}$$

where Γ[a,b] is the generalized incomplete gamma function $\int_a^b t^{-1} e^{-t} dt$. Equation 36 was substituted for Equation 35 to improve the performance of nonlinear regression algorithms. This equation was then curve-fit to the experimental data obtained and utilized in the previous sections. Table 13 (Section 9.2.2) showed the results of that analysis.

Note: All other approaches described in the literature are limited to fast strain rates as reported by the authors. The article by Carew et al. stated that their approach fails to converge

for long ramp times [15]. The approach described by Myers et al. utilizes extrapolation based on a linear least squares fit of the first 200 ms of relaxation data [76]. As loading time of the experiment increases, the slope of that linear least squares fit changes dramatically. The authors admitted that this approach assumes a linear rate of relaxation over the loading portion of the loading curve. That assumption is not invalid for long loading times. Nigul and Nigul report that determining the constants of the QLV theory following a finite ramp time can be done using their approach if experiments are carried out under a number of restrictions [83]. One of which is, "due to fast straining of the sample, the quantity t_0/τ_2 is kept several orders of magnitude smaller than unity." Thus, the closer this value gets to zero (i.e. as loading time increases), the more error is introduced. They suggest that at a value of 10^{-3}, or less, the error in their approach is negligible. For the strain rates we found acceptable for this dissertation, t_0/τ_2 is an order of magnitude larger. Thus, the error using this approach would not be negligible.

APPENDIX B

MATHEMATICA 4.2 CODES

CURVE-FITTING ALGORITHM

```
<<LinearAlgebra`GaussianElimination`
<<NumericalMath`PolynomialFit`
<<Statistics`NonlinearFit`
<<Statistics`DescriptiveStatistics`
<<Statistics`NormalDistribution`
<<Statistics`ConfidenceIntervals`
 Off[General::"spell1"]
directory="c:/Temp/";
Time1=StringJoin[directory,"ramptime(1sp).txt"];
Force1 = StringJoin[directory,"rampstress(19).txt"];
FileStream=OpenRead[Time1];
Time1=ReadList[FileStream,  Number];
Close[FileStream];
Stream = OpenRead[Force1];
Force1=ReadList[Stream,  Number];
Close[Stream];
yy=Length[Time1]
y=Length[Force1]
Datafirst=Table[0ij,{i,1,yy},{j,1,2}];
Dataorig1=Table[0ij,{i,1,yy},{j,1,2}];
Do[
     Datafirst[[i,1]]=Time1[[i]];
     Datafirst[[i,2]]=Force1[[i]];
     ,{i,1,yy}];
Data1=Datafirst;
Dataorig1=Data1;
Clear[Datafirst];


directory="c:/Temp/";
Time2=StringJoin[directory,"statictime(1sp).txt"];
Force2 = StringJoin[directory,"staticstress(19).txt"];
FileStream=OpenRead[Time2];
Time2=ReadList[FileStream,  Number];
Close[FileStream];
Stream = OpenRead[Force2];
Force2=ReadList[Stream,  Number];
```

```
Close[Stream];
yy=Length[Time2]
y=Length[Force2]
Datasecond=Table[0ij,{i,1,yy},{j,1,2}];
Dataorig2=Table[0ij,{i,1,yy},{j,1,2}];
Do[
     Datasecond[[i,1]]=Time2[[i]];
     Datasecond[[i,2]]=Force2[[i]];
     ,{i,1,yy}]
Data2=Datasecond;
Dataorig2=Data2;
Clear[Datasecond];
(* Plot of Original Data *)
A=ListPlot[Data1,PlotRange→All]
B=ListPlot[Data2,PlotRange→All]


 alpha=.0025;
elasticfit=NonlinearRegress[Data1,  (AA*(Exp[BB*i*alpha]-1)),
{i},{{AA,1,0,100000},{BB,50,0,100000}}, RegressionReport-
>BestFitParameters,Method ->LevenbergMarquardt];
Clear [AA,BB];
AA=BestFitParameters[[1,2]]/. elasticfit
BBinitial=BestFitParameters[[2,2]]/. elasticfit
tknot=18.3999999;
numberofinterations=1;
CCinitial=0.07;
tau2initial=1500;
tau1initial=.5;
iniCC=CCinitial;
initau1=tau1initial;
initau2=tau2initial;
iniBB=BBinitial;
iniAA=AAinitial;
 mm=Plot[(AA*(Exp[BBinitial*t*alpha]-1)),{t,.4,18.4}];
 Show[A,mm]
```

```
zz = Length[Data1] + Length[Data2];

model1[t_, BB_, CC_, tau2_, tau1_] =
  AA*BB*alpha/(1+CC Log[tau2/tau1])*
   ∫_0^(t-0.000001) (1+
      CC*(Gamma[0, (t-τ)/tau2, (t-τ)/tau1]))*
     E^(BB*alpha*τ) dτ;
model2[t_, BB_, CC_, tau2_, tau1_] =
  AA*BB*alpha/(1+CC Log[tau2/tau1])*
   ∫_0^tknot (1+CC*(Gamma[0, (t-τ)/tau2, (t-τ)/tau1]))*
     E^(BB*alpha*τ) dτ;
matrix = Table[0ij, {i, 1, zz}];
Do[
  matrix[[i]] = model1[Data1[[i, 1]], BB, CC, tau2, tau1];
  , {i, 1, Length[Data1]}];
Do[
  matrix[[i]] = model2[Data2[[i-Length[Data1], 1]],
    BB, CC, tau2, tau1];
  , {i, Length[Data1]+1, zz}];
dBB[BB_, CC_, tau2_, tau1_] = D[matrix, BB];
dCC[BB_, CC_, tau2_, tau1_] = D[matrix, CC];
dtau2[BB_, CC_, tau2_, tau1_] = D[matrix, tau2];
dtau1[BB_, CC_, tau2_, tau1_] = D[matrix, tau1];
 delta={0,0,0,0};
mu=1/100000;
BigD={{1,0,0,0},{0,1,0,0},{0,0,1,0},{0,0,0,1}};
BBinitialtemp=BBinitial;
CCinitialtemp=CCinitial;
tau2initialtemp=tau2initial;
tau1initialtemp=tau1initial;
sumofsquares=100000;
sumofsquareslast=100000;
initialguess={{BBinitial,CCinitial,tau2initial,tau1initial}};
BigF=Table[0ij,{i,1,zz},{j,1,4}];
residuals=Table[0i,{i,1,zz}];
residualstemp=Table[0i,{i,1,zz}];
stop={10,10,10,10};

 While[sumofsquareslast>.00000001&&mu<100000,
  holder=0;

BigBB=dBB[initialguess[[1,1]],initialguess[[1,2]],initialguess[[1
,3]],initialguess[[1,4]]];
```

```
BigCC=dCC[initialguess[[1,1]],initialguess[[1,2]],initialguess[[1
,3]],initialguess[[1,4]]];

Bigtau2=dtau2[initialguess[[1,1]],initialguess[[1,2]],initialgues
s[[1,3]],initialguess[[1,4]]];Bigtau1=dtau1[initialguess[[1,1]],i
nitialguess[[1,2]],initialguess[[1,3]],initialguess[[1,4]]];
  Do[
     BigF[[n,1]]=BigBB[[n]];
    BigF[[n,2]]=BigCC[[n]];
    BigF[[n,3]]=Bigtau2[[n]];
    BigF[[n,4]]=Bigtau1[[n]];
     ,{n,1,zz}];
  Do[
    residuals[[n]]=Data1[[n,2]]-
model1[Data1[[n,1]],initialguess[[1,1]],initialguess[[1,2]],initi
alguess[[1,3]],initialguess[[1,4]]];
    ,{n,1,Length[Data1]}];
 Do[
    residuals[[n]]=Data2[[n-Length[Data1],2]]-model2[Data2[[n-
Length[Data1],1]],initialguess[[1,1]],initialguess[[1,2]],initial
guess[[1,3]],initialguess[[1,4]]];
    ,{n,Length[Data1]+1,zz}];
Dtemp=Transpose[BigF].BigF;
BigD[[1,1]]=Dtemp[[1,1]];
BigD[[2,2]]=Dtemp[[2,2]];
BigD[[3,3]]=Dtemp[[3,3]];
BigD[[4,4]]=Dtemp[[4,4]];
While[holder==0&&mu<100000,
  lu=LUFactor[(Transpose[BigF].BigF+mu*BigD)];
  delta=LUSolve[lu,Transpose[BigF].residuals];
  sumofsquares=residuals.residuals;
  BBinitialtemp=BBinitial+delta[[1]];
  CCinitialtemp=CCinitial+delta[[2]];
  tau2initialtemp=tau2initial+delta[[3]];
  tau1initialtemp=tau1initial+delta[[4]];

initialguesstemp={{BBinitialtemp,CCinitialtemp,tau2initialtemp,ta
u1initialtemp}};
 Do[
          residualstemp[[n]]=Data1[[n,2]]-
model1[Data1[[n,1]],initialguesstemp[[1,1]],initialguesstemp[[1,2
]],initialguesstemp[[1,3]],initialguesstemp[[1,4]]];
          ,{n,1,Length[Data1]}];
      Do[
          residualstemp[[n]]=Data2[[n-Length[Data1],2]]-
model2[Data2[[n-
Length[Data1],1]],initialguesstemp[[1,1]],initialguesstemp[[1,2]]
,initialguesstemp[[1,3]],initialguesstemp[[1,4]]];
          ,{n,Length[Data1]+1,zz}];
      sumofsquarestemp=residualstemp.residualstemp;

If[BBinitialtemp>0&&CCinitialtemp>0&&tau2initialtemp>0&&tau1initi
altemp>0&&sumofsquarestemp<sumofsquares,
```

```
          mu=mu/100000;
          BBinitial=delta[[1]]+BBinitial;
          CCinitial=delta[[2]]+CCinitial;
          tau2initial=delta[[3]]+tau2initial;
          tau1initial=delta[[4]]+tau1initial;

initialguess={{BBinitial,CCinitial,tau2initial,tau1initial}};
          Print[initialguess];
          Print[sumofsquarestemp];
          sumofsquareslast=sumofsquares-sumofsquarestemp;
          numberofinterations=numberofinterations+1;
          Print[numberofinterations];
          holder=1,
          mu=mu*10];];]

BigBB=dBB[initialguess[[1,1]],initialguess[[1,2]],initialguess[[1
,3]],initialguess[[1,4]]];
BigCC=dCC[initialguess[[1,1]],initialguess[[1,2]],initialguess[[1
,3]],initialguess[[1,4]]];
Bigtau2=dtau2[initialguess[[1,1]],initialguess[[1,2]],initialgues
s[[1,3]],initialguess[[1,4]]];Bigtau1=dtau1[initialguess[[1,1]],i
nitialguess[[1,2]],initialguess[[1,3]],initialguess[[1,4]]];
Do[
     BigF[[n,1]]=BigBB[[n]];
    BigF[[n,2]]=BigCC[[n]];
    BigF[[n,3]]=Bigtau2[[n]];
    BigF[[n,4]]=Bigtau1[[n]];
     ,{n,1,zz}];
covariancematrix=Inverse[Transpose[BigF].BigF];
Print["covariancematrix"]
covariancematrix//MatrixForm
correlationmatrix=Table[0ij,{i,1,4},{j,1,4}];
Do[
Do[correlationmatrix[[i,j]]=covariancematrix[[i,j]]/Sqrt[(covaria
ncematrix[[i,i]]*covariancematrix[[j,j]])]
         ,{j,1,4}];
    ,{i,1,4}];
Print["correlationmatrix"]
correlationmatrix//MatrixForm
Print["Determinant of the correlationmatrix"]
Det[correlationmatrix]


 predyvalues=Table[0ij,{i,1,Length[Data1]}];
yvalues=Table[0ij,{i,1,Length[Data1]}];
Do[

predyvalues[[n]]=model1[Data1[[n,1]],initialguesstemp[[1,1]],init
ialguesstemp[[1,2]],initialguesstemp[[1,3]],initialguesstemp[[1,4
]]];
    ,{n,1,Length[Data1]}];
Do[
    yvalues[[n]]=Data1[[n,2]];
    ,{n,1,Length[Data1]}];
```

```
averageyvalues=Sum[yvalues[[i]],{i,1,Length[Data1]}]/Length[Data1
];
regressvar=Sum[(predyvalues[[i]]-
averageyvalues)^2,{i,1,Length[Data1]}];
residualvar=Sum[(yvalues[[i]]-
predyvalues[[i]])^2,{i,1,Length[Data1]}];
rsquared=regressvar/(regressvar+residualvar)
 predyvalues=Table[0ij,{i,1,Length[Data2]}];
yvalues=Table[0ij,{i,1,Length[Data2]}];
Do[

predyvalues[[n]]=model2[Data2[[n,1]],initialguesstemp[[1,1]],init
ialguesstemp[[1,2]],initialguesstemp[[1,3]],initialguesstemp[[1,4
]]];
    ,{n,1,Length[Data2]}];
Do[
    yvalues[[n]]=Data2[[n,2]];
    ,{n,1,Length[Data2]}];
averageyvalues=Sum[yvalues[[i]],{i,1,Length[Data2]}]/Length[Data2
];
regressvar=Sum[(predyvalues[[i]]-
averageyvalues)^2,{i,1,Length[Data2]}];
residualvar=Sum[(yvalues[[i]]-
predyvalues[[i]])^2,{i,1,Length[Data2]}];
rsquared=regressvar/(regressvar+residualvar)

 predyvalues=Table[0ij,{i,1,zz}];
yvalues=Table[0ij,{i,1,zz}];
Do[

predyvalues[[n]]=model1[Data1[[n,1]],initialguesstemp[[1,1]],init
ialguesstemp[[1,2]],initialguesstemp[[1,3]],initialguesstemp[[1,4
]]];
    ,{n,1,Length[Data1]}];
Do[

predyvalues[[n+Length[Data1]]]=model2[Data2[[n,1]],initialguesste
mp[[1,1]],initialguesstemp[[1,2]],initialguesstemp[[1,3]],initial
guesstemp[[1,4]]];
    ,{n,1,Length[Data2]}];
Do[
    yvalues[[n]]=Data1[[n,2]];
    ,{n,1,Length[Data1]}];
Do[
    yvalues[[n+Length[Data1]]]=Data2[[n,2]];
    ,{n,1,Length[Data2]}];
averageyvalues=Sum[yvalues[[i]],{i,1,zz}]/zz;
regressvar=Sum[(predyvalues[[i]]-averageyvalues)^2,{i,1,zz}];
residualvar=Sum[(yvalues[[i]]-predyvalues[[i]])^2,{i,1,zz}];
rsquared=regressvar/(regressvar+residualvar)
```

```
alpha = .00154;
elasticfit = NonlinearRegress[Data1, (AA*(Exp[BB*i*alpha] - 1)), {i}, {{AA, 1, 0, 100000}, {BB, 50, 0, 100000}},
  RegressionReport -> BestFitParameters, Method -> LevenbergMarquardt];
Clear[AA, BB];
AA = BestFitParameters[[1, 2]] /. elasticfit
BBinitial = BestFitParameters[[2, 2]] /. elasticfit
tknot = 18.3999999;
numberofinterations = 1;
CCinitial = 0.07;
tau2initial = 1500;
tau1initial = .5;
iniCC = CCinitial;
initau1 = tau1initial;
initau2 = tau2initial;
iniBB = BBinitial;
iniAA = AAinitial;

mm = Plot[(AA*(Exp[BBinitial*t*alpha] - 1)), {t, .4, 18.4}];

Show[A, mm]

zz = Length[Data1] + Length[Data2];

model1[t_, BB_, CC_, tau2_, tau1_] =
  AA*BB*alpha / (1 + CC Log[tau2 / tau1]) * ∫_0^(t-0.0000001) (1 + CC*(Gamma[0, (t - τ) / tau2, (t - τ) / tau1]))*E^(BB*alpha*τ) dτ;
model2[t_, BB_, CC_, tau2_, tau1_] =
  AA*BB*alpha / (1 + CC Log[tau2 / tau1]) * ∫_0^tknot (1 + CC*(Gamma[0, (t - τ) / tau2, (t - τ) / tau1]))*E^(BB*alpha*τ) dτ;
matrix = Table[0ij, {i, 1, zz}];
Do[
  matrix[[i]] = model1[Data1[[i, 1]], BB, CC, tau2, tau1];
  , {i, 1, Length[Data1]}];
Do[
  matrix[[i]] = model2[Data2[[i - Length[Data1], 1]], BB, CC, tau2, tau1];
  , {i, Length[Data1] + 1, zz}];
dBB[BB_, CC_, tau2_, tau1_] = D[matrix, BB];
dCC[BB_, CC_, tau2_, tau1_] = D[matrix, CC];
dtau2[BB_, CC_, tau2_, tau1_] = D[matrix, tau2];
dtau1[BB_, CC_, tau2_, tau1_] = D[matrix, tau1];
```

BOOTSTRAPING ALGORITHIM

```
numofboots=100;
 initialguessfixed=initialguesstemp;
AAfixed=AA;
count=1;
CCtable= Table[0i,{i,1,numofboots}];
tau1table= Table[0i,{i,1,numofboots}];
tau2table= Table[0i,{i,1,numofboots}];
BBtable= Table[0i,{i,1,numofboots}];
AAtable= Table[0i,{i,1,numofboots}];

 Do[
  random1=Random[Integer,{1,6}];
  random2=Random[Integer,{1,6}];
  If[random1==1,smoothfile="smoothfile1.txt"];
  If[random1==2,smoothfile="smoothfile2.txt"];
  If[random1==3,smoothfile="smoothfile3.txt"];
  If[random1==4,smoothfile="smoothfile4.txt"];
  If[random1==5,smoothfile="smoothfile5.txt"];
  If[random1==6,smoothfile="smoothfile6.txt"];
  If[random2==1,errorfile="errorfile1.txt"];
  If[random2==2,errorfile="errorfile2.txt"];
  If[random2==3,errorfile="errorfile3.txt"];
  If[random2==4,errorfile="errorfile4.txt"];
  If[random2==5,errorfile="errorfile5.txt"];
  If[random2==6,errorfile="errorfile6.txt"];
 directory="c:/Temp/";
smoothdata=StringJoin[directory,smoothfile];
errordata = StringJoin[directory,errorfile];
FileStream=OpenRead[smoothdata];
smooth=ReadList[FileStream,  Number];
Close[FileStream];
Stream = OpenRead[errordata];
error=ReadList[Stream,  Number];
Close[Stream];
yy=Length[smooth];
y=Length[error];
Datasmooth=smooth;
Dataerror=error;
```

```
Clear[AA, BB, CC, tau2, tau1];
eq1[t_, AA_, BB_, CC_, tau2_, tau1_] =
  AA*BB*alpha/(1+CC Log[tau2/tau1])*
   ∫_0^(t-0.0000001) (1+CC*(Gamma[0, (t-τ)/tau2, (t-τ)/tau1]))*
     E^(BB*alpha*τ) dτ;
eq2[t_, AA_, BB_, CC_, tau2_, tau1_] =
  AA*BB*alpha/(1+CC Log[tau2/tau1])*
   ∫_0^tknot (1+CC*(Gamma[0, (t-τ)/tau2, (t-τ)/tau1]))*E^(BB*alpha*τ) dτ;
```

```
Do[
Data1[[k,2]]=eq1[Data1[[k,1]],AAfixed,initialguessfixed[[1,1]],in
itialguessfixed[[1,2]],initialguessfixed[[1,3]],initialguessfixed
[[1,4]]]+Datasmooth[[k]]+Random[NormalDistribution[0,Dataerror[[1
]]]];,
    {k,1,Length[Data1]}];
Do[
    Data2[[k-Length[Data1],2]]=eq2[Data2[[k-
Length[Data1],1]],AAfixed,initialguessfixed[[1,1]],initialguessfi
xed[[1,2]],initialguessfixed[[1,3]],initialguessfixed[[1,4]]]+Dat
asmooth[[k]]+Random[NormalDistribution[0,Dataerror[[1]]]];,
    {k,Length[Data1]+1,zz}];
 alpha=.00154;
elasticfit=NonlinearRegress[Data1,  (AA*(Exp[BB*i*alpha]-1)),
{i},{{AA,1,0,100000},{BB,50,0,100000}}, RegressionReport-
>BestFitParameters,Method ->LevenbergMarquardt];
Clear [AA,BB];
AA=BestFitParameters[[1,2]]/. elasticfit;
BBinitial=BestFitParameters[[2,2]]/. elasticfit;
tknot=18.3999999;
numberofinterations=1;
CCinitial=0.072;
tau2initial=1470;
tau1initial=.65;
iniCC=CCinitial;
initau1=tau1initial;
initau2=tau2initial;
iniBB=BBinitial;
iniAA=AAinitial;
```

```
zz = Length[Data1] + Length[Data2];


model1[t_, BB_, CC_, tau2_, tau1_] =
  AA*BB*alpha/(1 + CC Log[tau2/tau1])*
   ∫_0^(t-0.0000001) (1 + CC*(Gamma[0, (t - τ)/tau2, (t - τ)/tau1]))*
    E^(BB*alpha*τ) dτ;
model2[t_, BB_, CC_, tau2_, tau1_] =
  AA*BB*alpha/(1 + CC Log[tau2/tau1])*
   ∫_0^tkmot (1 + CC*(Gamma[0, (t - τ)/tau2, (t - τ)/tau1]))*E^(BB*alpha*τ) dτ;
matrix = Table[0ij, {i, 1, zz}];
Do[
  matrix[[i]] = model1[Data1[[i, 1]], BB, CC, tau2, tau1];
  , {i, 1, Length[Data1]}];
Do[
  matrix[[i]] = model2[Data2[[i - Length[Data1], 1]], BB, CC, tau2, tau1];
  , {i, Length[Data1] + 1, zz}];
dBB[BB_, CC_, tau2_, tau1_] = D[matrix, BB];
dCC[BB_, CC_, tau2_, tau1_] = D[matrix, CC];
dtau2[BB_, CC_, tau2_, tau1_] = D[matrix, tau2];
dtau1[BB_, CC_, tau2_, tau1_] = D[matrix, tau1];



delta={0,0,0,0};
mu=1/100000;
BigD={{1,0,0,0},{0,1,0,0},{0,0,1,0},{0,0,0,1}};
BBinitialtemp=BBinitial;
CCinitialtemp=CCinitial;
tau2initialtemp=tau2initial;
tau1initialtemp=tau1initial;
sumofsquares=100000;
sumofsquareslast=100000;
initialguess={{BBinitial,CCinitial,tau2initial,tau1initial}};
BigF=Table[0ij,{i,1,zz},{j,1,4}];
residuals=Table[0i,{i,1,zz}];
residualstemp=Table[0i,{i,1,zz}];
stop={10,10,10,10};

 While[sumofsquareslast>.00000001&&mu<100000,
      holder=0;

BigBB=dBB[initialguess[[1,1]],initialguess[[1,2]],initialguess[[1,3]],initialg
uess[[1,4]]];

BigCC=dCC[initialguess[[1,1]],initialguess[[1,2]],initialguess[[1,3]],initialg
uess[[1,4]]];

Bigtau2=dtau2[initialguess[[1,1]],initialguess[[1,2]],initialguess[[1,3]],init
ialguess[[1,4]]];Bigtau1=dtau1[initialguess[[1,1]],initialguess[[1,2]],initial
guess[[1,3]],initialguess[[1,4]]];
      Do[
```

```
            BigF[[n,1]]=BigBB[[n]];
          BigF[[n,2]]=BigCC[[n]];
          BigF[[n,3]]=Bigtau2[[n]];
          BigF[[n,4]]=Bigtau1[[n]];
              ,{n,1,zz}];
        Do[
          residuals[[n]]=Data1[[n,2]]-
model1[Data1[[n,1]],initialguess[[1,1]],initialguess[[1,2]],initialguess[[1,3]
],initialguess[[1,4]]];
          ,{n,1,Length[Data1]}];
        Do[
          residuals[[n]]=Data2[[n-Length[Data1],2]]-model2[Data2[[n-
Length[Data1],1]],initialguess[[1,1]],initialguess[[1,2]],initialguess[[1,3]],
initialguess[[1,4]]];
          ,{n,Length[Data1]+1,zz}];
        Dtemp=Transpose[BigF].BigF;
        BigD[[1,1]]=Dtemp[[1,1]];
        BigD[[2,2]]=Dtemp[[2,2]];
        BigD[[3,3]]=Dtemp[[3,3]];
        BigD[[4,4]]=Dtemp[[4,4]];
        While[holder==0&&mu<100000,
          lu=LUFactor[(Transpose[BigF].BigF+mu*BigD)];
          delta=LUSolve[lu,Transpose[BigF].residuals];
          sumofsquares=residuals.residuals;
          BBinitialtemp=BBinitial+delta[[1]];
          CCinitialtemp=CCinitial+delta[[2]];
          tau2initialtemp=tau2initial+delta[[3]];
          tau1initialtemp=tau1initial+delta[[4]];

initialguesstemp={{BBinitialtemp,CCinitialtemp,tau2initialtemp,tau1initialtemp
}};
          Do[
            residualstemp[[n]]=Data1[[n,2]]-
model1[Data1[[n,1]],initialguesstemp[[1,1]],initialguesstemp[[1,2]],initialgue
sstemp[[1,3]],initialguesstemp[[1,4]]];
            ,{n,1,Length[Data1]}];
          Do[
            residualstemp[[n]]=Data2[[n-Length[Data1],2]]-model2[Data2[[n-
Length[Data1],1]],initialguesstemp[[1,1]],initialguesstemp[[1,2]],initialguess
temp[[1,3]],initialguesstemp[[1,4]]];
            ,{n,Length[Data1]+1,zz}];
          sumofsquarestemp=residualstemp.residualstemp;

If[BBinitialtemp>0&&CCinitialtemp>0&&tau2initialtemp>0&&tau1initialtemp>0&&sum
ofsquarestemp<sumofsquares,
            mu=mu/100000;
            BBinitial=delta[[1]]+BBinitial;
            CCinitial=delta[[2]]+CCinitial;
            tau2initial=delta[[3]]+tau2initial;
            tau1initial=delta[[4]]+tau1initial;
            initialguess={{BBinitial,CCinitial,tau2initial,tau1initial}};
            Print[initialguess];
            sumofsquareslast=sumofsquares-sumofsquarestemp;
            numberofinterations=numberofinterations+1;
            holder=1,
            mu=mu*10];];]
      Print[initialguess];
      Print[count];
      CCtable[[count]]=CCinitial;
      tau1table[[count]]=tau1initial;
      tau2table[[count]]=tau2initial;
      BBtable[[count]]=BBinitial;
      AAtable[[count]]=AA;
      count=count+1;
```

```
    ,{vv,1,numofboots}];
```

VALIDATION PROGRAM

```
Clear[AA,BB,ω,PEAKS,tknot,ϵ1,ϵ0,t,n,alpha,q,w,v,τ];
n=0;
alpha = 0.0037
ω=Pi/3;
tknot=6.2;
t=tknot+(2n+1)π/ω;
ϵ1=t*alpha;
ϵ0=tknot*alpha;
AA= 19.0;
BB=32.7;
CC=.0433;
tau1 = .35;
tau2=452;
```

```
n = 1;
PEAKS = Table[0 i, {i, 0, 9}];
ϵ = alpha * (τ);
q[τ_] =
 AA * BB
  ((1 + CC * (Gamma[0, (t - τ) / tau2, (t - τ) / tau1])) /
     (1 + CC * Log[tau2 / tau1]) * (E^(BB*ϵ) * ∂τ ϵ));
Stress1 = NIntegrate[q[τ], {τ, 0, tknot - .000001}];
Do[
    Stress2 = 0;
    t = tknot + (2  (n - 1) + 1) π / ω;
    ϵprime =
  ((ϵ1 + ϵ0) / 2) - ((ϵ1 - ϵ0) / 2) * (Cos[ω * (τ - tknot)]);
 v[τ_] =
  AA * BB ( (1 + CC * (Gamma[0, (t - τ) / tau2, (t - τ) / tau1])) / (1 + CC * Log[tau2 / tau1]) *
     (E^(BB*ϵprime) * ∂τ ϵprime) );
    Stress2 = NIntegrate [v[τ], {τ, tknot, t - .000001}];
    PEAKS[[n]] = Stress1 + Stress2
    , {n, 1, 10}]
PEAKS
Pipe1 = "peaks.dat";
OpenWrite[Pipe1];
WriteString[Pipe1, PEAKS[[1]], "\n", PEAKS[[2]], "\n",
  PEAKS[[3]], "\n", PEAKS[[4]], "\n", PEAKS[[5]], "\n",
  PEAKS[[6]], "\n", PEAKS[[7]], "\n", PEAKS[[8]], "\n",
  PEAKS[[9]], "\n"];
    Close[Pipe1];
```

```
n = 1;
VALLEYS = Table[0 i, {i, 0, 9}];
Do[
    Stress2 = 0;
    t = tknot + (2 n) π / ω;
    eprime =
  ((ϵ1 + ϵ0) / 2) - ((ϵ1 - ϵ0) / 2) * (Cos[ω * (τ - tknot)]);
 w[τ_] =
  AA * BB ( (1 + CC * (Gamma[0, (t - τ) / tau2, (t - τ) / tau1])) / (1 + CC * Log[tau2 / tau1]) *
     (E^(BB*eprime) * ∂τ eprime) );
    Stress2 = NIntegrate [w[τ], {τ, tknot, t - .000001}];
    VALLEYS[[n]] = Stress1 + Stress2
    , {n, 1, 10}]
VALLEYS
Pipe2 = "valleys.dat";
OpenWrite[Pipe2];
WriteString[Pipe2, VALLEYS[[1]], "\n", VALLEYS[[2]],
  "\n", VALLEYS[[3]], "\n", VALLEYS[[4]], "\n", VALLEYS[[5]],
  "\n", VALLEYS[[6]], "\n", VALLEYS[[7]], "\n", VALLEYS[[8]],
  "\n"];
    Close[Pipe2];
```

DMA PROGRAM

```
<<Statistics`NonlinearFit`
 Off[General::"spell1"]
directory="c:/Temp/";
elapsedtime=StringJoin[directory,"elapsedtime.txt"];
load=StringJoin[directory,"load.txt"];
disp = StringJoin[directory,"disp.txt"];
FileStream=OpenRead[elapsedtime];
elapsedtime=ReadList[FileStream,  Number];
Close[FileStream];
Stream = OpenRead[load];
load=ReadList[Stream,  Number];
Close[Stream];
Stream2 = OpenRead[disp];
disp=ReadList[Stream2,  Number];
Close[Stream2];
 yyy=Length[elapsedtime]
yy=Length[load]
y=Length[disp]
timeloadData=Table[0ij,{i,1,yy},{j,1,2}];
timedispData=Table[0ij,{i,1,yy},{j,1,2}];
loaddispData=Table[0ij,{i,1,yy},{j,1,2}];
temppeaks=Table[0ij,{i,1,500},{j,1,2}];
tempvalleys=Table[0ij,{i,1,500},{j,1,2}];
freqsdisp=Table[0i,{i,1,500}];
freqsload=Table[0i,{i,1,500}];
Do[
     timeloadData[[i,1]]=elapsedtime[[i]];
         timedispData[[i,1]]=elapsedtime[[i]];
     timeloadData[[i,2]]=load[[i]];
         loaddispData[[i,2]]=load[[i]];
         timedispData[[i,2]]=disp[[i]];
         loaddispData[[i,1]]=disp[[i]];
     ,{i,1,yy}]
(* Plot of Original Data *)
AA=ListPlot[timeloadData,PlotJoined->True,PlotStyle-
>Hue[.6],PlotLabel→"Load versus Time"];
BB=ListPlot[timedispData,PlotJoined->True,PlotStyle-
>Hue[0],PlotLabel→"Disp versus Time"];
CC=ListPlot[loaddispData,PlotJoined->True,PlotLabel→"Load versus
Disp"];
Show[AA,BB]

freq=100;
 Clear[shift,A,diff,BestFitParameters];
fit=NonlinearRegress[timedispData,shift+A Sin[2 Pi (freq
t+diff)],{t},{shift,A,diff},RegressionReport→BestFitParameters];
BestFitParameters=BestFitParameters/. fit;
shiftdisp=shift/. BestFitParameters;
Adisp=A/. BestFitParameters;
```

```
diffdisp=diff/. BestFitParameters;
Clear[shift,A,diff,BestFitParameters];
fit=NonlinearRegress[timeloadData,shift+A Sin[2 Pi (freq
t+diff)],{t},{shift,A,diff},RegressionReport→BestFitParameters];
BestFitParameters=BestFitParameters/. fit;
shiftload=shift/. BestFitParameters;
Aload=A/. BestFitParameters;
diffload=diff/. BestFitParameters;
Print["Amp Displacement"]
peakdisp=Abs[Adisp]
Print["Amp Load"]
peakload=Abs[Aload]
Print["Delta"]
delta= ArcTan[Tan[2*Pi*(diffload-diffdisp)]]-.00112*freq
Print["Tan(delta)"]
tandelta=Tan[delta]
Print["Complex Modulus"];
complex=peakload/peakdisp
Print["Storage"]
Storage=peakload/peakdisp*Cos[delta]
Print["Loss"]
loss=peakload/peakdisp*Sin[delta]
Print["Hysteresis"]
hysteresis=Chop[Integrate[(shiftload+peakload Sin[2 Pi*freq
t+delta])*D[shiftdisp+peakdisp Sin[2 Pi*freq t],t],{t,0,1/freq}]]

hyst=ParametricPlot[{shiftdisp+peakdisp Sin[2 Pi*freq
t],shiftload+peakload Sin[2 Pi*freq
t+(delta)]},{t,0,1/freq},PlotStyle->Hue[0]]
Show[CC,hyst]
test=Plot[shiftdisp+Adisp Sin[2 Pi (freq
t+diffdisp)],{t,0,elapsedtime[[Length[elapsedtime]]]},PlotLabel→
"Disp versus Time"];
Show[test,BB]

 test2=Plot[shiftload+Aload Sin[2 Pi (freq
t+diffload)],{t,0,elapsedtime[[Length[elapsedtime]]]},PlotLabel→
"Load versus Time"]

Show[test2,AA]
 test3=Plot[ Sin[2 Pi (freq t)],{t,0,0.01},PlotLabel→"Disp
versus Time"];
 test4=Plot[ Sin[2 Pi (freq t)+delta],{t,0,.01},PlotLabel→"Load
versus Time",PlotStyle->Hue[.6]]
 Show[test3,test4]

 ListPlot[Abs[Fourier[load]
],PlotJoined→True,PlotRange→{{0,250},{0,20}}];

 N[25/elapsedtime[[Length[elapsedtime]]]]

 ListPlot[Abs[Fourier[disp]
],PlotJoined→True,PlotRange→{{0,250},{0,.03}}];
```

BIBLIOGRAPHY

1. Abramowitch, S.D., et al., *A Biomechanical and Histological Analysis of the Structure and Function of the Healing Medial Collateral Ligament in a Goat Model.* Knee Surg Sports Traumatol Arthrosc, 2003. **11**(11): p. 155-62.

2. Abramowitch, S.D., et al. *Effect of Initial Graft Tension on the Biomechanical Properties of ACL Reconstruction Grafts.* in *46th Annual Meeting of Orthopaedic Research Society*. 2000. Orlando, Florida.

3. Abramowitch, S.D. and S.L.-Y. Woo, *An Improved Method to Analyze the Stress Relaxation of Ligaments Following a Finite Ramp Time Based on the Quasi-Linear Viscoelastic Theory.* Journal of Biomechanical Engineering, 2003. **Accepted**.

4. Abramowitch, S.D. and S.L.-Y. Woo, *An Improved Method to Analyze the Stress Relaxation of Ligaments Following a Finite Ramp Time Based on the Quasi-Linear Viscoelastic Theory.* Journal of Biomechanical Engineering, 2004. **126**(1): p. 92-97.

5. Abramowitch, S.D., et al., *An Evaluation of the Quasi-linear Viscoelastic Properties of the Healing Medial Collateral Ligament in a Goat Model.* Annals of Biomedical Engineering, 2004. **32**(3): p. 329-335.

6. Abramowitch, S.D., et al., *The healing medial collateral ligament following a combined anterior cruciate and medial collateral ligament injury--a biomechanical study in a goat model.* J Orthop Res, 2003. **21**(6): p. 1124-30.

7. Aimedieu, P., Jr., et al., *Dynamic stiffness and damping of porcine muscle specimens.* Med Eng Phys, 2003. **25**(9): p. 795-9.

8. Amiel, D., et al., *Stress deprivation effect on metabolic turnover of the medial collateral ligament collagen. A comparison between nine- and 12-week immobilization.* Clinical Orthopaedics & Related Research, 1983(172): p. 265-70.

9. Best, T.M., et al., *Characterization of the passive responses of live skeletal muscle using the quasi-linear theory of viscoelasticity.* J Biomech, 1994. **27**(4): p. 413-9.

10. Birk, D.E., et al., *Collagen Fibrillogenesis In Vitro: Interaction of Types I and V Collagen Regulates Fibril Diameter.* J Cell Sci, 1990. **95**(Pt 4): p. 649-57.

11. Bonifasi-Lista, C., et al. *Strain- and Rate-Dependent Viscoelastic Properties of Human MCL in Tension*. in *48th Annual Meeting of the Orthopaedic Research Society*. 2002. Dallas, TX.

12. Boorman, R.S., N.G. Shrive, and C.B. Frank, *Immobilization increases the vulnerability of rabbit medial collateral ligament autografts to creep.* Journal of Orthopaedic Research, 1998. **16**(6): p. 682-9.

13. Bouchoucha, M., et al., *Variation of rheological properties of the human rectal wall with distending volume.* Clin Invest Med, 1994. **17**(2): p. 107-14.

14. Bray, R.C., R.M. Rangayyan, and C.B. Frank, *Normal and Healing Ligament Vascularity: A Quantitative Histological Assessment in the Adult Rabbit Medial Collateral Ligament.* J Anat, 1996. **188**(Pt 1): p. 87-95.

15. Carew, E.O., et al., *Quasi-Linear Viscoelastic theory applied to internal shearing of porcine aortic valve leaflets.* J Biomech Eng, 1999. **121**(4): p. 386-92.

16. Celechovsky, C., et al. *Analysis of Collagens Synthesized by Cells Harvested from MCL in the Early Stages of Healing*. in *47th Annual Meeting of Orthopaedic Research Society*. 2001. San Fransisco, CA.

17. Chimich, D., et al., *The Effects of Initial End Contact on Medial Collateral Ligament Healing: A Morphological and Biomechanical Study in a Rabbit Model.* J Orthop Res, 1991. **9**(1): p. 37-47.

18. Chimich, D., et al., *Water content alters viscoelastic behaviour of the normal adolescent rabbit medial collateral ligament.* J Biomech, 1992. **25**(8): p. 831-7.

19. Clineff, T.D., et al. *Experimental & Theoretical Evaluation of the Viscoelastic Properties of the Healing Collateral Ligament.* in *ASME Summer Bioengineering Conference*. 1999. Big Sky, MT.

20. Cox, R.H., *Viscoelastic properties of canine pulmonary arteries.* Am J Physiol, 1984. **246**(1 Pt 2): p. H90-6.

21. Dahlqvist, A., et al., *Viscoelasticity of rabbit vocal folds after injection augmentation.* Laryngoscope, 2004. **114**(1): p. 138-42.

22. Derscheid, G.L. and J.G. Garrick, *Medial collateral ligament injuries in football. Nonoperative management of grade I and grade II sprains.* Am J Sports Med, 1981. **9**(6): p. 365-8.

23. Dortmans, L.J., A.A. Sauren, and E.P. Rousseau, *Parameter estimation using the quasi-linear viscoelastic model proposed by Fung.* J Biomech Eng, 1984. **106**(3): p. 198-203.

24. Elliott, D.M., et al., *Effect of altered matrix proteins on quasilinear viscoelastic properties in transgenic mouse tail tendons.* Ann Biomed Eng, 2003. **31**(5): p. 599-605.

25. Fetto, J.F. and J.L. Marshall, *Medial Collateral Ligament Injuries of the Knee: A Rationale for Treatment.* Clinical Orthopaedics & Related Research, 1978(132): p. 206-18.

26. Fetto, J.F. and J.L. Marshall, *The Natural History and Diagnosis of Anterior Cruciate Ligament Insufficiency.* Clinical Orthopaedics & Related Research, 1980(147): p. 29-38.

27. Frank, C., et al., *A quantitative analysis of matrix alignment in ligament scars: a comparison of movement versus immobilization in an immature rabbit model.* J Orthop Res, 1991. **9**(2): p. 219-27.

28. Frank, C., et al., *Collagen fibril diameters in the healing adult rabbit medial collateral ligament.* Connect Tissue Res, 1992. **27**(4): p. 251-63.

29. Frank, C., D. McDonald, and N. Shrive, *Collagen fibril diameters in the rabbit medial collateral ligament scar: a longer term assessment.* Connect Tissue Res, 1997. **36**(3): p. 261-9.

30. Frank, C., et al., *Rabbit medial collateral ligament scar weakness is associated with decreased collagen pyridinoline crosslink density.* J Orthop Res, 1995. **13**(2): p. 157-65.

31. Frank, C., N. Schachar, and D. Dittrich, *Natural history of healing in the repaired medial collateral ligament.* J Orthop Res, 1983. **1**(2): p. 179-88.

32. Frank, C., et al., *Medial collateral ligament healing. A multidisciplinary assessment in rabbits.* American Journal of Sports Medicine, 1983. **11**(6): p. 379-89.

33. Frank, C.B., D.A. Hart, and N.G. Shrive, *Molecular biology and biomechanics of normal and healing ligaments--a review.* Osteoarthritis Cartilage, 1999. **7**(1): p. 130-40.

34. Fung, Y.C., *Biomechanics: Mechanical Properties of Living Tissues*. 2nd ed, ed. Y.C. Fung. 1993, New York, NY: Springer.

35. Fung, Y.-C.B., *Stress-Strain-History Relations of Soft Tissues in Simple Elongation*, in *Biomechanics: Its Foundations and Objectives*, Y.-C.B. Fung and M. Anliker, Editors. 1972, Prentice-Hall Inc.: Englewood Cliffs, N.J. p. 181-208.

36. Funk, J.R., et al., *Linear and quasi-linear viscoelastic characterization of ankle ligaments.* J Biomech Eng, 2000. **122**(1): p. 15-22.

37. Gomez, M.A., et al., *Medical collateral ligament healing subsequent to different treatment regimens.* Journal of Applied Physiology, 1989. **66**(1): p. 245-52.

38. Hart, D.A., et al., *Complexity of Determining Cause and Effect In Vivo after Antisense Gene Therapy.* Clin Orthop, 2000(379 Suppl): p. S242-51.

39. Hart, D.P. and L.E. Dahners, *Healing of the medial collateral ligament in rats. The effects of repair, motion, and secondary stabilizing ligaments.* J Bone Joint Surg Am, 1987. **69**(8): p. 1194-9.

40. Hart, R.A., S.L. Woo, and P.O. Newton, *Ultrastructural morphometry of anterior cruciate and medial collateral ligaments: an experimental study in rabbits.* J Orthop Res, 1992. **10**(1): p. 96-103.

41. Hildebrand, K.A., et al., *The effects of platelet-derived growth factor-BB on healing of the rabbit medial collateral ligament. An in vivo study.* Am J Sports Med, 1998. **26**(4): p. 549-54.

42. Hirshman, H.P., D.M. Daniel, and K. Miyasaka, *The fate of the unoperated knee ligament injuries*, in *Knee Ligaments: Structure , Function, Injury and Repair*, A.W. Danil D, O'Connor J, Editor. 1990, Raven Press: New York. p. 481-503.

43. Hoel, P.G., *Introduction to Mathematical Statistics*. 1971, San Diego: John Wiley & Sons, Inc.

44. Iatridis, J.C., et al., *The viscoelastic behavior of the non-degenerate human lumbar nucleus pulposus in shear.* J Biomech, 1997. **30**(10): p. 1005-13.

45. Indelicato, P.A., *Non-operative treatment of complete tears of the medial collateral ligament of the knee.* Journal of Bone & Joint Surgery - American Volume, 1983. **65**(3): p. 323-9.

46. Indelicato, P.A., *Isolated medial collateral ligament injuries in the knee.* J Am Acad Orthop Surg, 1995. **3**(1): p. 9-14.

47. Ingenito, E.P., L. Mark, and B. Davison, *Effects of acute lung injury on dynamic tissue properties.* J Appl Physiol, 1994. **77**(6): p. 2689-97.

48. Johnson, G.A., et al., *Tensile and viscoelastic properties of human patellar tendon.* Journal of Orthopaedic Research, 1994. **12**(6): p. 796-803.

49. Jokl, P., et al., *Non-operative treatment of severe injuries to the medial and anterior cruciate ligaments of the knee.* J Bone Joint Surg Am, 1984. **66**(5): p. 741-4.

50. Kannus, P., *Long-term results of conservatively treated medial collateral ligament injuries of the knee joint.* Clin Orthop, 1988(226): p. 103-12.

51. Kannus, P. and M. Jarvinen, *Conservatively treated tears of the anterior cruciate ligament. Long-term results.* J Bone Joint Surg Am, 1987. **69**(7): p. 1007-12.

52. Kannus, P. and M. Jarvinen, *Incidence of knee injuries and the need for further care. A one-year prospective follow-up study.* J Sports Med Phys Fitness, 1989. **29**(4): p. 321-5.

53. Kastelic, J. and E. Baer, *Deformation in tendon collagen.* Symp Soc Exp Biol, 1980. **34**: p. 397-435.

54. Kastelic, J., A. Galeski, and E. Baer, *The multicomposite structure of tendon.* Connect Tissue Res, 1978. **6**(1): p. 11-23.

55. Kim, S.M., T.M. McCulloch, and K. Rim, *Comparison of viscoelastic properties of the pharyngeal tissue: human and canine.* Dysphagia, 1999. **14**(1): p. 8-16.

56. Kwan, M.K., T.H. Lin, and S.L. Woo, *On the viscoelastic properties of the anteromedial bundle of the anterior cruciate ligament.* J Biomech, 1993. **26**(4-5): p. 447-52.

57. Kwan, M.K., T.H. Lin, and S.L.-Y. Woo, *On the viscoelastic properties of the anteromedial bundle of the anterior cruciate ligament.* Journal of Biomechanics, 1993. **26**(4-5): p. 447-52.

58. Lam, T.C., C.B. Frank, and N.G. Shrive, *Calibration characteristics of a video dimension analyser (VDA) system.* J Biomech, 1992. **25**(10): p. 1227-31.

59. Lam, T.C., C.B. Frank, and N.G. Shrive, *Changes in the cyclic and static relaxations of the rabbit medial collateral ligament complex during maturation.* J Biomech, 1993. **26**(1): p. 9-17.

60. Lam, T.C., et al., *The effects of temperature on the viscoelastic properties of the rabbit medial collateral ligament.* J Biomech Eng, 1990. **112**(2): p. 147-52.

61. Laros, G.S., C.M. Tipton, and R.R. Cooper, *Influence of physical activity on ligament insertions in the knees of dogs.* Journal of Bone & Joint Surgery - American Volume, 1971. **53**(2): p. 275-86.

62. Larsen, N.P., M.R. Forwood, and A.W. Parker, *Immobilization and retraining of cruciate ligaments in the rat.* Acta Orthopaedica Scandinavica, 1987. **58**(3): p. 260-4.

63. Lauder, T.D., et al., *Sports and physical training injury hospitalizations in the army.* Am J Prev Med, 2000. **18**(3 Suppl): p. 118-28.

64. Lee, T.Q. and M. Dante, *Application of a continuous video digitizing system for tensile testing of bone soft tissue bone complex.* ASME Adv. Bioeng., 1992. **BED-22**: p. 87-90.

65. Lee, T.Q. and S.L. Woo, *A new method for determining cross-sectional shape and area of soft tissues.* J Biomech Eng, 1988. **110**(2): p. 110-4.

66. Lim, K.O. and D.R. Boughner, *The low frequency dynamic viscoelastic properties of human aortic valve tissue.* Circ Res, 1976. **39**(2): p. 209-14.

67. Lin, H.C., M. Kwan, and S.L.-Y. Woo. *On the stress relaxation properties of anterior cruciate ligament (ACL)*. in *Amer. Soc. Mech. Eng*. 1987.

68. Lin, H.C., M.K. Kwan, and S.L.-Y. Woo. *On the stress relaxation properties of anterior cruciate ligament (ACL).* in *ASME Adv Bioeng.* 1987.

69. Linsenmayer, T.F., et al., *Type V collagen: molecular structure and fibrillar organization of the chicken alpha 1(V) NH2-terminal domain, a putative regulator of corneal fibrillogenesis.* Journal of Cell Biology, 1993. **121**(5): p. 1181-9.

70. Loitz-Ramage, B.J., C.B. Frank, and N.G. Shrive, *Injury size affects long-term strength of the rabbit medial collateral ligament.* Clinical Orthopaedics & Related Research, 1997(337): p. 272-80.

71. Lyon, R.M., et al. *Stress relaxation of the anterior cruciate ligament (ACL) and the patellar tendon.* in *Ortho. Res. Soc*. 1988.

72. Messina, D.F., W.C. Farney, and J.C. DeLee, *The incidence of injury in Texas high school basketball. A prospective study among male and female athletes.* Am J Sports Med, 1999. **27**(3): p. 294-9.

73. Miller, C.E., M.A. Vanni, and B.B. Keller, *Characterization of passive embryonic myocardium by quasi-linear viscoelasticity theory.* J Biomech, 1997. **30**(9): p. 985-8.

74. Miyasaka, K.C., et al., *The incidence of knee ligament injuries in the general population.* Am J Knee Surg, 1991. **4**: p. 3-8.

75. Musahl, V., et al., *The use of porcine small intestinal submucosa to enhance the healing of the medial collateral ligament--a functional tissue engineering study in rabbits.* J Orthop Res, 2004. **22**(1): p. 214-20.

76. Myers, B.S., J.H. McElhaney, and B.J. Doherty, *The viscoelastic responses of the human cervical spine in torsion: experimental limitations of quasi-linear theory, and a method for reducing these effects.* J Biomech, 1991. **24**(9): p. 811-7.

77. Navajas, D., et al., *Dynamic response of the isolated passive rat diaphragm strip.* J Appl Physiol, 1992. **73**(6): p. 2681-92.

78. Neubert, H.K.P., *A simple model representing internal damping in solid materials.* Aeronaut, 1963. **14**: p. 187-197.

79. Newton, P.O., et al., *Ultrastructural changes in knee ligaments following immobilization.* Matrix, 1990. **10**(5): p. 314-9.

80. Newton, P.O., et al., *Immobilization of the knee joint alters the mechanical and ultrastructural properties of the rabbit anterior cruciate ligament.* J Orthop Res, 1995. **13**(2): p. 191-200.

81. Ng, G.Y., et al., *Long-term study of the biochemistry and biomechanics of anterior cruciate ligament-patellar tendon autografts in goats.* J Orthop Res, 1996. **14**(6): p. 851-6.

82. Ng, G.Y., et al., *Biomechanics of patellar tendon autograft for reconstruction of the anterior cruciate ligament in the goat: three-year study.* J Orthop Res, 1995. **13**(4): p. 602-8.

83. Nigul, I. and U. Nigul, *On algorithms of evaluation of Fung's relaxation function parameters.* J Biomech, 1987. **20**(4): p. 343-52.

84. Niyibizi, C., et al., *Type V collagen is increased during rabbit medial collateral ligament healing.* Knee Surg Sports Traumatol Arthrosc., 2000. **8**(5): p. 281-285.

85. Niyibizi, C., et al., *Identification and immunolocalization of type X collagen at the ligament-bone interface.* Biochem Biophys Res Commun, 1996. **222**(2): p. 584-9.

86. Niyibizi, C., et al., *Collagens in an adult bovine medial collateral ligament: immunofluorescence localization by confocal microscopy reveals that type XIV collagen predominates at the ligament-bone junction.* Matrix Biology, 1995. **14**(9): p. 743-51.

87. Noyes, F.R., *Functional properties of knee ligaments and alterations induced by immobilization: a correlative biomechanical and histological study in primates.* Clinical Orthopaedics & Related Research, 1977(123): p. 210-42.

88. Noyes, F.R., et al., *The symptomatic anterior cruciate-deficient knee. Part II: the results of rehabilitation, activity modification, and counseling on functional disability.* J Bone Joint Surg Am, 1983. **65**(2): p. 163-74.

89. Noyes, F.R., et al., *Biomechanics of ligament failure. II. An analysis of immobilization, exercise, and reconditioning effects in primates.* J Bone Joint Surg Am, 1974. **56**(7): p. 1406-18.

90. Ohland, K.J., et al. *Healing of Combined Injuries of the Rabbit Medial Collateral Ligament and Its Insertions: A Long Term Study on the Effects of Conservative vs. Surgical Treatment*. in *The Winter Annual Meeting of the American Society of Mechanical Engineers*. 1991. Atlanta, GA.

91. Ohno, K., et al., *Healing of the medial collateral ligament after a combined medial collateral and anterior cruciate ligament injury and reconstruction of the anterior*

cruciate ligament: comparison of repair and nonrepair of medial collateral ligament tears in rabbits. J Orthop Res, 1995. **13**(3): p. 442-9.

92. Papageorgiou, C.D., et al., *A multidisciplinary study of the healing of an intraarticular anterior cruciate ligament graft in a goat model.* Am J Sports Med, 2001. **29**(5): p. 620-6.

93. Patel, D.J., W.K. Tucker, and J.S. Janicki, *Dynamic elastic properties of the aorta in radial direction.* J Appl Physiol, 1970. **28**(5): p. 578-82.

94. Pereira, J.M., J.M. Mansour, and B.R. Davis, *Dynamic measurement of the viscoelastic properties of skin.* J Biomech, 1991. **24**(2): p. 157-62.

95. Press, W.H., et al., *Chapter 15: Modeling of Data*, in *Numerical Recipies in C: The Art of Scientific Computing*. 1992, Cambridge University Press: New York, NY. p. 681-688.

96. Provenzano, P., et al., *Nonlinear ligament viscoelasticity.* Ann Biomed Eng, 2001. **29**(10): p. 908-14.

97. Provenzano, P.P., et al., *Subfailure damage in ligament: a structural and cellular evaluation.* J Appl Physiol, 2002. **92**(1): p. 362-71.

98. Provenzano, P.P., et al., *Application of nonlinear viscoelastic models to describe ligament behavior.* Biomech Model Mechanobiol, 2002. **1**(1): p. 45-57.

99. Puso, M.A. and J.A. Weiss, *Finite element implementation of anisotropic quasi-linear viscoelasticity using a discrete spectrum approximation.* Journal of Biomechanical Engineering, 1998. **120**(1): p. 62-70.

100. Reider, B., et al., *Treatment of isolated medial collateral ligament injuries in athletes with early functional rehabilitation. A five-year follow-up study.* American Journal of Sports Medicine, 1994. **22**(4): p. 470-7.

101. Rosner, B.A., *Fundamentals of Biostatistics*. 1990, Belmont, California: Duxbury Press.

102. Sauren, A.A. and E.P. Rousseau, *A concise sensitivity analysis of the quasi-linear viscoelastic model proposed by Fung.* J Biomech Eng, 1983. **105**(1): p. 92-5.

103. Sauren, A.A., et al., *The mechanical properties of porcine aortic valve tissues.* J Biomech, 1983. **16**(5): p. 327-37.

104. Scheffler, S.U., et al., *Structure and Function of the Healing Medial Collateral Ligament in a Goat Model.* Annals of Biomedical Engineering, 2001. **29**: p. 173-180.

105. Shrive, N., et al., *Soft-tissue "flaws" are associated with the material properties of the healing rabbit medial collateral ligament.* Journal of Orthopaedic Research, 1995. **13**(6): p. 923-9.

106. Smutz, W.P., et al., *Accuracy of a video strain measurement system.* Journal of Biomechanics, 1996. **29**(6): p. 813-7.

107. Tanaka, E., et al., *The proteoglycan contents of the temporomandibular joint disc influence its dynamic viscoelastic properties.* J Biomed Mater Res, 2003. **65A**(3): p. 386-92.

108. Thomopoulos, S., et al., *Variation of biomechanical, structural, and compositional properties along the tendon to bone insertion site.* J Orthop Res, 2003. **21**(3): p. 413-9.

109. Thomopoulos, S., G.R. Williams, and L.J. Soslowsky, *Tendon to bone healing: differences in biomechanical, structural, and compositional properties due to a range of activity levels.* J Biomech Eng, 2003. **125**(1): p. 106-13.

110. Thornton, G.M., et al., *Early medial collateral ligament scars have inferior creep behaviour.* J Orthop Res, 2000. **18**(2): p. 238-46.

111. Thornton, G.M., et al., *Ligament creep cannot be predicted from stress relaxation at low stress: a biomechanical study of the rabbit medial collateral ligament.* J Orthop Res, 1997. **15**(5): p. 652-6.

112. Thornton, G.M., N.G. Shrive, and C.B. Frank, *Healing ligaments have decreased cyclic modulus compared to normal ligaments and immobilization further compromises healing ligament response to cyclic loading.* J Orthop Res, 2003. **21**(4): p. 716-22.

113. Toms, S.R., et al., *Quasi-linear viscoelastic behavior of the human periodontal ligament.* J Biomech, 2002. **35**(10): p. 1411-5.

114. Van Kleunen, J.P. and D.M. Elliott. *Effect of a Natural Crosslinking Agent (Genipin) on Tendon Longitudinal and Transverse Tensile Properties*. in *Summer Bioengineering Conference*. 2003. Key Biscayne, FL.

115. Weiss, J.A., et al., *Evaluation of a new injury model to study medial collateral ligament healing: primary repair versus nonoperative treatment.* Journal of Orthopaedic Research, 1991. **9**(4): p. 516-28.

116. Wiig, M.E., et al., *Type I procollagen gene expression in normal and early healing of the medial collateral and anterior cruciate ligaments in rabbits: an in situ hybridization study.* Journal of Orthopaedic Research, 1991. **9**(3): p. 374-82.

117. Woo, S.L.-Y., *Mechanical properties of tendons and ligaments. I. Quasi-static and nonlinear viscoelastic properties.* Biorheology, 1982. **19**(3): p. 385-96.

118. Woo, S.L.-Y., et al., *Anatomy, biology, and biomechanics of tendon, ligament, and meniscus*, in *Orthopaedic Basic Science*, S.R. Simon, Editor. 1994, American Academy of Orthopaedic Surgeons: Rosemont, IL. p. 45-87.

119. Woo, S.L.-Y., et al., *Anatomy, biology, and biomechanics of tendon and ligament*, in *American Academy of Orthopaedic Surgeons- Orthopaedic Basic Science Biology and Biomechanics of the Musculoskeletal System*, B. J.A., E. T.A., and S. S.R., Editors. 2000: Rosemont, IL. p. 581-616.

120. Woo, S.L.-Y., et al., *The use of a laser micrometer system to determine the cross-sectional shape and area of ligaments: a comparative study with two existing methods.* Journal of Biomechanical Engineering, 1990. **112**(4): p. 426-31.

121. Woo, S.L.-Y., M.A. Gomez, and W.H. Akeson, *The time and history-dependent viscoelastic properties of the canine medical collateral ligament.* Journal of Biomechanical Engineering, 1981. **103**(4): p. 293-8.

122. Woo, S.L.-Y., et al., *New experimental procedures to evaluate the biomechanical properties of healing canine medial collateral ligaments.* J Orthop Res, 1987. **5**(3): p. 425-32.

123. Woo, S.L.-Y., et al., *Measurement of mechanical properties of ligament substance from a bone-ligament-bone preparation.* J Orthop Res, 1983. **1**(1): p. 22-9.

124. Woo, S.L.-Y., et al., *The biomechanical and morphological changes in the medial collateral ligament of the rabbit after immobilization and remobilization.* J Bone Joint Surg Am, 1987. **69**(8): p. 1200-11.

125. Woo, S.L.-Y., et al., *Mechanical properties of tendons and ligaments. II. The relationships of immobilization and exercise on tissue remodeling.* Biorheology, 1982. **19**(3): p. 397-408.

126. Woo, S.L.-Y., et al., *Tensile properties of the human femur-anterior cruciate ligament-tibia complex. The effects of specimen age and orientation.* American Journal of Sports Medicine, 1991. **19**(3): p. 217-25.

127. Woo, S.L.Y., et al., *The response of ligaments to injury: Healing of the collateral ligaments*, in *Knee Ligaments: Structure, Function, Injury, and Repair*, D.M. Daniel, W.H. Akeson, and J.J. O'Connor, Editors. 1990, Raven Press: New York. p. 351-364.

128. Woo, S.L.-Y., et al., *Treatment of the medial collateral ligament injury. II: Structure and function of canine knees in response to differing treatment regimens.* American Journal of Sports Medicine, 1987. **15**(1): p. 22-9.

129. Woo, S.L.-Y., G.A. Johnson, and B.A. Smith, *Mathematical modeling of ligaments and tendons.* J Biomech Eng, 1993. **115**(4B): p. 468-73.

130. Woo, S.L.-Y., et al., *Effects of immobilization and exercise on the strength characteristics of bone-medial collateral ligament-bone complex.* ASME Biomechanical Symposium, 1979. **32**: p. 67-70.

131. Woo, S.L.-Y., et al., *Temperature dependent behavior of the canine medial collateral ligament.* J Biomech Eng, 1987. **109**(1): p. 68-71.

132. Woo, S.L.-Y., et al., *Medial collateral knee ligament healing. Combined medial collateral and anterior cruciate ligament injuries studied in rabbits.* Acta Orthopaedica Scandinavica, 1997. **68**(2): p. 142-8.

133. Woo, S.L.-Y., K.J. Ohland, and P.J. McMahon, *Biology, Healing and Repair of Ligaments*, in *Biology and Bimechanics of the Traumetized Synovial Joint: The Knee as a Model*, G.A.H. Finerman and F.R. Noyes, Editors. 1992, American Academy of Orthoaedic Suregons: Chicago, IL. p. 241-273.

134. Woo, S.L.-Y., K.J. Ohland, and J.A. Weiss, *Aging and sex-related changes in the biomechanical properties of the rabbit medial collateral ligament.* Mech Ageing Dev, 1990. **56**(2): p. 129-42.

135. Woo, S.L.-Y., et al., *Effects of postmortem storage by freezing on ligament tensile behavior.* J Biomech, 1986. **19**(5): p. 399-404.

136. Woo, S.L.-Y., et al., *Tensile properties of the medial collateral ligament as a function of age.* Journal of Orthopaedic Research, 1986. **4**(2): p. 133-41.

137. Woo, S.L.-Y., et al., *The effects of strain rate on the properties of the medial collateral ligament in skeletally immature and mature rabbits: a biomechanical and histological study.* Journal of Orthopaedic Research, 1990. **8**(5): p. 712-21.

138. Woo, S.L.-Y., et al., *Quasi-linear viscoelastic properties of normal articular cartilage.* J Biomech Eng, 1980. **102**(2): p. 85-90.

139. Woo, S.L.-Y., et al. *Engineering the Healing of the Rabbit Medial Collateral Ligament*. in *3rd International Conference on Cellular Engineering*. 1997. San Remo, Italy.

140. Woo, S.L.-Y., T.M. Vogrin, and S.D. Abramowitch, *Healing and repair of ligament injuries in the knee.* J Am Acad Orthop Surg, 2000. **8**(6): p. 364-72.

141. Yamaji, T., et al., *Medial collateral ligament healing one year after a concurrent medial collateral ligament and anterior cruciate ligament injury: an interdisciplinary study in rabbits.* Journal of Orthopaedic Research, 1996. **14**(2): p. 223-7.

142. Yamashita, J., et al., *Collagen and bone viscoelasticity: a dynamic mechanical analysis.* J Biomed Mater Res, 2002. **63**(1): p. 31-6.

143. Yin, F.C., P.H. Chew, and S.L. Zeger, *An approach to quantification of biaxial tissue stress-strain data.* J Biomech, 1986. **19**(1): p. 27-37.

144. Yin, F.C., et al., *A video-dimension analyxer.* IEEE Transactions on Biomedical Engineering, 1972. **19**(5): p. 376-81.

145. Zheng, Y.P. and A.F. Mak, *Extraction of quasi-linear viscoelastic parameters for lower limb soft tissues from manual indentation experiment.* J Biomech Eng, 1999. **121**(3): p. 330-9.